Zoological Journal of the Linnean Society, 2006, **146**, 407–452. With 14 figures

Phylogeny of South American *Bufo* (Anura: Bufonidae) inferred from combined evidence

JENNIFER B. PRAMUK*

Department of Ecology and Evolutionary Biology, Natural History Museum and Biodiversity Research Center, Division of Herpetology, The University of Kansas, Lawrence, KS 66045, USA

Received July 2004; accepted for publication October 2005

Despite the considerable research that has focused on the evolutionary relationships and biogeography of the genus *Bufo,* an evolutionary synthesis of the entire group has not yet emerged. In the present study, almost 4 kb of DNA sequence data from mitochondrial (12S, $tRNA^{Val}$, and 16S) and nuclear (POMC; Rag-1) genes, and 83 characters from morphology were analysed to infer a phylogeny of South American toads. Phylogenies were reconstructed with parsimony and maximum likelihood and Bayesian model-based methods. The results of the analysis of morphological data support the hypothesis that within *Bufo*, some skull characters (e.g. frontoparietal width), correlated with the amount of cranial ossification, are prone to homoplasy. Unique and unreversed morphological synapomorphies are presented that can be used to diagnose recognized species groups of South American toads. The results of all phylogenetic analyses support the monophyly of most species groups of South American *Bufo*. In most DNA-only and combined analyses, the South American (minus the *B. guttatus* and part of the '*B. spinulosus*' groups), North American, Central American, and African lineages form generally well-supported clades: (((((((South America) (North America + Central America)) Eurasia) Africa) Eurasia) South America) West Indies) South America). This result confirms and extends prior studies recovering South American *Bufo* as polyphyletic. The biogeographical results indicate that: (1) The origin of *Bufo* predates the fragmentation of Gondwana; (2) Central and North American species compose the sister group to a large, 'derived' clade of South American *Bufo*; and (3) Eurasian species form the sister group to the New World clade. *Zoological Journal of the Linnean Society*, 2006, **146**, 407–452.

ADDITIONAL KEYWORDS: amphibia – Bayesian analysis – biogeography – Gondwana – mitochondrial ribosomal DNA – morphology – osteology – POMC – Rag-1 – South America.

INTRODUCTION

Bufonidae, commonly known as the true toads, is a family of neobatrachian frogs composed of approximately 471 species in 33 genera (AmphibiaWeb: http://amphibiaweb.org). Synapomorphies of Bufonidae include the presence of a Bidder's organ (rudimentary ovaries present in males; absent in some *Dendrophryniscus*), parotoid glands (Ford & Cannatella, 1993), and an edentate maxilla and premaxilla. Bufonidae is nearly cosmopolitan in distribution, occurring in all areas except the Australo-Papuan Realm (excluding Sulawesi), Madagascar, and the Arctic and Antarctic (Duellman & Sweet, 1999). The geographical distribution of the ~258 species in *Bufo* (AmphibiaWeb) is broader than that of any other amphibian genus and is one of the largest distributions of all vertebrate genera. At this time, there are no synapomorphies to define *Bufo* and several investigators (e.g. Graybeal & Cannatella, 1995; Graybeal, 1997) have questioned the monophyly of the genus. Among amphibians, the relationships of the genus *Bufo* are especially poorly understood, as their morphological and ecological conservatism has challenged systematists attempting to resolve their relationships.

Some aspects of the biology and systematics of *Bufo* have been studied in depth (e.g. Blair, 1972a, b; Martin, 1972a, b; Graybeal, 1997; Cunningham & Cherry, 2000, 2004; Pauly, Hillis & Cannatella, 2004), but an evolutionary synthesis of the entire genus has not emerged. Most prior attempts to infer the phylogeny of true toads were primarily phenetic, based on

*Current address: Department of Integrative Biology, Brigham Young University, Provo, UT 84602, USA. E-mail: pramuk@byu.edu

morphology (Tihen, 1960, 1962a, b; McDiarmid, 1971; Inger, 1972; Martin, 1972a, b; Grandison, 1981), experimental hybridization (Blair, 1963, 1966, 1972a), and chromosomes (Bogart, 1972). Immunological studies by Cardellini *et al*. (1984), Maxson (1981a, b, 1984), and Maxson, Song & Lopatra (1981) were limited by modest taxon sampling, whereas some of the more recent and comprehensive studies based on the analysis of DNA sequences (Graybeal, 1993, 1997) yielded conflicting topologies with poor branch support.

Despite considerable earlier work on phylogenetic relationships of bufonid frogs, there is little consensus about the relationships of South American *Bufo* beyond the composition of some species groups. For this study, nuclear and mitochondrial DNA (mtDNA) sequence data were combined and analysed with morphological data to infer the evolutionary history of South American toads in three discrete steps: (1) Molecular markers and morphological characters were used to infer interspecific phylogenetic relationships of South American *Bufo.* (2) The recovered morphological and combined phylogenies were used to address morphological character evolution within South American species. (3) The biogeographical history of South American *Bufo* was inferred by comparing resulting phylogenetic topologies with previously proposed biogeographical hypotheses.

From a body of multidisciplinary evidence spanning chromosomal, acoustical, morphological, and fossil data, Blair (1972b) hypothesized that toads of the genus *Bufo* included 'narrow-skulled' and 'broad-skulled' lineages, which he suggested resulted from an early evolutionary dichotomy in the genus. Blair (1972a, b) defined 'narrow-' vs. 'broad-skulled' groups based on the sizes of the frontoparietals; however, assignment to either the 'broad' or 'narrow' lineage was based on a synthesis of multiple types of data (e.g. chromosomes and call morphology). Therefore, a narrow-skulled taxon might have been placed in the broad-skulled lineage (e.g. *B. terrestris*); conversely, a broad-skulled toad might be assigned to the narrow-skulled lineage (e.g. *B. alvarius*). The work of Blair (1972a, b) and his coauthors on the evolution of *Bufo* is the most comprehensive to date, but it is based on a synthesis of overall similarity and offers conflicting interpretations of the evolution and biogeography of the genus.

Graybeal (1997) inferred a higher-level phylogeny of Bufonidae based on an analysis of molecular (cytochrome *b,* 12S, 16S, and c-mos) and morphological data. She had mixed success using mitochondrial protein coding and ribosomal genes to investigate bufonid relationships. In the same paper, she performed a 'total evidence' analysis (*sensu* Kluge, 1989) by adding 73 morphological characters derived from the literature and from an examination of specimens. The results of her total evidence analysis suggested that the genus *Bufo* is not monophyletic. In addition, Graybeal (1997) identified several clades within Bufonidae (e.g. the North American *B. boreas* group); however, the necessarily large scale of her analysis was such that tests of monophyly of all species groups within the family were not possible. Representation of South American *Bufo* in Graybeal's (1997) analysis was limited to nine species and they were not recovered as monophyletic (Graybeal, 1997: fig. 13). Overall, Graybeal's (1997) results suggest that there is little correlation between geographical area and phylogenetic relationships, which is contrary to the findings of other studies (Maxson, 1984; Pauly *et al.*, 2004). Unfortunately, even though Graybeal's study included the greatest taxonomic sampling yet to investigate relationships within Bufonidae, recent studies have revealed that many of her 16S sequences are of questionable quality (Harris, 2001; Pauly *et al.*, 2004), which might explain the conflicting topologies presented in her paper.

Within the past decade, several researchers have investigated the relationships within selected species groups of *Bufo*. Among the more recent morphological and/or molecular-based studies are the following: Goebel (1996) on the systematics of the *B. boreas* group of North America; Cordova (1999), Di Tada, Martino & Sinsch (2001) and Morrison (1994) on the *B. spinulosus* group of South America; Hass *et al*. (1995) on the '*B. margaritifera*' (= *margaritifer*) group of South America; Macey *et al*. (1998) on the *B. bufo* group of Asia; Masta *et al*. (2002) on the *B. americanus* group of North America; Mendelson (1997a) and Mulcahy & Mendelson (2000) on the *B. valliceps* group of North and Central America; Pauly *et al.* (2004) on the relationships of Nearctic *Bufo*; Pramuk, Hass & Hedges (2001) and Pramuk (2002) on the *B. peltocephalus* group of the West Indies; Wanzhao *et al*. (2000) on East Asian *Bufo* and Cunningham & Cherry (2000, 2004) on African *Bufo*. However, none of these focused specifically on the evolution of multiple species groups within the South American radiation.

The large size of the genus *Bufo* has necessitated the grouping of morphologically similar taxa into species groups. These groupings are convenient for systematists to organize the vast diversity of the genus. It has been 14 years since Duellman & Schulte (1992) defined eight phenetic species groups within South America and provided a diagnosis for each; little has changed regarding the content and characteristics defining these assemblages, although since then, quite a few new species have been described. A summary of the content and general geographical distribution of each South American species group is provided in Table 1. Fortunately, several investigators (e.g. F. Baldissera, M. Hoogmoed, P. Narvaes, & C. Vélez-R.) in South America are working on the alpha taxonomy

Table 1. Species composition of the eight traditionally recognized groups of South American *Bufo* (modified from those presented by Duellman & Schulte, 1992), their geographical distributions, and morphological characters used to diagnose them. Groups listed in quotes were not supported as monophyletic in this study. SVL, snout–vent length

Species group	Approximate geographical distribution	Traditionally used diagnostic characters
PREDOMINANTLY SOUTH AMERICAN SPECIES GROUPS		
***B. crucifer* group**	Argentina to E Brazil and Paraguay	Well-developed cranial crests
B. crucifer (may contain = 5 spp.)*†		
B. granulosus group (as defined by Narvaes, 2003)		Prenasal bones; subtriangular parotoid glands; relatively short hindlimbs
B. azarai Gallardo, 1965	Argentina and Paraguay	
B. bergi Céspedez, 2000	Argentina and Paraguay	
B. dorbignyi Duméril & Bibron, 1841	S Brazil, Argentina, and Uruguay	
B. fernandezae Gallardo, 1957	S Brazil, Argentina, and Uruguay	
B. granulosus Spix, 1824*†	SE to NE Brazil	
B. humboldti (Gallardo, 1965)*†	Colombia, Venezuela, Guiana, Suriname, and Trinidad	
B. major Müller & Helmich, 1936†	Argentina, Bolivia, Paraguay, and Amazonian Brazil	
B. merianae Gallardo, 1965	Amazonian regions of Venezuela, Guiana, and Suriname	
B. mirandaribeiroi (Gallardo, 1965)†	C Brazil	
B. nattereri Bokermann, 1967	Roraima, Brazil	
B. pygmaeus Myers & Carvalho, 1952	Rio de Janeiro, Brazil	
***B. guttatus* group**		Well-developed omosternum; smooth skin on dorsum; large SVL (in some spp.)
B. anderssoni Melin, 1941	Rio Uaupes, Brazil	
B. blombergi Myers & Funkhouser, 1951†	N Ecuador to W Colombia	
B. caeruleostictus Günther, 1859†	W Ecuador	
B. glaberrimus Günther, 1868*†	Amazonian Colombia, Ecuador, and Peru	
B. guttatus Schneider, 1799*†	Amazonian Ecuador, Colombia, Venezuela, Guyanas, Bolivia, and Brazil	
B. haematiticus Cope, 1862*†	E Honduras, S Costa Rica, N Colombia, and Venezuela to W Ecuador	
***B. margaritifer* group**		Hypertrophied supra- and postorbital crests (especially in females)
B. alatus Thominot, 1884	E Colombia, S Venezuela, and Brazil	
B. castaneoticus Caldwell, 1991*	Xingu, Brazil	
B. ceratophrys Boulenger, 1882	E Ecuador and Columbia; Venezuela	
B. cristinae Vélez-R. & Ruiz-C., 2002	Colombia	
B. dapsilis Myers & Carvalho, 1945*	Amazonian Colombia, Brazil, Peru, and Ecuador	
B. iserni (Jiménez de la Espada, 1875)	R'o Chanchamayo and R'o Perene, Peru	
B. margaritifer (Laurenti, 1768)*†	Throughout S Central and South America	
B. nasicus Werner, 1903†§	E Venezuela and NW Guyana	
B. roqueanus Melin, 1941	S Ecuador, Peruvian lowlands along E Andes	
B. sclerocephalus Mijares-Urrutia & Arends, 2001	Falcón, Venezuela	

Table 1. *Continued*

Species group	Approximate geographical distribution	Traditionally used diagnostic characters
***B. marinus* group**		Large SVL, conspicuous parotoid glands; well-developed cranial crests
B. arenarum Hensel, 1867*†	S Brazil, northern Argentina, Uruguay, and Bolivia	
B. ictericus Spix, 1824*	Brazil, E Paraguay, and Misiones, Argentina	
B. jimi Stevaux, 2002	NE Brazil	
B. marinus (Linnaeus, 1758)*†	S North America, Central America to N South America	
B. poeppigii Tschudi, 1845*†	Andean slopes of Ecuador, Peru, Bolivia	
B. rubescens Lutz, 1925* (= *B. rufus* Garman, 1877 '1876'; *fide* Frost, 2002)	Goiás and Minas Gerais, Brazil	
B. schneideri Werner, 1894*† (= *B. paracnemis* Lutz, 1925; *fide* Frost, 2002)	Atlantic coast of Brazil to Paraguay; C Bolivia; N and C Argentina, and Uruguay	
'*B. spinulosus* group'		Narrow frontoparietals with cranial crests absent; tympanum absent in some species
B. amabilis Pramuk & Kadivar, 2003†	Ecuador	
B. arequipensis Vellard, 1959*†	Arequipa region and S Pacific Peru	
B. arunco (Molina, 1782)	C Chilean arid steppe	
B. atacamensis Cei, 1962*†	Atacama Desert, Chile	
B. chilensis (Tschudi, 1838)*†	C Chile	
B. cophotis Boulenger, 1900*†§	Atlantic and Amazonian Andes, N Peru	
B. corynetes Duellman & Ochoa, 1991†§	Urubamba Province, Cusco, Peru	
B. limensis Werner, 1901*†	Arid coastal region of Peru	
B. rubropunctatus Guichenot, 1848†	Argentina, S Chile	
B. spinulosus (Wiegmann, 1834)*†	Andean Argentina, Chile, Bolivia, Peru, S Ecuador	
B. variegatus (Günther, 1870)*†§	Argentina, adjacent Chile southward to Magellanic Islands of Chile, Argentina	
B. vellardi Leviton & Duellman, 1978*†	N Peru	
'*B. veraguensis* group'		Weakly developed cranial crests
B. amboroensis Harvey & Smith, 1993*	Cochabamba and Santa Cruz, Bolivia	
B. arborescandens Duellman & Schulte, 1992	Amazonian Peru	
B. chavin Lehr *et al.*, 2001*†	E Andean slopes of C Peru	
B. fissipes Boulenger, 1903	Peru and Bolivia	
B. inca Stejneger, 1913	C Peru	
B. justinianoi Harvey & Smith, 1994	La Paz, Santa Cruz, and Cochabamba, Bolivia	
B. nesiotes Duellman & Toft, 1979*	Huanuco, Peru	
B. quechua Gallardo, 1961	Bolivian Andes	
B. rumbolli Carrizo, 1992	NW Argentina	

Table 1. *Continued*

Species group	Approximate geographical distribution	Traditionally used diagnostic characters
B. veraguensis Schmidt, 1857*†	SE Peru, valleys of Bolivia	
Not assigned to a species group		
B. ocellatus Günther, 1858*†	Brazil	Stout habitus, distinctive leopard-spotted dorsum
PREDOMINANTLY CENTRAL AMERICAN SPECIES		
***B. valliceps* group** (modified from Mendelson, 1997a)		Weakly developed omosternum (some spp.)
B. campbelli Mendelson, 1994	Atlantic versant of Mexico to Honduras	Well-developed cranial crests
B. cavifrons Firschein, 1950	Veracruz, Mexico	
B. cristatus Wiegmann, 1833*B. leucomyos* McCranie & Wilson, 2000	Veracruz and Puebla, Mexico Atlantic versant, N Honduras	
B. luetkenii Boulenger, 1891*†	S Chiapas Mexico to C Costa Rica	
B. macrocristatus Firschein & Smith, 1957	Chiapas, Mexico, and Guatemala	
B. mazatlanensis Taylor, 1940	N Sonroa to Colima, Mexico	
B. melanochlorus Cope, 1878	SW Costa Rica	
B. nebulifer (Girard, 1854)	Gulf Coast of US to C Veracruz, Mexico	
B. spiculatus Mendelson, 1997b	Oaxaca, Mexico	
B. tutelarius Mendelson, 1997c	Chiapas, Mexico, and Guatemala	
B. valliceps Wiegmann, 1833*†	C Veracruz, Mexico to Costa Rica	
OTHER CENTRAL/SOUTH AMERICAN SPECIES		
B. coccifer Cope, 1866*†	Michoacán, Mexico, to W Panama	
B. coniferus Cope, 1862*†	NC Nicaragua to N Ecuador	

* and † indicate species included in molecular and morphological data sets, respectively.
Based on the results of the present study, species indicated with § should be reassigned to other species groups (see text for details).

of several of the more widespread and intractable species groups (e.g. the *B. granulosus* and *B. margaritifer* groups); undoubtedly, their contents and diagnoses will change following the findings of these authors.

Until now, the monophyly of South American species groups has not been tested in a phylogenetic framework. In this study, molecular and morphological data were analysed to examine the phylogenetic relationships within and among the South American species groups and the biogeographical history of *Bufo*. The morphological analyses were also used to examine diagnostic characters for each species group and the evolution of cranial characters in the genus.

MATERIAL AND METHODS

TAXON SAMPLING

In this study, ingroup taxa were selected to cover all proposed lineages or species groups within South America. In total, sequences from 89 specimens representing 74 species were collected, including data for 66 *Bufo*, four non-*Bufo* bufonids, and four outgroup taxa. Taxon sampling spanned 36 South American species (representing ~60% of the diversity in South America), in addition to 35 individuals from North America, Eurasia, and Africa. The selection of outgroups necessitated the consideration of recent studies of hyloid (Darst & Cannatella, 2004; Wiens *et al.*, 2005b) and bufonid (Graybeal, 1997; Pauly *et al.*, 2004) relationships. For the molecular and combined analyses, hyloid outgroups were selected based on their position relative to *Bufo* in the earlier studies and included *Leptodactylus*, *Ceratophrys*, *Eleutherodactylus*, *Hyla*, and the bufonid *Melanophryniscus*, which has been shown recently to be basal within Bufonidae (Darst & Cannatella, 2004; Wiens *et al*., 2005b). The taxa included in the morphological data set differed from those utilized in the molecular analysis because tissue samples or osteological prepara-

tions were not available for all taxa. Morphological transformation series were collected and scored from 58 ingroup species of *Bufo*, four non-*Bufo* bufonids, and two outgroup taxa: the bufonid *Melanophryniscus* and a nonbufonid (the leptodactylid *Leptodactylus ocellatus*).

Morphological data and analysis

In this analysis, characters of cranial and axial osteology described by previous authors (Lynch, 1971; Martin, 1972a, b; Pregill, 1981; Cannatella, 1985; Morrison, 1994; Mendelson, 1997a; Pramuk, 2000, 2002) were examined; these characters were combined with additional transformation series that were discovered upon examination of the specimens. In addition to osteological characters, soft anatomical and integumentary characters (e.g. morphology of parotoid glands) were included in the analysis. One character relating to inguinal fat bodies was coded from the literature (Da Silva & Mendelson, 1999).

The specimens used in this study were dried skeletons, cleared and stained, and whole alcohol-preserved specimens in The University of Kansas Natural History Museum and Biodiversity Research Center Herpetological Collections (KU). In addition, specimens were loaned from a variety of institutions (see Appendix 1). Some specimens were cleared and stained by the author using the protocol of Taylor & Van Dyke (1985), whereas others were skeletonized by hand or with the assistance of dermestid beetle larvae. Morphological observations and illustrations were made with a stereo dissection microscope equipped with a camera lucida. The dorsal, ventral, and lateral views of the skulls of one or more representatives of each species group were drawn to illustrate the osteological cranial characters described herein.

The complete data matrix containing all morphological character states is presented in Table 2. Except where noted, transformation series used in this analysis were scored directly from specimens. In cases of an unknown character state (e.g. when a damaged specimen was lacking a particular element) or logical inconsistency (e.g. the state of the prenasal bones in species lacking these elements), the characters were coded as unknown. Many specimens were skeletonized or cleared and stained for this project. Multiple specimens were examined for each character when possible; however, the rarity of skeletonized or cleared and stained material for many taxa (e.g. *B. humboldti*) precluded this.

Morphological transformation series were coded as binary and multistate characters and were analysed with parsimony and Bayesian methods. Whether or not to order multistate characters in an analysis is controversial at best (Mickevich, 1982; Mabee, 1989; Mickevich & Weller, 1990; Hauser & Presch, 1991; Slowinski, 1993; Wiens, 2001). Therefore, in an attempt to investigate the effect of character ordering on the resulting topologies, data were analysed with unordered as well as with ordered multistate characters for which there is variation along an axis (characters 2, 6, 15, 26, 34, 37, 39, 48, 50, 52, 55, 56, and 62). The program MACCLADE (Maddison & Maddison, 1992) was used to enter, edit, and manipulate the morphological data. Parsimony analyses were performed using PAUP* (ver. 4.0b10; Swofford, 2000). A heuristic search was performed with tree–bisection–reconnection (TBR) branch swapping, with 100 random taxon addition replicates, saving all minimum trees at each replicate. No limit was imposed on the maximum number of trees to be saved, and PAUP* was instructed to increase automatically the maximum by 100 if/when the default value of 100 trees was reached. Summary values (e.g. tree length, consistency index) were reported by PAUP*. Nonparametric bootstrapping (Felsenstein, 1985) with 200 bootstrap pseudoreplicates and ten random taxon addition sequence replicates was performed to determine support for individual branches.

A Bayesian analysis of morphological data was performed with MRBAYES (ver. 3.0b4; Huelsenbeck & Ronquist, 2001) and employed the maximum likelihood (ML) model for morphological character data (Markov k or Mk) of Lewis (2001). To find the best-fitting model for the morphological data, a preliminary analysis was run of two likelihood models for morphological character evolution, one that assumes equal rates of change among characters (Mk) and one that uses the gamma distribution to incorporate unequal rates among characters (Mk + G). Each initial analysis was run for 4.0×10^6 generations. Harmonic means resulting from the two analyses were compared using the Bayes factor (following Nylander *et al.*, 2004; Wiens, Bonett & Chippindale, 2005). The Bayes factor (B_{10}) is calculated as the difference of the two harmonic means of the log likelihoods, multiplied by two (Kass & Rafferty, 1995; Nylander *et al.*, 2004; Wiens *et al.*, 2005a). The Bayes factor strongly favoured the Mk model (mean likelihood = –2113.96) over the Mk + G model (mean likelihood = –2131.39) with $B_{10} = 34.86$ (a Bayes factor = 10 is considered strongly favoured). After selection of the best-fitting model, two replicate analyses of the morphological data were performed with MRBAYES using 20×10^6 generations each, with four chains and default priors, the temperature set at 0.4 and trees sampled every 1000 generations. The two replicate analyses converged on very similar topologies and branch support. Nodes with Bayesian posterior probabilities (bpp) of 0.95 or

Table 2. Taxon by character matrix used in the morphological and combined analyses

Taxon	01	02	03	04	05	06	07	08	09	10	11	12	13	14	15	16	17	18	19	20	21	22	23	24	25
Outgroups																									
Leptodactylus	0	0	0	0	0	0	0	0	0	0	0	0	0	0	0	0	0	0	0	0	0	0	0	0	0
Melanophryniscus	1	0	1	0	0	0	0	1	0	0	0	0	0	0	2	1	1	?	0	0	0	0	0	1	2
Non-*Bufo* bufonids																									
Osornophryne	1	1	0	0	0	0	0	0	2	1	0	0	0	0	2	1	1	?	1	0	0	0	0	0	0
Pedostibes	0	0	0	0	1	0	0	0	2	3	0	0	0	0	2	1	0	1	1	0	0	1	0	1	0
Schismaderma	0	0	0	0	0	1	0	0	0	1	0	0	0	0	0	0	1	1	0	0	0	0	0	0	2
Truebella skoptes	1	0	0	1	1	0	0	0	2	1	1	0	0	0	1	1	1	?	0	0	0	0	0	1	2
Truebella tothastes	1	0	0	1	1	0	0	0	2	1	1	0	0	0	1	1	1	?	0	0	0	0	0	1	2
North America																									
B. americanus	0	2	0	0	0	1	0	1	0	2	0	0	0	0	2	0	0	0	1	0	0	1	0	0	0
B. alvarius	0	2	0	0	0	1	0	1	2	0	0	0	0	0	2	0	0	1	1	0	0	1	0	0	0
B. boreas	0	1	0	0	1	1	0	0	0	2	0	0	0	0	1	0	0	0	0	0	2	1	0	0	0
B. cognatus	0	1	0	0	0	1	0	1	1	2	0	0	0	0	2	0	0	0	0	0	0	1	0	0	0
B. debilis	0	1	0	0	0	1	0	0	1	2	0	2	0	0	2	1	0	1	1	0	1	1	0	1	2
B. exsul	0	1	1	0	1	1	0	0	0	2	0	0	0	0	1	1	0	1	0	0	2	1	0	0	0
B. fowleri	0	1	0	0	0	1	0	1	1	3	0	0	0	0	2	0	0	0	1	0	0	1	0	0	0
B. punctatus	0	1	0	0	0	1	0	1	2	3	0	0	0	0	2	0	0	1	1	0	1	1	0	0	2
B. quercicus	0	1	0	0	0	1	0	0	1	0	0	2	0	0	2	1	0	1	1	0	1	1	0	0	2
B. terrestris	0	2	0	0	0	1	0	1	1	2	0	0	0	0	2	0	0	0	1	0	0	1	0	0	0
B. woodhousii	0	2	0	0	0	1	0	1	1	3	0	0	0	0	2	0	0	0	0	0	0	1	0	0	0
Central America																									
B. coccifer	0	2	0	0	0	1	0	1	1	2	0	0	0	0	2	0	0	0	1	0	1	1	0	1	0
B. coniferus	0	2	0	0	0	1	0	1	1	2	0	0	0	0	2	0	0	1	1	0	1	1	0	1	0
B. luetkenii	0	2	0	0	0	1	0	1	2	2	0	0	0	0	2	0	0	0	1	0	1	0/1	0	0	0
B. valliceps	0	2	0	0	0	1	0	1	2	2	0	0	0	0	2	0	0	0	1	0	1	0/1	0	0	0
Eurasia																									
B. asper	0	2	0	0	0	2	0	1	2	3	0	0	0	0	2	0	0	1	1	0	1	1	0	0	0
B. bufo	0	0	0	0	0	1	0	0	0	3	1	0	0	0	1	0	0	0	0	0	0	1	0	0	0
B. juxtasper	0	2	0	0	0	2	0	0	2	1	0	0	0	0	2	0	0	1	1	0	1	1	0	0	0
B. macrotis	0	0	0	0	0	0	0	0	0	1	0	0	0	0	0	1	0	1	0	0	0	1	0	1	0
B. melanostictus	0	1	0	0	0	0	0	1	0	2	0	0	0	0	2	0	0	0	1	0	0	1	0	1	0
B. viridis	0	0	0	0	0	1	0	0	0	3	1	0	0	0	1	0	0	0	0	0	0	1	0	0	0
Africa																									
B. maculatus	0	1	0	0	0	0	0	1	2	2	0	0	0	0	2	1	0	1	1	0	0	0	0	0	1
B. pardalis	0	1	0	0	0	0	0	0	2	3	0	0	0	0	2	0	0	1	1	0	0	0	0	0	0
B. regularis	0	1	0	0	0	0	0	1	2	2	0	0	0	0	2	0	0	1	1	0	0	0	0	0	0
B. xeros	0	1	0	0	0	0	0	1	2	2	0	0	0	0	2	0	0	1	0	0	0	0	0	0	0
West Indies																									
B. lemur	1	2	0	0	0	3	1	1	2	3	0	2	0	1	2	1	0	?	1	0	?	1	1	?	2
South America																									
B. crucifer	0	2	0	0	0	1	0	0	2	2	0	1	0	0	2	0	0	0	2	0	0	1	0	0	0
B. ocellatus	?	?	?	0	0	?	?	?	?	?	?	?	0	?	?	?	?	?	?	?	?	?	?	?	?
B. granulosus group																									
B. goeldi	0	2	0	0	0	3	1	1	2	2	0	2	0	1	2	1	0	0	2	0	?	1	1	?	2
B. humboldti	0	2	0	0	0	3	1	1	2	2	0	2	0	1	2	1	0	0	2	0	?	1	0	?	2
B. granulosus	0	2	0	0	0	3	1	1	2	2	0	2	0	1	2	1	0	0	2	0	?	1	0	?	2
B. mirandaribeiroi	0	2	0	0	0	3	1	1	2	2	0	2	0	1	2	1	0	0	2	0	?	1	0	?	2
B. guttatus group																									
B. blombergi	0	1	0	0	0	1	0	0	2	1	0	1	0	0	2	1	0	0	1	1	0	1	0	0	0
B. caeruleostictus	0	1	0	0	0	1	0	0	2	2	0	0	0	0	2	0	0	0	1	1	0	1	0	0	0
B. guttatus	0	1	0	0	0	1	0	0	2	2	0	1	0	0	2	1	0	0	1	1	0	1	0	0	0
B. haematiticus	0	1	0	0	0	1	0	0	2	1	0	1	0	0	2	0	0	1	1	1	0	1	0	0	0

Table 2. *Continued*

Taxon	01	02	03	04	05	06	07	08	09	10	11	12	13	14	15	16	17	18	19	20	21	22	23	24	25
B. nasicus	0	?	?	0	0	?	?	?	?	?	?	?	0	?	?	?	?	?	?	?	?	?	?	?	?
B. margaritifer group																									
B. margaritifer 1	0	2	0	1	2	0	1	1	2	2	0	2	1	0	2	1	0	0	1	0	1	1	0	1	0
B. margaritifer 2	0	1	0	1	2	0	1	1	2	2	0	2	1	0	2	1	0	0	1	0	1	1	0	1	0
B. marinus group																									
B. arenarum	0	2	0	0	0	1	0	1	2	2	0	2	0	0	2	0	0	0	2	0	0	1	0	0	0
B. marinus	0	2	0	0	0	1	0	1	2	2	0	2	0	0	2	0	0	0	2	0	0	1	0	0	0
B. poeppigii	0	2	0	0	0	1	0	1	1	2	0	2	0	0	2	0	0	0	2	0	0	1	0	0	0
B. scheideri	0	2	0	0	0	1	0	1	2	2	0	2	0	0	2	0	0	0	2	0	0	1	0	0	0
B. spinulosus group																									
B. amabilis	0	1	0	0	0	0	0	0	1	2	0	0	0	0	1	1	0	1	0	0	0	1	0	0	0
B. arequipensis	0	1	0	0	0	0	0	0	1	2	0	0	0	0	1	0	0	0	1	0	0	1	0	0	0
B. atacamensis	0	1	0	0	0	0	0	0	1	3	0	0	0	0	1	0	0	?	0	0	0	1	0	0	1
B. chilensis	0	1	1	0	0	0	0	0	0	2	0	0	0	0	1	0	0	?	0	0	0	1	0	0	1
B. cophotis	0	0	0	0	0	2	0	0	0	2	0	0	0	0	0	1	1	?	0	0	2	0	0	1	2
B. corynetes	0	0	1	0	0	2	0	0	0	1	0	0	0	0	0	1	1	?	0	0	2	0	0	1	2
B. limensis	0	1	0	0	0	0	0	0	1	2	0	0	0	0	1	0	0	0	1	0	0	1	0	0	0
B. rubropunctatus	0	0	1	0	0	0	0	0	0	1	0	0	0	0	1	1	0	?	1	0	0	1	0	0	1
B. spinulosus	0	1	0	0	0	0	0	0	0	2	0	0	0	0	1	1	0	0	0	0	0	1	0	0	0
B. variegatus	0	0	1	0	0	2	0	0	0	2	0	0	0	0	0	1	1	0	0	0	2	0	0	1	2
B. vellardi	0	1	0	0	0	0	0	0	0	2	0	0	0	0	1	1	0	0	0	0	0	1	0	0	0
B. veraguensis group																									
B. veraguensis	0	1	0	0	1	0	0	0	1	3	0	0	0	0	2	1	0	?	1	0	1	1	0	1	1
B. chavin	0	1	0	0	1	0	0	0	1	3	0	0	0	0	2	1	0	?	1	0	1	1	0	1	0
B. sp.	0	1	0	0	1	0	0	0	2	3	0	0	0	0	2	1	0	1	1	0	1	1	0	1	0

Taxon	26	27	28	29	30	31	32	33	34	35	36	37	38	39	40	41	42	43	44	45	46	47	48	49	50
Outgroups																									
Leptodactylus	0	0	0	0	0	0	2	0	2	0	0	1	0	0	0	0	0	0	0	0	1	0	0	0	0
Melanophryniscus	0	0	0	1	0	0	1	0	2	0	1	2	1	0	0	0	0	0	0	2	0	1	2	1	1
Non-*Bufo* bufonids																									
Osornophryne	0	1	0	1	2	0	0	0	2	0	1	0	1	?	1	0	0	2	1	2	?	?	?	?	2
Pedostibes	0	0	0	1	1	0	0	1	0	0	1	0	0	1	1	0	0	0	0	0	1	1	2	1	1
Schismaderma	0	0	0	1	1	0	1	1	2	0	1	0	0	0	1	0	0	0	0	0	0	1	2	1	0
Truebella skoptes	0	0	0	1	0	0	0	0	2	0	1	1	0	0	1	0	0	3	1	2	1	0	0	?	0
Truebella tothastes	0	0	0	1	0	0	0	0	2	0	1	1	0	0	1	0	0	3	0	2	1	1	2	1	0
North America																									
B. americanus	0	1	0	0	1	0	2	1	2	0	1	2	0	0	0	0	0	0	0	1	0	0	2	1	0
B. alvarius	0	1	0	0	1	0	2	1	0	0	1	0	0	0	0	0	0	2	0	0	0	0	2	1	0
B. boreas	0	0	0	0	1	0	2	1	1	0	1	0	0	0	0	0	0	0	0	1	0	0	2	1	0
B. cognatus	0	1	0	1	1	0	2	1	2	0	1	2	0	0	0	0	0	0	0	1	0	0	2	1	0
B. debilis	2	0	0	0	1	0	1	0	2	0	1	2	0	0	1	0	0	0	0	1	0	1	2	1	0
B. exsul	0	0	0	0	1	0	1	1	1	0	1	0	0	0	0	0	0	0	0	1	0	0	2	1	0
B. fowleri	0	1	0	0	1	0	2	0	1	0	1	0	0	0	1	0	0	0	0	1	0	0	2	1	0
B. punctatus	2	0	0	0	1	0	2	0	2	0	1	2	0	0	0	0	0	0	0	1	0	1	2	1	0
B. quercicus	2	0	0	0	1	0	2	0	2	0	1	2	1	0	0	0	0	0	0	1	0	1	2	1	0
B. terrestris	0	1	0	0	1	0	2	1	2	0	1	0	0	0	0	0	0	0	0	1	0	0	1	1	0
B. woodhousii	0	1	0	0	1	0	2	1	2	0	1	2	0	0	1	0	0	0	0	1	0	0	2	1	0
Central America																									
B. coccifer	0	1	1	0	1	0	2	0	1	0	1	1	0	0	0	0	0	1	0	0	0	0	1	1	1
B. coniferus	0	1	1	0	1	0	1	1	1	0	1	1	0	0	0	0	0	1	0	0	0	0	1	1	1

Table 2. *Continued*

Taxon	26	27	28	29	30	31	32	33	34	35	36	37	38	39	40	41	42	43	44	45	46	47	48	49	50
B. luetkenii	0	1	1	0	1	0	2	0	1	0	1	2	0	0	0	0	0	1	0	0	0	0	1	1	1
B. valliceps	0	1	1	0	1	0	2	0	1	0	1	2/1	0	0	0	0	0	1	0	0	0	0	1	1	1
Eurasia																									
B. asper	2	1	0	0	1	0	1	1	0	0	1	1	0	1	1	0	0	0	0	3	1	0	1	1	1
B. bufo	1	1	0	1	1	0	2	0	0	0	1	0	0	1	0	0	0	1	0	0	0	0	1	1	0
B. juxtasper	0	1	0	0	1	0	1	1	0	0	1	1	0	1	1	0	0	0	0	3	1	0	2	1	1
B. macrotis	0	0	0	0	1	0	1	0	1	0	1	0	0	0	0	0	0	0	0	0	0	0	1	1	1
B. melanostictus	0	1	0	0	1	0	2	0	1	0	1	0	0	0	0	0	0	1	0	0	0	1	2	1	1
B. viridis	0	0	0	0	1	0	2	0	1	0	1	0	0	1	0	0	0	1	0	0	0	1	2	1	0
Africa																									
B. maculatus	0	0	0	0	1	0	2	0	2	0	1	2	0	1	0	0	0	0	0	0	0	0	1	1	1
B. pardalis	1	1	1	0	1	0	2	1	2	0	1	0	0	0	0	0	0	1	0	0	0	0	2	1	?
B. regularis	0	1	1	0	1	0	2	0	2	0	1	2	0	0	0	0	0	0	0	0	0	0	2	1	0
B. xeros	1	1	1	0	1	0	2	1	2	0	1	2	0	1	0	0	0	0	0	0	0	1	2	1	0
West Indies																									
B. lemur	0	1	0	0	2	0	1	1	1	0	1	0	0	0	0	1	0	?	0	0	0	1	2	1	1
South America																									
B. crucifer	0	1	0	0	1	0	1	1	0	0	1	0	0	0	0	0	0	1	0	0	0	0	1	1	1
B. ocellatus	?	?	?	0	?	0	?	?	?	?	1	?	?	?	0	?	?	?	?	0	?	?	?	?	?
B. granulosus group																									
B. goeldi	2	1	0	0	2	0	1	0	1	0	1	2	0	0	0	1	1	?	0	0	0	0	2	1	1
B. humboldti	2	1	0	0	2	0	1	0	1	0	1	2	0	0	0	1	1	?	0	0	0	0	2	1	1
B. granulosus	2	1	0	0	2	0	1	0	1	0	1	1	0	0	0	1	1	?	0	0	0	0	2	1	1
B. mirandaribeiroi	2	1	0	0	2	0	1	0	1	0	1	2	0	0	0	1	1	?	0	0	0	0	2	1	1
B. guttatus group																									
B. blombergi	0	0	0	1	2	0	2	1	1	1	0	1	0	0	1	0	0	1	0	0	2	0	2	1	1
B. caeruleostictus	0	0	0	0	2	0	2	1	1	1	0	1	0	0	1	0	0	0	0	0	2	0	1	1	1
B. guttatus	0	0	0	0	2	0	2	1	1	1	0	0	0	0	1	0	0	0	0	0	2	0	2	1	1
B. haematiticus	0	0	0	0	2	0	2	1	1	1	0	0	0	0	1	0	0	1	0	0	2	0	2	1	1
B. nasicus	?	?	?	?	?	?	?	?	?	?	?	?	?	?	?	?	?	?	0	?	2	0	?	1	1
B. margaritifer group																									
B. margaritifer 1	2	0	0	1	1	0	0	1	1	0	1	1	1	0	1	0	0	2	0	0	0	0	2	1	0
B. margaritifer 2	2	0	0	1	1	0	0	1	1	0	1	1	1	0	1	0	0	0	0	0	0	0	2	1	1
B. marinus group																									
B. arenarum	0	1	0	0	2	1	2	1	0	0	1	?	0	0	0	0	0	1	0	0	0	0	0	1	1
B. marinus	0	1	0	0	2	1	2	1	0	0	1	1	0	0	0	0	0	1	0	0	0	0	2	1	1
B. poeppigii	0	1	0	0	2	1	2	1	0	0	1	1	0	0	0	0	0	1	0	0	0	0	2	1	1
B. scheideri	0	1	0	0	2	1	2	1	0	0	1	1	0	0	0	0	0	1	0	0	0	0	0	1	1
B. spinulosus group																									
B. amabilis	0	0	0	0	1	0	2	1	1	0	1	0	0	2	0	0	0	0	0	0	0	0	2	1	0
B. arequipensis	1	0	0	0	1	0	2	1	1	0	1	0	0	0	0	0	0	0	0	0	0	0	2	1	0
B. atacamensis	0	0	0	0	1	0	2	1	1	0	1	0	0	0	0	0	0	0	0	0	0	0	2	1	0
B. chilensis	0	0	0	0	1	0	2	0	1	0	1	0	0	0	0	0	0	1	0	0	0	0	0	1	0
B. cophotis	1	0	0	1	1	0	1	1	1	0	1	1	0	0	1	0	0	0	0	0	1	0	2	1	0
B. corynetes	0	0	0	1	1	0	1	0	1	0	1	1	0	1	1	0	0	3	0	0	1	1	2	1	0
B. limensis	0	0	0	0	1	0	2	1	1	0	1	0	0	0	0	0	0	1	0	0	0	0	2	1	1
B. rubropunctatus	0	0	0	0	1	0	2	0	1	0	1	0	0	0	0	0	0	3	0	0	0	0	1	0	0
B. spinulosus	0	0	0	0	1	0	2	1	1	0	1	0	0	2	0	0	0	0	0	0	0	0	2	1	0
B. variegatus	0	0	0	0	1	0	2	0	1	0	1	1	1	0	1	0	0	3	0	0	1	0	2	1	0
B. vellardi	0	0	0	1	1	0	2	1	1	0	1	0	0	2	1	0	0	0	0	0	0	0	2	1	0
B. veraguensis group																									
B. veraguensis	0	0	0	1	1	0	0	0	2	0	1	2	1	1	1	0	0	1	0	0	0	0	2	1	1
B. chavin	1	1	0	1	1	0	0	0	2	0	1	1	1	1	1	0	0	1	0	0	0	0	0	1	1
B. sp.	1	1	0	1	1	0	0	0	2	0	1	1	1	1	1	0	0	1	0	0	0	0	0	0	1

Table 2. *Continued*

Taxon	51	52	53	54	55	56	57	58	59	60	61	62	63	64	65	66	67	68	69	70	71	72	73	74	75
Outgroups																									
Leptodactylus	0	0	0	0	0	2	0	0	0	0	0	?	0	0	0	0	0	0	0	0	0	0	0	?	0
Melanophryniscus	0	2	1	1	2	0	0	1	0	1	0	2	0	0	0	0	0	0	0	0	0	0	0	1	2
Non-*Bufo* bufonids																									
Osornophryne	1	2	?	1	2	0	0	1	0	1	0	2	1	0	0	0	0	0	0	0	0	0	0	0	?
Pedostibes	0	0	0	1	1	1	0	1	0	1	1	2	1	0	0	0	0	0	1	0	0	1	?	1	?
Schismaderma	1	0	0	1	1	0	0	1	0	1	1	0	0	0	0	0	0	0	1	0	0	0	0	2	0
Truebella skoptes	1	2	1	1	2	0	1	1	0	1	0	2	0	0	0	0	0	0	0	0	0	0	0	0	?
Truebella tothastes	1	2	1	1	2	0	1	1	0	1	0	2	0	0	0	0	0	0	0	0	0	0	0	1	?
North America																									
B. americanus	0	2	1	0	1	1	0	0	0	1	0	0	1	2	1	0	0	2	1	1	1	0	1	2	0
B. alvarius	0	2	1	0	1	1	1	1	0	1	0	0	1	0	1	0	0	1	1	1	0	1	2	2	1
B. boreas	0	2	1	0	1	1	1	0	0	1	0	0	1	0	1	0	0	0	0	2	0	0	1	2	0
B. cognatus	0	2	1	0	1	1	0	1	0	1	0	0	0	2	1	1	0	2	0	1	1	0	2	2	1
B. debilis	1	2	1	0	1	0	0	1	0	1	0	2	1	0	0	0	1	1	1	0	0	0	2	2	0
B. exsul	1	2	1	0	1	1	0	0	0	1	0	0	0	0	0	0	0	0	0	2	0	0	2	2	?
B. fowleri	0	1	0	0	1	1	0	0	0	1	0	0	?	?	?	?	?	2	?	1	0	0	?	?	0
B. punctatus	0	2	1	0	1	0	0	1	0	1	0	0	1	0	1	0	1	1	1	0	0	0	2	2	1
B. quercicus	1	2	1	0	1	0	1	0	0	1	0	2	1	2	0	0	0	2	1	0	1	0	2	2	1
B. terrestris	0	1	1	0	1	1	0	0	0	1	0	0	1	2	1	1	1	2	1	1	1	1	1	2	0
B. woodhousii	0	2	1	0	1	1	0	0	0	1	0	0	1	2	1	1	0	2	1	1	1	0	1	2	0
Central America																									
B. coccifer	0	2	1	0	1	1	1	0	0	1	0	0	1	3	1	1	1	1	1	0	0	1	2	2	1
B. conifer	1	2	1	0	1	1	1	0	0	1	1	2	1	3	1	1	1	1	1	0	0	1	2	2	1
B. luetkenii	0	2	1	0	1	1	1	0	0	1	0	0	1	3	1	1	1	1	1	0	0	1	2	2	1
B. valliceps	0	2	1	0	1	1	1	0	0	0	0	0	1	3	1	1	1	1	1	0	0	1	2	2	0
Eurasia																									
B. asper	0	2	0	1	1	2	0	0	0	1	0	0	1	0	0	0	0	1	1	0	0	1	2	1	0
B. bufo	0	2	1	1	2	1	0	0	0	1	0	0	1	0	0	0	0	0	0	0	0	0	1	2	?
B. juxtasper	0	2	0	1	1	2	1	1	0	1	0	0	1	0	0	0	0	1	1	0	0	1	1	1	0
B. macrotis	1	2	1	1	2	1	1	1	0	1	0	1	1	0	0	0	0	0	0	0	0	0	?	?	1
B. melanostictus	0	2	1	1	1	0	1	1	0	1	0	0	1	0	1	1	1	1	1	0	0	1	1	2	1
B. viridis	1	2	1	1	2	0	0	0	0	1	0	0	0	0	0	0	0	0	0	0	0	0	1	2	1
Africa																									
B. maculatus	1	2	1	1	1	1	1	1	0	1	0	0	?	0	?	?	?	?	?	?	0	0	1	2	0
B. pardalis	1	2	1	1	1	1	1	0	0	1	0	0	1	0	0	0	0	0	0	0	0	0	1	2	0
B. regularis	1	2	1	1	1	1	1	0	0	1	0	0	1	0	0	0	0	0	0	0	0	0	1	2	0
B. xeros	1	2	1	1	1	1	1	0	0	1	0	?	1	?	0	0	?	?	?	0	0	0	?	2	0
West Indies																									
B. lemur	1	2	?	0	1	1	0	0	0	1	1	1	1	1	1	1	1	1	1	0	0	1	2	2	?
South America																									
B. crucifer	0	1	1	1	1	1	1	1	0	1	0	0	1	1	1	0	0	1	1	0	0	1	2	2	0
B. ocellatus	?	?	?	?	1	?	?	?	1	1	1	1	1	0	0	0	1	1	?	0	1	1	2	?	?
B. granulosus group																									
B. goeldi	1	2	1	0	0	1	1	1	1	1	0	2	1	1	1	1	1	1	1	0	0	1	2	2	0
B. humboldti	1	2	1	0	0	1	1	1	1	1	0	?	1	1	1	1	1	1	1	0	0	1	2	2	0
B. granulosus	1	2	1	0	0	1	1	1	1	1	0	0/2	1	1	1	1	1	1	1	0	0	1	2	2	0
B. mirandaribeiroi	1	2	1	0	0	1	1	1	1	1	0	2	1	1	1	1	1	1	1	0	0	1	2	?	?
B. guttatus group																									
B. blombergi	0	1	1	0	1	1	1	1	0	0	0	0	1	1	0	0	0	1	1	0	0	1	2	1	?
B. caeruleostictus	0	1	1	0	1	1	1	1	0	0	0	0	1	1	0	0	0	1	1	0	0	1	2	1	1
B. guttatus	0	1	1	0	1	1	1	1	0	0	0	0	1	1	0	0	0	1	1	0	0	1	2	1	?
B. haematiticus	0	2	0	0	0	1	1	1	0	0	0	0	1	1	0	0	0	1	1	0	0	1	2	1	1

Table 2. *Continued*

Taxon	51	52	53	54	55	56	57	58	59	60	61	62	63	64	65	66	67	68	69	70	71	72	73	74	75
B. nasicus	?	1	?	?	?	1	?	?	?	0	0	0	?	0	?	?	?	?	?	?	?	1	2	1	?
B. margaritifer group																									
B. margaritifer 1	0	2	1	1	1	0	1	1	0	1	0	0	1	1	1	0	0	0	1	0	0	1	2	2	0
B. margaritifer 2	0	2	1	1	1	0	1	1	0	1	0	0	1	1	1	0	0	0	1	0	0	1	2	2	0
B. marinus group																									
B. arenarum	0	0	1	0	2	1	1	1	0	1	0	0	1	1	1	1	1	1	1	0	0	1	2	2	0
B. marinus	0	0	1	0	0	1	1	1	0	1	0	0	1	1	1	1	1	1	1	0	0	1	2	2	0
B. poeppigii	0	0	1	0	0	1	1	1	0	1	0	0	1	1	1	1	1	1	1	0	0	1	2	2	0
B. scheideri	0	0	1	0	0	1	1	1	0	1	0	0	1	1	1	1	1	1	1	0	0	1	2	2	0
B. spinulosus group																									
B. arequipensis	1	2	1	0	1	0	1	1	0	1	0	0	1	0	0	0	0	0	1	0	0	0	2	2	0
B. atacamensis	1	1	1	0	1	1	1	0	0	1	0	0	0	0	0	0	0	0	1	0	0	0	2	2	2
B. chilensis	1	1	1	1	2	1	1	1	0	1	0	0	1	0	0	0	0	0	1	0	0	0	2	2	?
B. cophotis	0	2	1	1	2	1	0	1	0	1	0	1	1	0	0	0	0	0	0	0	0	0	3	2	1
B. corynetes	1	2	1	1	2	0	0	1	0	1	0	1	1	0	0	0	0	0	0	0	0	0	3	1	1
B. limensis	0	2	1	0	1	1	1	0	0	1	0	0	1	0	0	0	0	0	1	0	0	0	2	1	2
B. rubropunctatus	0	1	1	0	2	1	0	1	0	1	0	0	1	0	0	0	0	0	1	0	0	0	3	2	?
B. amabilis	0	1	1	0	1	1	1	0	0	1	0	0	0	0	0	0	0	0	1	0	0	0	2	2	0
B. spinulosus	0	2	1	0	1	1	1	1	0	1	0	0	1	0	0	0	0	0	1	0	0	0	2	2	2
B. variegatus	1	2	1	1	2	1	0	1	0	1	0	1	1	0	0	0	0	0	0	0	0	0	3	1	2
B. vellardi	0	1	1	1	1	1	1	1	0	1	0	0	1	0	0	0	0	0	1	0	0	0	2	2	2
B. veraguensis group																									
B. veraguensis	0	2	1	1	1	1	1	0	0	1	0	2	1	2	1	1	1	1	1	0	0	1	2	1	?
B. chavin	0	2	?	?	?	1	?	0	0	1	0	?	?	?	?	?	?	0	?	?	0	1	2	1	?
B. sp.	0	2	?	1	1	1	1	?	0	1	0	?	?	0	?	?	?	0	?	?	?	1	2	?	?

Taxon	76	77	78	79	80	81	82	83
Outgroups								
Leptodactylus	0	0	0	0	0	0	0	0
Melanophryniscus	1	0	0	1	0	0	0	0
Non-*Bufo* bufonids								
Osornophryne	1	1	0	0	0	1	0	0
Pedostibes	1	?	0	0	0	?	0	0
Schismaderma	0	0	0	1	1	1	0	0
Truebella skoptes	1	0	1	1	0	0	0	0
Truebella tothastes	1	0	1	1	0	0	0	0
North America								
B. americanus	0	0	0	0/1	0	0	0	0
B. alvarius	0	0	0	1	0	0	1	0
B. boreas	0	0	0	1	0	0	0	0
B. cognatus	0	0	0	1	0	0	0	0
B. debilis	0	0	0	1	0	0	0	0
B. exsul	0	0	0	1	0	0	0	0
B. fowleri	0	0	0	?	0	0	0	0
B. punctatus	0	0	0	1	0	0	0	0
B. quercicus	0	0	0	1	0	0	0	0
B. terrestris	0	0	0	0/1	0	0	0	0
B. woodhousii	0	0	0	0/1	0	0	0	0
Central America								
B. coccifer	0	0	0	1	0	0	0	0
B. coniferus	0	0	0	0	0	1	0	0

Table 2. *Continued*

Taxon	76	77	78	79	80	81	82	83
B. luetkenii	0	0	0	1	0	0	0	0
B. valliceps	0	0	0	0/1	0	1	0	0
Eurasia								
B. bufo	0	0	0	0/1	0	0	0	0
B. asper	0	0	0	0	0	0	0	0
B. juxtasper	0	0	0	0	0	0	0	0
B. macrotis	0	0	0	?	0	0	0	0
B. melanostictus	0	0	0	1	0	0	0	0
B. viridis	0	0	0	1	0	0	0	0
Africa								
B. maculatus	0	0	0	?	0	0	0	0
B. pardalis	0	0	0	0	0	1	0	0
B. regularis	0	0	0	1	0	0	0	0
B. xeros	0	0	0	?	0	?	0	0
West Indies								
B. lemur	0	0	0	1	0	0	0	0
South America								
B. crucifer	0	0	0	0	0	1	0	0
B. ocellatus	0	0	0	0	0	0	0	0
B. granulosus group								
B. goeldi	0	0	0	?	0	0	0	0
B. humboldti	0	0	0	?	0	0	0	0
B. granulosus	0	0	0	1	0	0	0	0
B. mirandaribeiroi	0	0	0	?	0	0	0	0
B. guttatus group								
B. blombergi	0	0	0	0	1	1	0	0
B. caeruleostictus	0	0	0	?	0	1	0	0
B. guttatus	0	0	0	0	1	1	0	0
B. haematiticus	0	0	0	0	1	1	0	0
B. nasicus	0	0	0	?	1	1	0	0
B. margaritifer group								
B. margaritifer 1	0	0	0	0	1	1	0	0
B. margaritifer 2	0	0	0	0	1	1	0	0
B. marinus group								
B. arenarum	0	0	0	1	0	1	0	0
B. marinus	0	0	0	1	0	1	0	0
B. scheideri	0	0	0	0/1	0	1	0	0
B. poeppigii	0	0	0	1	0	0/1	0	0
B. spinulosus group								
B. amabilis	0	0	0	?	0	0	0	0
B. arequipensis	0	0	0	?	0	1	0	0
B. atacamensis	0	0	0	1	0	0	0	0
B. chilensis	0	0	0	1	0	0	0	0
B. cophotis	1	0	0	1	0	0	0	1
B. corynetes	1	1	0	?	0	1	1	1
B. limensis	0	0	0	1	0	1	0	0
B. rubropunctatus	0	0	0	1	0	0	0	0
B. spinulosus	0	0	0	1	0	0	0	0
B. variegatus	1	0	0	?	0	1	0	0
B. vellardi	0	0	0	1	0	1	0	0
B. veraguensis group								
B. veraguensis	1	0	0	?	0	0	0	0
B. chavin	?	0	0	?	0	?	0	0
B. sp.	?	0	0	1	0	?	0	0

greater were considered well supported (Alfaro, Zoller & Lutzoni, 2003).

Molecular data and analysis

Because estimates of divergence times for *Bufo* vary considerably, genes with disparate rates of evolutionary change were sequenced to target a wide range of signal. Recently, investigators have begun to include more slowly evolving nuclear genes with mtDNA data to resolve deep and shallow divergences within Anura and to incorporate independently evolving molecular markers (e.g. Hillis, 1987; Pennington, 1996). For this study, regions of the 12S–16S mitochondrial genome were sequenced to give a signal at intermediate and recent levels of divergence. The 12S–16S fragment was obtained with several sets of overlapping primers used previously for *Bufo* (Goebel, Donnelly & Atz, 1999; Pramuk *et al.*, 2001) or modified from published primers. Portions of the nuclear proopiomelanocortin-A gene (POMC) and the recombination-activating gene 1 (Rag-1) were sequenced in order to provide a signal at deeper levels of divergence and were selected based on their proven phylogenetic utility for other groups of vertebrates. POMC and Rag-1 are single-copy nuclear genes proven useful for resolving deeper evolutionary relationships among jawed vertebrates (Venkatesh, Erdmann & Brenner, 2001), as well as amphibians (POMC: Alrubaian *et al.*, 2002; Wiens *et al.*, 2005b; Rag-1: Hoegg *et al.*, 2004; Wiens *et al.*, 2005a). POMC and Rag-1 primers were used directly or modified from those used previously for anurans (Wiens *et al.*, 2005b, Hoegg *et al.*, 2004, respectively). All primers used in this study are listed in Table 3.

In total, data for samples were sequenced from 89 specimens, but with fewer (77) individuals sequenced for the Rag-1 data set. To verify sequence identity, multiple individuals were sequenced for some polytypic and geographically widespread species (e.g. members of the *B. margaritifer* group). Previously published data for the 12S–16S fragment (Pauly *et al.*, 2004) were used for the outgroups *Ceratophrys cornuta*, *Eleutherodactylus w-nigrum*, and *Hyla cinerea* (AY326014, AY326004, AY680271, respectively). In addition, published data for POMC (Wiens *et al.*, 2005b) were used for *Ceratophrys cornuta* (AY819091) and *Hyla cinerea* (AY819116). A complete list of voucher specimens, their associated locality data, and GenBank accession numbers can be found in Appendix 2.

Prior to extraction, tissues were stored at –80 °C or fixed in 95–100% EtOH. The DNA was extracted from small amounts (~50 ng) of muscle or liver tissue with the Dneasy Tissue Kit (Qiagen Inc.) and visualized on 1% high-melt agarose gels in TAE buffer. A polymerase chain reaction (PCR) was performed in 50-μL reactions containing 0.5 units of *Taq* polymerase (Fisher), ~1 μg of genomic DNA, 10 pmol of each primer, 15 nmol of each dNTP, 50 nmol of $MgCl_2$, and buffer. Amplification followed published PCR conditions (Palumbi, 1996) and was performed on a Bio-Rad (MyCycler) thermal cycler. Cycle sequencing reactions were completed with Big Dye Sequencing Kits (ABI Inc.). Amplified DNA was purified [with either CleanSEQ magnetic beads (Agencourt) or Sephadex

Table 3. The amplification and sequencing primers used for the continuous 12S–16S region of the mitochondrial genome, and portions of the nuclear genes POMC and Rag-1. Position refers to the location in the *Xenopus* mitochondrial genome. The Goebel number refers to primers listed in Goebel *et al.* (1999: table 3). POMC and Rag-1 primers are from Wiens *et al.* (2005b) and Hoegg *et al.* (2004), respectively. Other primers were modified by the author as indicated

Primer name	Position	Primer sequence (5′→3′)	Goebel
12SZL	2206–2225	AAAGGTTTGGTCCTAGCCTT	35
12H2(R) mod.	2484–2503	GGTATGTAATCCCAGTTTG	N/A
12L6 mod.	2487–2508	ACTGGGATTAGATACCCCACTA	N/A
12SKH	2975–2996	TCCRGTAYRCTTACCDTGTTACGA	70
12Sc(L.)	2834–2853	AAGGCGGATTTAGHAGTAAA	65
16H14(R) mod.	3753–3774	TCTTGTTACTAGTTTTAACAT	85
16L10	3622–3641	AGTGGGCCTAAAAGCAGCCA	82
16H10	4054–4076	TGATTACGCTACCTTCGCACGGT	92
16L9	3956–3976	CGCCTGTTTACCAAAAACAT	88
16H13	4551–4572	CCGGTCTGAACTCAGATCACGTA	96
POMC1	—	GAATGTATYAAAGMMTGCAAGATGGWCCT	—
POMC2	—	TAYTGRCCCTTYTTGTGGGCRTT	—
POMC2B mod.	—	GCATTYTTGAAAAGAGTCATTARTGGAGTCTG	—
RAG-1 MartFl1	—	AGCTGCAGYCARTAYCAYAARATGTA	—
RAG-1 AmpR1	—	AACTCAGCTGCATTKCCAATRTCA	—

columns] and sequencing was performed directly using a Beckman Coulter CEQ 8000 XL (KU) or ABI 3100 [Brigham Young University (BYU)] automated sequencer. The programs SEQUENCHER 3.1.1 (Gene Codes Corp.) and SE-AL (ver. 1.d1; Rambaut, 1996) were used to edit sequences. CLUSTALX (Thompson *et al*., 1997) was employed to perform preliminary alignment using default parameters (gap opening = 15; gap extension = 6.666; delay divergent sequences = 30%; transition:transversion = 50%), with adjustments by eye. Alignment of the protein coding sequences was straightforward and they were translated into amino acids to verify alignment. Although they were relatively uncommon (~1–2%) within nuclear genes, heterozygous bases were coded with IUPAC symbols. Alignment of the 12S–16S ribosomal genes was more complicated. Published secondary structure models of the 16S and 12S genes for *Eleutherodactylus cuneatus* and *Xenopus laevis* (De Rijk *et al*., 1994; Van de Peer *et al*., 1994) were used to discover the secondary structure of the nonprotein coding genes. Alignments of ribosomal DNA were adjusted to agree with known secondary structure, and insertions and deletions were preferentially placed into loop regions rather than stems. Regions of the mtDNA that remained unalignable were deleted from the analyses.

Maximum parsimony (MP), ML, and Bayesian analyses were performed on separate molecular partitions, and were also performed on the combined data sets. Initially, data from each of the three DNA fragments (12S–16S, POMC, Rag-1) and morphology were analysed separately. By comparing nonparametric bootstrap (npb) values and bpp supporting nodes of the resulting trees, and the topologies resulting from the separately analysed data sets, areas of strongly supported incongruence resulting from two or more data subsets were investigated (following Wiens, 1998). Strong support for individual nodes was defined as nodes with bpp = 0.95 (Alfaro *et al.*, 2003) or npb = 70 (Hillis & Bull, 1993; but see their caveats). No strongly supported conflicting relationships were recovered, so all data were combined for all subsequent analyses (Wiens, 1998). MP analyses were performed with PAUP* (ver. 4.0b10; Swofford, 2000) using a heuristic search with 100 random addition sequence replicates and TBR branch swapping. Nodal support for parsimony results was assessed through nonparametric bootstrap analysis with 200 bootstrap pseudoreplicates and ten random taxon addition replicates.

The most appropriate model of gene evolution for the ML (and Bayesian) analysis was estimated through likelihood ratio tests of the entire mitochondrial fragment (12S, $tRNA^{Val}$, and 16S) and separately for each nuclear gene, with MODELTEST ver. 3.06 (Posada & Crandall, 1998). ML analyses were performed on separate and combined data sets. For ML searches of all combined DNA data, MODELTEST selected the best model as GTR + I + G (base frequencies: A: 0.2917; C: 0.2054; G: 0.2226; T: 0.2803; rate matrix: A–C: 0.7394, A–G: 2.3595, A–T: 0.6279, C–G: 0.4620, C–T: 3.3126, G–T: 1.0000; shape parameter for gamma distribution: 1.9537; proportion of invariant sites: 0.4041). ML searches (Felsenstein, 1981) were run using 100 random addition replicates and TBR branch swapping. Confidence in the resulting topology was assessed with npb (Felsenstein, 1985) with 200 bootstrap replicates, and heuristic searches of one random addition with TBR branch swapping per replicate.

The data sets were analysed in combined, mixed-model analyses using MRBAYES 3.04b (Ronquist & Huelsenbeck, 2003). The analysis of combined data utilized four model partitions for the morphological, 12S–16S, POMC, and Rag-1 data sets (see Table 4). To check for congruence on an identical topology, a mini-

Table 4. Major data partitions analysed in this study, their characteristics resulting from maximum parsimony analysis, and the appropriate model selected by MODELTEST (Posada & Crandall, 1998) or via the Bayes factor for morphology (following Nylander *et al*., 2004; Wiens *et al.*, 2005a) and used in separate and combined Bayesian and maximum likelihood (ML) data partitions

Partition (no. taxa)	No. characters (parsimony informative)	No. MP trees	TL	CI	RI	ML model
Morphology (64)	83 (83)	5 077	537	0.245	0.666	Mk
12S–16S mtDNA (89)	2563 (1180)	6	10 618	0.258	0.518	GTR + I + G
POMC (89)	550 (173)	93 200	467	0.504	0.730	GTR + G
RAG-1 (77)	791 (232)	31	697	0.501	0.658	GTR + I + G
All DNA data (89)	3904 (1473)	4	11 104	0.244	0.542	Mixed
All nuclear data (89)	1341 (377)	72	1 189	0.470	0.645	Mixed
All data (89)	3987 (1484)	2	10 588	0.254	0.551	Mixed

CI, consistency index (excluding uninformative characters); G, gamma; Mk, Markov k; MP, most parsimonious; RI, retention index; TL, tree length.

mum of two replicate searches was performed for each separate and combined data set on the BYU BioAg Computational Cluster. Analyses were initiated with random starting trees and each analysis was run for 20×10^6 generations, with four Markov chains employed, the temperature set at 0.4, and with the chain sampled every 1000th generation. The application TRACER (ver. 1.2; Rambaut & Drummond, 2003) was used to view output of the *sump* file generated by MRBAYES. To determine the burn-in, log-likelihood plots were examined for stationarity (where plotted values reach an asymptote). Trees generated prior to reaching stationarity were discarded as burn-in. Most analyses reached stationarity relatively quickly (all reached stationarity after 160 000 generations).

RESULTS

PHYLOGENETIC RELATIONSHIPS

Morphological data

Of the 83 morphological characters employed in this analysis, 15 were unique and unreversed (the characters are described in Appendix 3). The MP analysis of the unordered morphological data yielded 5077 most-parsimonious trees (refer to Table 4 for summaries of tree statistics for all analysed data subsets). The results of the Bayesian analysis of ordered characters were almost identical to the parsimony analysis of unordered characters, whereas the parsimony analysis of ordered data differed in that the clade containing *Truebella*, *Melanophryniscus*, and *Osornophryne* was more derived and nested within *Bufo.* Because all trees converged on a broadly similar topology, I have chosen to focus the discussion on the topology presented in Figure 1 (resulting from the parsimony analysis of unordered characters). The strict consensus tree (Fig. 1) indicates that most groups currently recognized within South American *Bufo* are supported as monophyletic (*B. margaritifer*, *marinus*, *granulosus*, *guttatus*, *valliceps*, and *veraguensis* groups), with the exception of the *B. spinulosus* group, which comprises several separate lineages. The smaller species currently assigned to this group (*B. cophotis*, *B. corynetes*, and *B. variegatus*) are supported (bpp = 98) as a basal clade within *Bufo*. Other *B. spinulosus* group species (*B. atacamensis*, *B. limensis*, *B. amabilis*, *B. spinulosus*, and *B. vellardi*) fall out in lineages separate from the smaller *B. spinulosus* group species, with *B. exsul* and *B. boreas* (lightly ossified species from western North America) falling out in between them.

All consensus trees resulting from Bayesian and parsimony analyses of the morphology reveal little about the relationships among South American toads. Within the strict consensus tree (Fig. 1), species defined as having 'narrow' skulls are indicated with grey branches (these individuals are defined as having character 72, state 0; see Appendix 3). This topology manifests a pattern in which most 'narrow-skulled' species (e.g. *B. boreas*, *B. bufo*, *B. debilis*, *B. spinulosus*) fall outside of a clade containing mostly 'broad-skulled' species (e.g. *B. granulosus*, *B. guttatus*, *B. marinus*, *B. valliceps*). In some instances, some species (e.g. ((*B. boreas* + *B. exsul*) *B. spinulosus*)) having disparate geographical distributions are weakly supported as sharing a recent common ancestor. A close relationship between these groups is not supported by molecular data, and a shared history, as indicated by the morphology, is an artefact resulting from convergence on and characters correlated with, a lightly ossified skull.

Molecular and combined data

DNA sequence data were obtained for 2563 aligned bases of the continuous 12S–16S mitochondrial RNA gene region, including the intervening $tRNA^{Val}$, in addition to 550 bases of POMC and 791 bp of Rag-1, for a total of 3987 bp. For the final alignment of the mtDNA sequences, positional homology was ambiguous for seven regions totalling 91 bases, and they were excluded from the analysis.

The results of MP, ML, and Bayesian analyses of all molecular data subsets were broadly congruent; only a few of the deeper nodes with poor support in the data subsets changed position among analyses and are discussed herein. Because the resulting MP, ML, and Bayesian topologies were very similar and Bayesian analysis is the only method that allows for the combination of mixed models, only the latter results are presented and discussed in detail.

Bayesian topologies of the mtDNA (12S–16S) and nuclear (POMC and Rag-1) data subsets are shown in Figures 2 and 3, respectively. The two topologies are broadly congruent, with differences only occurring in some of the poorly supported clades. One major difference between the analyses of these subsets is the position of the North American clade (monophyletic in both trees, with bpp = 1.0), which in the mtDNA tree (Fig. 2), is unresolved with the Central and South American clades. In contrast, the nuclear data place the North American clade as sister to the Central American clade (bpp = 0.89). In the tree derived from the nuclear data, the NA + CA clade is recovered as the sister group to a weakly supported clade containing Eurasian, African, and South American taxa (although this relationship is poorly supported: bpp = 0.73; Fig. 3).

Bayesian analysis of combined DNA and DNA + morphology yielded consensus trees (50% majority rule) broadly congruent with those resulting from MP and ML analyses. In the following discussion

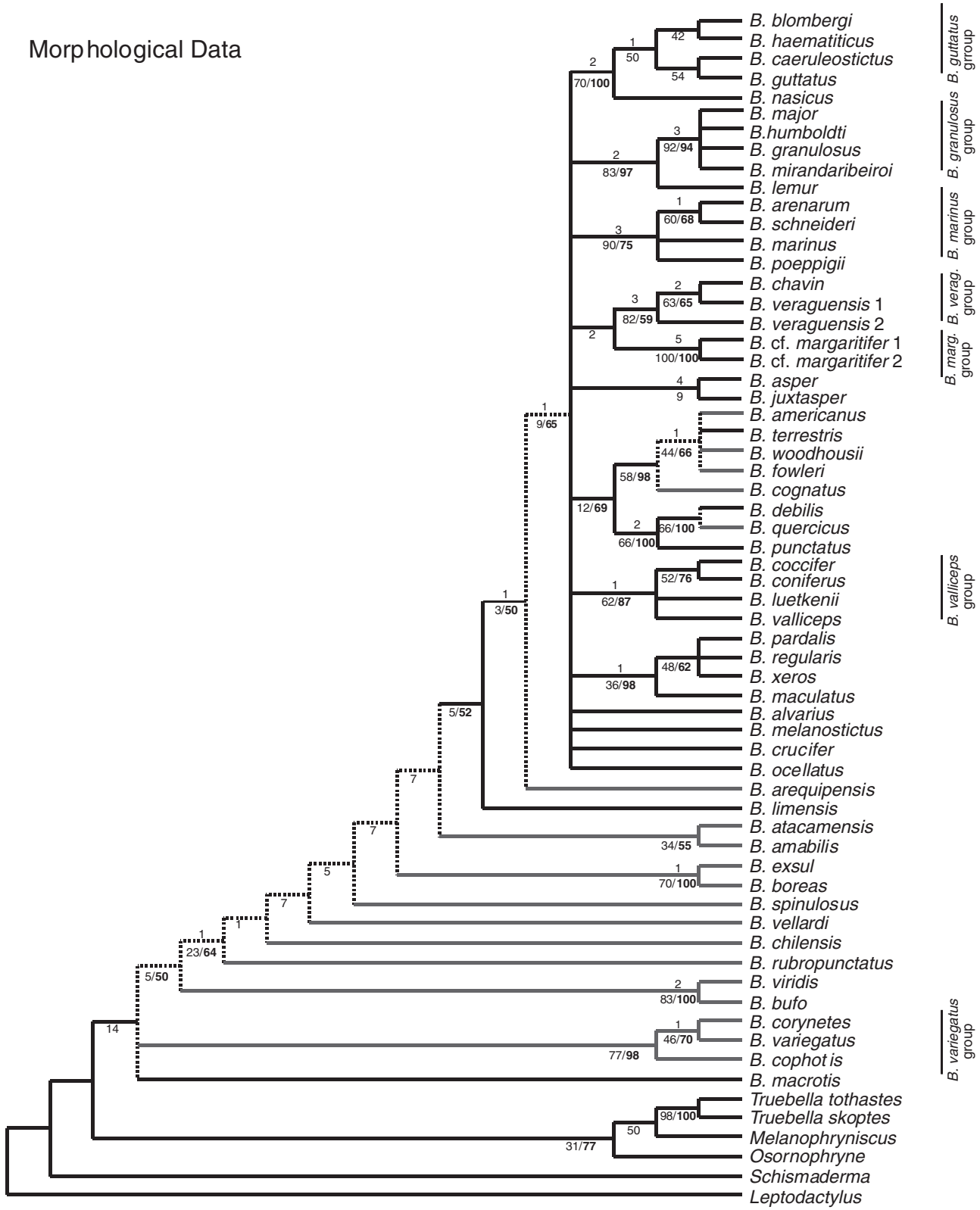
Morphological Data
B. blombergi
B. haematiticus
B. caeruleostictus
B. guttatus
B. nasicus
B. major
B.humboldti
B. granulosus
B. mirandaribeiroi
B. lemur
B. arenarum
B. schneideri
B. marinus
B. poeppigii
B. chavin
B. veraguensis 1
B. veraguensis 2
B. cf. margaritifer 1
B. cf. margaritifer 2
B. asper
B. juxtasper
B. americanus
B. terrestris
B. woodhousii
B. fowleri
B. cognatus
B. debilis
B. quercicus
B. punctatus
B. coccifer
B. coniferus
B. luetkenii
B. valliceps
B. pardalis
B. regularis
B. xeros
B. maculatus
B. alvarius
B. melanostictus
B. crucifer
B. ocellatus
B. arequipensis
B. limensis
B. atacamensis
B. amabilis
B. exsul
B. boreas
B. spinulosus
B. vellardi
B. chilensis
B. rubropunctatus
B. viridis
B. bufo
B. corynetes
B. variegatus
B. cophotis
B. macrotis
Truebella tothastes
Truebella skoptes
Melanophryniscus
Osornophryne
Schismaderma
Leptodactylus
B. guttatus group
B. granulosus group
B. marinus group
B. verag. group
B. marg. group
B. valliceps group
B. variegatus group

Figure 1. Strict consensus of 5077 most-parsimonious trees resulting from the analysis of morphological data alone (64 taxa) with all characters unordered and equally weighted (tree length = 537; consistency index = 0.245; retention index = 0.666). Bremer (1988, 1994) support values are presented above the branches. Bootstrap values and Bayesian posterior probabilities are shown below the nodes (the latter are in bold). The skull (frontoparietal) type of each clade is indicated as follows: black line, 'broad skull'; grey line, 'narrow skull'; dashed line, equivocal.

of phylogenetic relationships, refer to the labelled clades in Figure 4. In the Bayesian topology resulting from the analysis of all data, relationships within New World *Bufo* are fully resolved, with bpp values for most nodes = 0.95 (Fig. 4). This topology recovers a large, strongly supported South American clade (bpp = 1.0) as sister to the well-supported (North + Central American) clade (bpp = 1.0); together, these groups comprise a large New World clade (bpp = 1.0). Within this deeply nested group of South American *Bufo*, a clade containing the monophyletic *B. margaritifer* group (clade 1, Fig. 4) and *B. ocellatus* are sister to the clade containing *Rhamphophryne*, *B. chavin*, and *B. nesiotes* (clade 2; the latter two are assigned to the *B. veraguensis* group); sister to this clade is a lineage containing the remaining species in the *B. veraguensis* group included in this analysis (clade 3; *B. veraguensis* 1 + 2 and *B. amboroensis*). Part of the '*B. spinulosus* group' is weakly supported (clade 4; bpp = 0.91) as the sister to the *B. margaritifer* + '*B. veraguensis*' groups.

The *B. marinus* group is weakly supported as monophyletic (clade 5; bpp = 0.91) with *B. crucifer* at its base (bpp = 1.0); the sister to this clade is the monophyletic *B. granulosus* group (clade 6; bpp = 1.0). All of the above-mentioned monophyletic groups form a lineage referred to herein as the 'derived' South American clade (to distinguish it from other, more basal South American *Bufo*). In all analyses of all combined data, Eurasian species (clades 9, 10, and 12) are paraphyletic with two lineages falling out as sequential sister groups to the New World clade (bpp = 0.64 and .97).

PHYLOGENY, CRANIAL MORPHOLOGY, AND DIAGNOSTIC SYNAPOMORPHIES OF SOUTH AMERICAN SPECIES GROUPS OF *BUFO*

The results of this study indicate that the current taxonomy of South American *Bufo*, for the most part, accurately reflects the evolutionary history of the group. The results of all analyses support the monophyly of: (1) five lineages of 'South American' toads (as defined by Duellman & Schulte, 1992: the *B. granulosus*, *B. guttatus*, *B. margaritifer*, *B. marinus*, and *B. valliceps* groups); and (2) the Central and North American lineages. Most of the species groups of South American *Bufo* have at least one unique and unreversed morphological synapomorphy that can be used to assist in their diagnosis; these characters are discussed below. The nonmonophyletic groups are the *B. veraguensis* and *spinulosus* groups, with the former being monophyletic only in the morphological analysis and the latter polyphyletic in all analyses. Additional taxon sampling of the '*B. veraguensis* group' will be required to ascertain how many lineages are contained in this polyphyletic taxon. Terms for cranial characters follow Trueb (1993), and for convenience are shown in Figure 5. Dorsal (Fig. 6), ventral (Fig. 7), and lateral (Fig. 8) views of the skulls of one representative of each species group are illustrated and characters relating to them are described herein.

Bufo margaritifer group (clade 1)

This group of medium-sized toads has relatively lightly ossified crania with variable amounts of dermal ornamentation. Many have highly developed and dorsally projecting preorbital crests confluent with the postorbital crests; however, this character is highly variable and is also sexually dimorphic, with the crests being more developed in the females of some species (Fig. 8D). The crania of the species examined in this study share the following characters: relatively broad skulls that are wider than long, with the greatest width at the level of the quadratojugals (Fig. 6D); articulation of the nasals laterally with the pars facialis of the maxilla; sphenethmoid covered completely by medial articulation of the nasals and frontoparietals; jaw articulation posterior to the level of the fenestra ovalis; anterior margins of the nasals distinctly acuminate; and a complete temporal arcade (*sensu* Lynch, 1971) is formed by articulation of the frontoparietal and squamosal. The sacral diapophyses of the examined species in this group are not broadly dilated (Fig. 9D). One unique and unreversed synapomorphy supports the monophyly of the *B. margaritifer* group: character 13, expansion of the posterior ramus of the pterygoid (Fig. 8D). Members of this group also share nasals that articulate laterally with the preorbital processes of the maxillae (Fig. 8D); however, this character is also common to members of the *B. peltocephalus* and *B. granulosus* groups.

Bufo ocellatus, a taxon with uncertain affinities that was first assigned to the *B. margaritifer* group (= *margaritifer*; Boulenger, 1882) and later to the

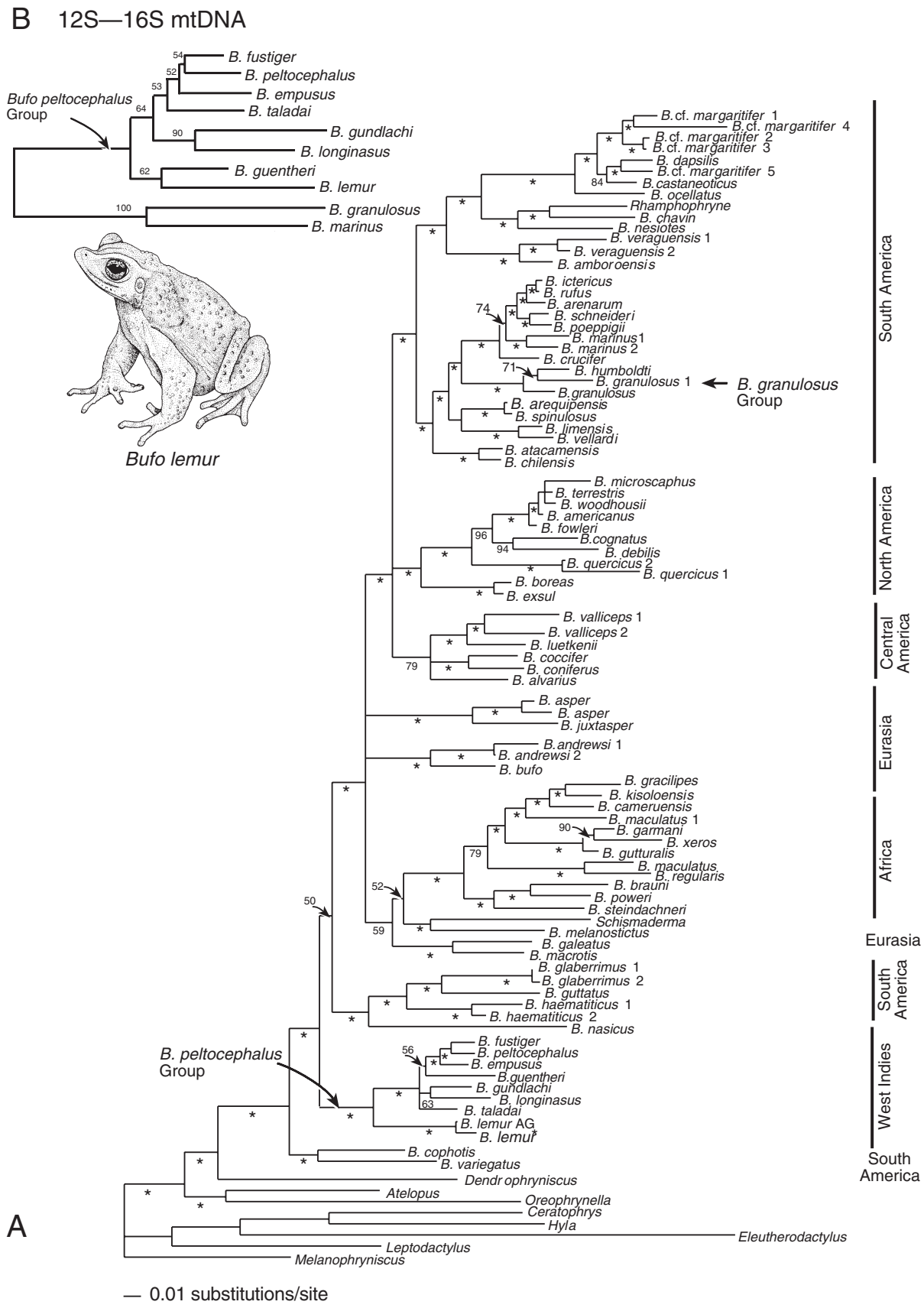
B 12S—16S mtDNA
Bufo peltocephalus Group
B. fustiger
B. peltocephalus
B. empusus
B. taladai
B. gundlachi
B. longinasus
B. guentheri
B. lemur
B. granulosus
B. marinus
Bufo lemur
B. cf. margaritifer 1
B. cf. margaritifer 4
B. cf. margaritifer 2
B. cf. margaritifer 3
B. dapsilis
B. cf. margaritifer 5
B. castaneoticus
B. ocellatus
Rhamphophryne
B. chavin
B. nesiotes
B. veraguensis 1
B. veraguensis 2
B. amboroensis
B. ictericus
B. rufus
B. arenarum
B. schneideri
B. poeppigii
B. marinus 1
B. marinus 2
B. crucifer
B. humboldti
B. granulosus 1
B. granulosus
B. arequipensis
B. spinulosus
B. limensis
B. vellardi
B. atacamensis
B. chilensis
B. granulosus Group
South America
B. microscaphus
B. terrestris
B. woodhousii
B. americanus
B. fowleri
B. cognatus
B. debilis
B. quercicus 2
B. quercicus 1
B. boreas
B. exsul
North America
B. valliceps 1
B. valliceps 2
B. luetkenii
B. coccifer
B. coniferus
B. alvarius
Central America
B. asper
B. asper
B. juxtasper
B. andrewsi 1
B. andrewsi 2
B. bufo
Eurasia
B. gracilipes
B. kisoloensis
B. cameruensis
B. maculatus 1
B. garmani
B. xeros
B. gutturalis
B. maculatus
B. regularis
B. brauni
B. poweri
B. steindachneri
Schismaderma
B. melanostictus
B. galeatus
B. macrotis
Africa
Eurasia
B. glaberrimus 1
B. glaberrimus 2
B. guttatus
B. haematiticus 1
B. haematiticus 2
B. nasicus
South America
B. peltocephalus Group
B. fustiger
B. peltocephalus
B. empusus
B. guentheri
B. gundlachi
B. longinasus
B. taladai
B. lemur AG
B. lemur
West Indies
B. cophotis
B. variegatus
Dendrophryniscus
Atelopus
Oreophrynella
Ceratophrys
Hyla
Eleutherodactylus
Leptodactylus
Melanophryniscus
South America
A
— 0.01 substitutions/site

Figure 2. A, Bayesian consensus tree inferred from 12S–16S mitochondrial DNA data sequenced for this study, combined with 1970 bp of previously published 12S and 16S data (Pramuk *et al.*, 2001) for eight additional individuals of the *Bufo peltocephalus* group; Bayesian posterior probabilities (multiplied by 100) are listed below the branches; values ≥ 97 are indicated with an asterisk. B, neighbour-joining tree inferred from 12S and 16S DNA from Pramuk *et al.* (2001); nonparametric bootstrap values are listed above the branches. *B. lemur* of Puerto Rico is illustrated, showing the unusual elongated snout morphology of West Indian toads. Note the more basal position of the West Indian *B. peltocephalus* group in (A) resulting from the more extensive taxon sampling in this study. **B. lemur* from Pramuk *et al.* (2001); AG, specimen of *B. lemur* sequenced for this study.

B. granulosus group (Leão & Cochran, 1952), is well supported as the sister to the *B. margaritifer* group (bpp = 1.0).

'Bufo veraguensis group' (clades 2 and 3)

These small- to medium-sized toads have moderately to lightly ossified skulls that lack dermal sculpturing. According to Duellman & Schulte (1992), there are no characters uniting members of the *B. veraguensis* group and as such, its monophyly is suspect. The lack of unique and unreversed morphological characters for this group (as it is currently defined) resulting from this study also attests to its nonmonophyly. Because there are few specimens in collections, the morphological analysis included only three individuals representing the ten species currently assigned to it (Table 1). The crania of examined species of this 'group' share the following characters: relatively broad skulls that are wider than long, with the greatest width at the level of the quadratojugals (Fig. 6E); nasals not expanded dorsolaterally; nasal and pars facialis of maxilla not in contact laterally; sphenethmoid visible dorsally and not covered completely by the nasals and frontoparietals; jaw articulation posterior or at the level of the fenestra ovalis; and a complete temporal arcade. The sacral diapophyses of the examined species of this group are relatively broadly dilated (Fig. 9E).

'Bufo spinulosus group' (clades 4 and 15)

Toads assigned to the *B. spinulosus* group are small to medium in size and have moderately to lightly ossified skulls that lack dermal sculpturing and exostosing. The *B. spinulosus* group was previously defined as having narrow frontoparietals and lacking cranial crests (Duellman & Schulte, 1992). Although there are no synapomorphies supporting the monophyly of these toads, there are broad similarities among members currently assigned to it. All members have relatively broad skulls that are wider than long, with the greatest width at the level of the quadratojugals (Fig. 6C, H). The nasals are not expanded dorsoventrally; therefore, the nasal bones and pars facialis of the maxilla are not in contact laterally. All examined species of this 'group' have the sphenethmoid visible dorsally (a consequence of a lightly ossified cranium). The level of jaw articulation is variable; in some species (e.g. *B. cophotis*, Fig. 8H), jaw articulation is anterior to the fenestra ovalis, whereas in others it is posterior (e.g. *B. amabilis*, Fig. 8C). None of the species assigned to this group has a complete temporal arcade. In addition, the shape of the otic ramus of the squamosal is variable: in *B. variegatus*, *B. corynetes*, and *B. chilensis*, the otic ramus is not enlarged, and in the other species assigned to the group it is slightly enlarged and overlaps the prootic laterally.

The basal position of two '*spinulosus*' group species (*B. variegatus* and *B. cophotis*; Fig. 4; clade 15) is not surprising, given that these taxa were formerly assigned to the *B. variegatus* group based on morphological differences (Martin, 1972a). A basal relationship for *B. variegatus* was also reported by Pauly *et al.* (2004). Duellman & Schulte (1992) reassigned these smaller taxa to the *B. spinulosus* group on the basis of their shared lack of cranial crests. Certain cranial characters of these basal species are apparently convergent on the lightly ossified, 'narrow-skulled' morphology of members of the *B. spinulosus* group, and therefore it is not surprising that earlier investigators were misled by the striking convergence of these distantly related taxa. I recommend that *B. cophotis* and *B. variegatus* (clade 15) be reassigned to the *B. variegatus* group. Based on the placement of *B. corynetes* in the morphological analysis (Fig. 1), I tentatively assign it to the *B. variegatus* group as well.

Bufo marinus group (clade 5)

Toads of the *B. marinus* group have extremely well-ossified and exostosed crania that are ornamented with deep striations, pits, and rugosities. The cranium of examined specimens of this group share the following characters: relatively broad skulls that are wider than long, with the greatest width at the level of the quadratojugals (Fig. 5A, B); sphenethmoid covered completely by medial articulation of nasals and

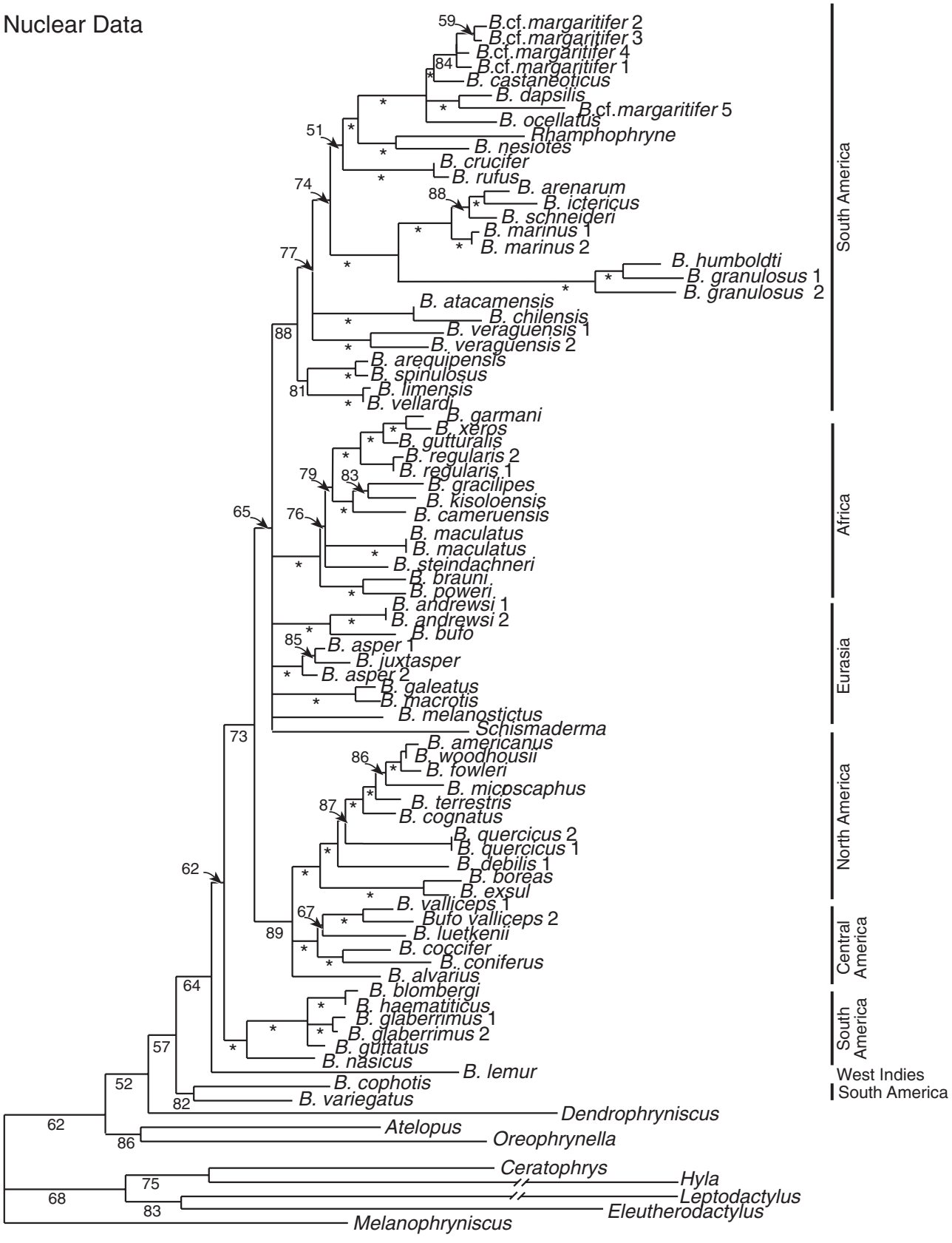
Nuclear Data
B.cf.margaritifer 2
B.cf.margaritifer 3
B.cf.margaritifer 4
B.cf.margaritifer 1
B. castaneoticus
B. dapsilis
B.cf.margaritifer 5
B. ocellatus
Rhamphophryne
B. nesiotes
B. crucifer
B. rufus
B. arenarum
B. ictericus
B. schneideri
B. marinus 1
B. marinus 2
B. humboldti
B. granulosus 1
B. granulosus 2
B. atacamensis
B. chilensis
B. veraguensis 1
B. veraguensis 2
B. arequipensis
B. spinulosus
B. limensis
B. vellardi
B. garmani
B. xeros
B. gutturalis
B. regularis 2
B. regularis 1
B. gracilipes
B. kisoloensis
B. cameruensis
B. maculatus
B. maculatus
B. steindachneri
B. brauni
B. poweri
B. andrewsi 1
B. andrewsi 2
B. bufo
B. asper 1
B. juxtasper
B. asper 2
B. galeatus
B. macrotis
B. melanostictus
Schismaderma
B. americanus
B. woodhousii
B. fowleri
B. microscaphus
B. terrestris
B. cognatus
B. quercicus 2
B. quercicus 1
B. debilis 1
B. boreas
B. exsul
B. valliceps 1
Bufo valliceps 2
B. luetkenii
B. coccifer
B. coniferus
B. alvarius
B. blombergi
B. haematiticus
B. glaberrimus 1
B. glaberrimus 2
B. guttatus
B. nasicus
B. lemur
B. cophotis
B. variegatus
Dendrophryniscus
Atelopus
Oreophrynella
Ceratophrys
Hyla
Leptodactylus
Eleutherodactylus
Melanophryniscus
South America
Africa
Eurasia
North America
Central America
South America
West Indies
South America
0.005 substitutions/site

Figure 3. The consensus tree resulting from Bayesian analysis of the combined nuclear (POMC + Rag-1) data. This analysis employed a mixed model for the two nuclear genes (GTR + G and GTR + I + G for the POMC and Rag-1 data sets, respectively). Bayesian posterior probabilities (multiplied by 100) are shown below the branches; values ≥ 97 are indicated with an asterisk.

frontoparietals; nasals not expanded dorsolaterally (as they are in *B. granulosus*), and forming a nearly transverse suture with the frontoparietals; jaw articulation lies posterior to the level of the fenestra ovalis; and a complete temporal arcade. The *B. marinus* group is distinctive among all *Bufo* examined in sharing the following unique and unreversed synapomorphy: character 31, the point of articulation between the medial ramus of the pterygoid and parasphenoid alae formed by a jagged or 'scalloped' suture. The sacral diapophyses of members of this group are not expanded (Fig. 9C) and are more cylindrical than most species of *Bufo* examined. In addition, the anterior edge of the sacral diapophyses is angled posterolaterally to the longitudinal axis of the vertebrae. Species assigned to this group have distinctively large parotoid glands.

The *B. marinus* group is monophyletic in all analyses. Cei (1972) proposed that this group is closely related to members of the Central American *B. valliceps* group (contained within clade 8); however, this was not supported by the analyses in which the *B. marinus* group (+ *B. crucifer*) is sister to the *B. granulosus* group (clades 5 and 6, respectively). A close relationship between *B. crucifer* and the *B. marinus* lineage has been proposed previously based on overall similarity (Cei, 1972) and mtDNA data (Pauly *et al.*, 2004).

Bufo crucifer group (sister to clade 5)

The skull of *B. crucifer* is heavily ossified, broadly rounded anteriorly, and wider than long, with the greatest width at the level of the quadratojugals (Fig. 6A). The articulation between the squamosal and frontoparietal over the crista parotica forms a complete temporal arcade. The sphenethmoid of one specimen (KU 93112; Fig. 6A) is visible dorsally. Overall, the skull of *B. crucifer* most resembles the skulls of members of the *B. marinus* lineage (e.g. *B. arenarum*, *B. ictericus*, *B. marinus*, *B. schneideri*, *B. poeppigii*, and *B. rufus*); among the similar features are the relatively heavy ossification, the full complement of cranial crests, and the broad overlap of the medial ramus of the pterygoid with the parasphenoid alae. However, these characters are not synapomorphies defining the *B. crucifer* + *B. marinus* groups, as they are shared by other clades of South American *Bufo* (e.g. the *B. granulosus* group).

Bufo granulosus group (clade 6)

Toads in this group are of small to medium size and have heavily ossified crania that are exostosed and display heavy dermal ornamentation (Fig. 6B). The crania are distinctive among species of South American *Bufo* because they have a 'closed orbit' (Martin, 1972a) with a complete margin of the orbit being formed by the articulation of the zygomatic ramus of the squamosal with the dorsal surface of the maxilla and the confluence of the preorbital and suborbital crests. The crania of examined species of this lineage share the following characters: relatively broad skulls that are wider than long, with the greatest width at the level of the quadratojugals (Fig. 6B); posterolaterally expanded nasals; lateral articulation of the nasal and pars facialis of the maxilla; dorsal sphenethmoid covered completely by medial articulation of the nasals and frontoparietals; jaw articulation anterior to the level of the fenestra ovalis (Fig. 8B); and a complete temporal arcade. The sacral diapophyses are broadly dilated (Fig. 9B). The monophyly of the *B. granulosus* group is supported by two unique and unreversed synapomorphies: character 59, the presence of an expanded, 'flag-shaped' dorsal crest of the ilium in lateral view (Fig. 10C); character 42, the presence of prenasal bones (Fig. 6B; Pramuk, 2000). All analyses of DNA and combined data support the *B. marinus* group + *B. crucifer* as sister to the *B. granulosus* group.

North American taxa (clade 7)

Analyses of combined data place the North American clade (clade 7) as sister to the Central American clade (clade 8); these clades together form the sister group to the 'derived' South American lineage. Relationships within the North American clade are consistent for the most part with prior hypotheses inferred from ND1, tRNA, and 16S mtDNA (Masta *et al.*, 2002) and from 12S–16S mtDNA data (Pauly *et al.*, 2004): ((((*B. americanus* + *B. woodhousii*) (*B. terrestris* + *B. fowleri*)) *B. microscaphus*) *B. cognatus*). One exception resulting from the present study is the position of *B. fowleri*, which is sister to *B. americanus* rather than *B. terrestris*. This unexpected relationship may indicate that the sample included in the present study (USNM 314864) is a hybrid. This specimen was collected from the northern half of Mississippi, where *B. americanus* is known to occur. However, upon examination of the voucher specimen, and with the aid

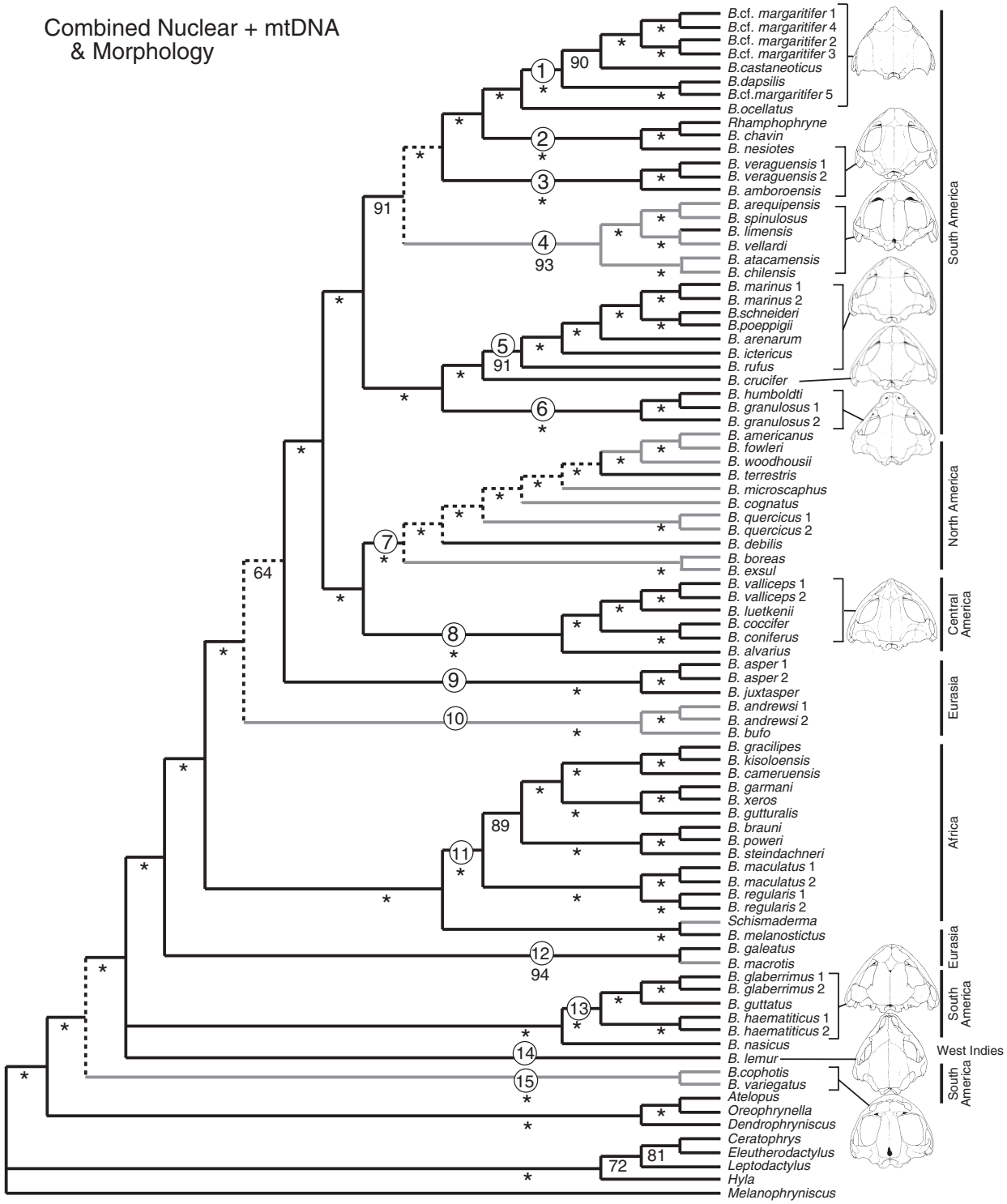

Figure 4. Bayesian topology inferred from the combined molecular and morphological data, analysed with the following maximum likelihood (ML) models: GTR + I + G (mitochondrial DNA + Rag-1), GTR + G (POMC), and Markov k (Mk; morphology). Bayesian posterior probabilities (multiplied by 100) are listed below the branches (values ≥ 97 are indicated with an asterisk). The skull (frontoparietal) type of each clade is indicated as follows: black line, 'broad skull'; grey line, 'narrow skull'; dashed line, equivocal. To give an indication of the variation in skull width and shape within *Bufo*, the skull of one representative of each South American species group (and *B. lemur* from the West Indies), is illustrated to the right of its respective clade.

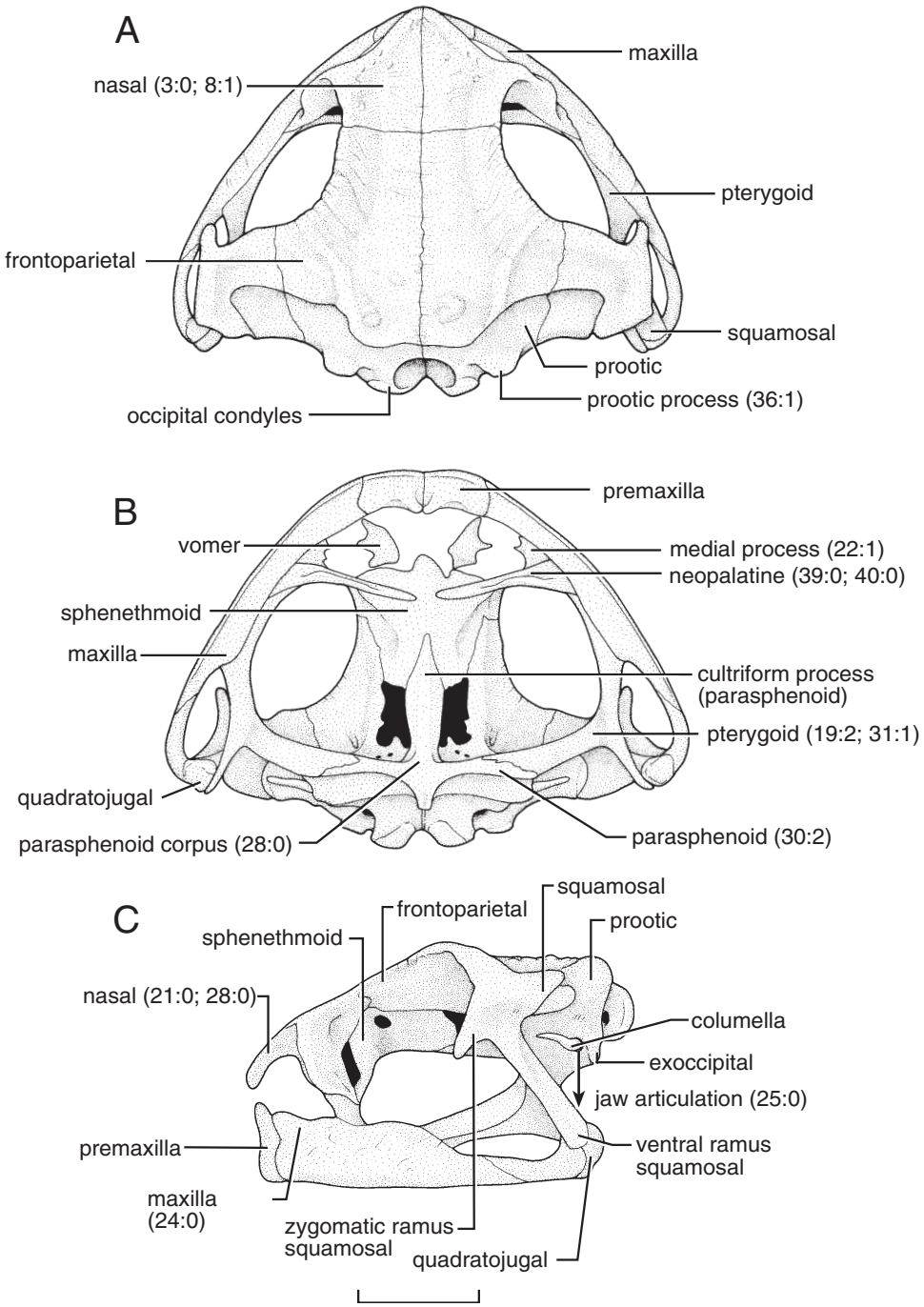

Figure 5. Skull of *Bufo marinus* (KU 152914) in (A) dorsal, (B) ventral, and (C) lateral aspects, illustrating cranial elements described in the text and used in the phylogenetic analyses. The numbers identify characters (and their assigned states) that are described in the text. Scale bar = 1 cm.

of a dichotomous key (Powell, Collins & Hooper, 1998), it was identified as *B. fowleri* with no external evidence indicating a hybrid origin. However, *B. fowleri* has been reported to hybridize with other species of North American *Bufo*, including *B. americanus* (Masta *et al*., 2002; Green & Parent, 2003).

Central American lineage (clade 8)

Although the *B. valliceps* group has been referred to as a 'South American species group' (*sensu* Duellman & Schulte, 1992) throughout this study, my results confirm earlier findings (Mulcahy & Mendelson, 2000; Pauly *et al.*, 2004) suggesting that this group is

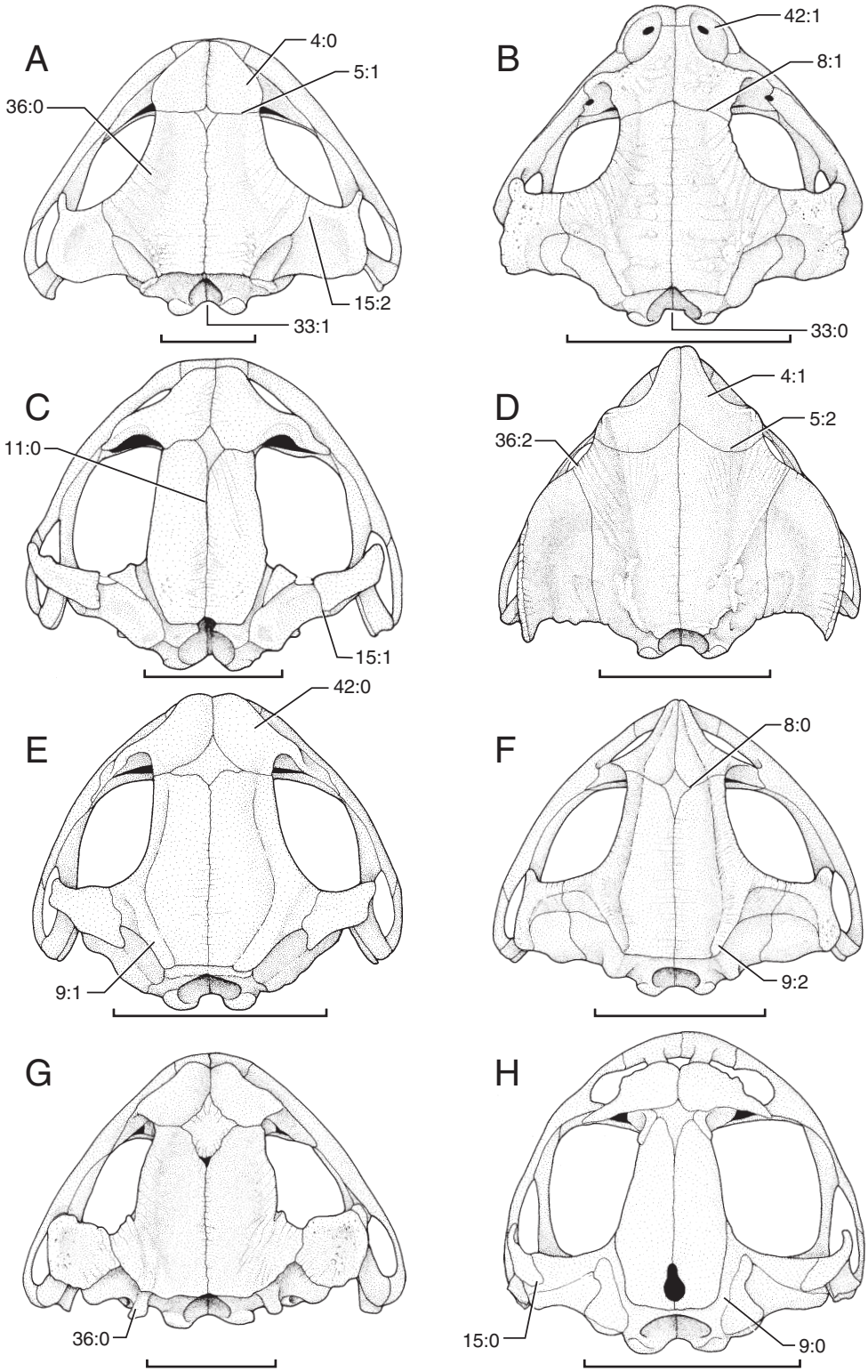

Figure 6. Dorsal aspect of the skulls of representative South American *Bufo*. A, *B. crucifer* (KU 93112). B, *B. granulosus* (*B. granulosus* group; KU 170090). C, *B. amabilis* (*B. spinulosus* group; KU 124587). D, *B. margaritifer* (*B. margaritifer* group; KU 152057). E, *B. veraguensis* (*B. veraguensis* group; KU 164084). F, *B. valliceps* (*B. valliceps* group; KU 59873). G, *B. caeruleostictus* (*B. guttatus* group; KU 152057). H, *B. cophotis* (*B. variegatus* group; KU 218525). Scale bars = 1 cm.

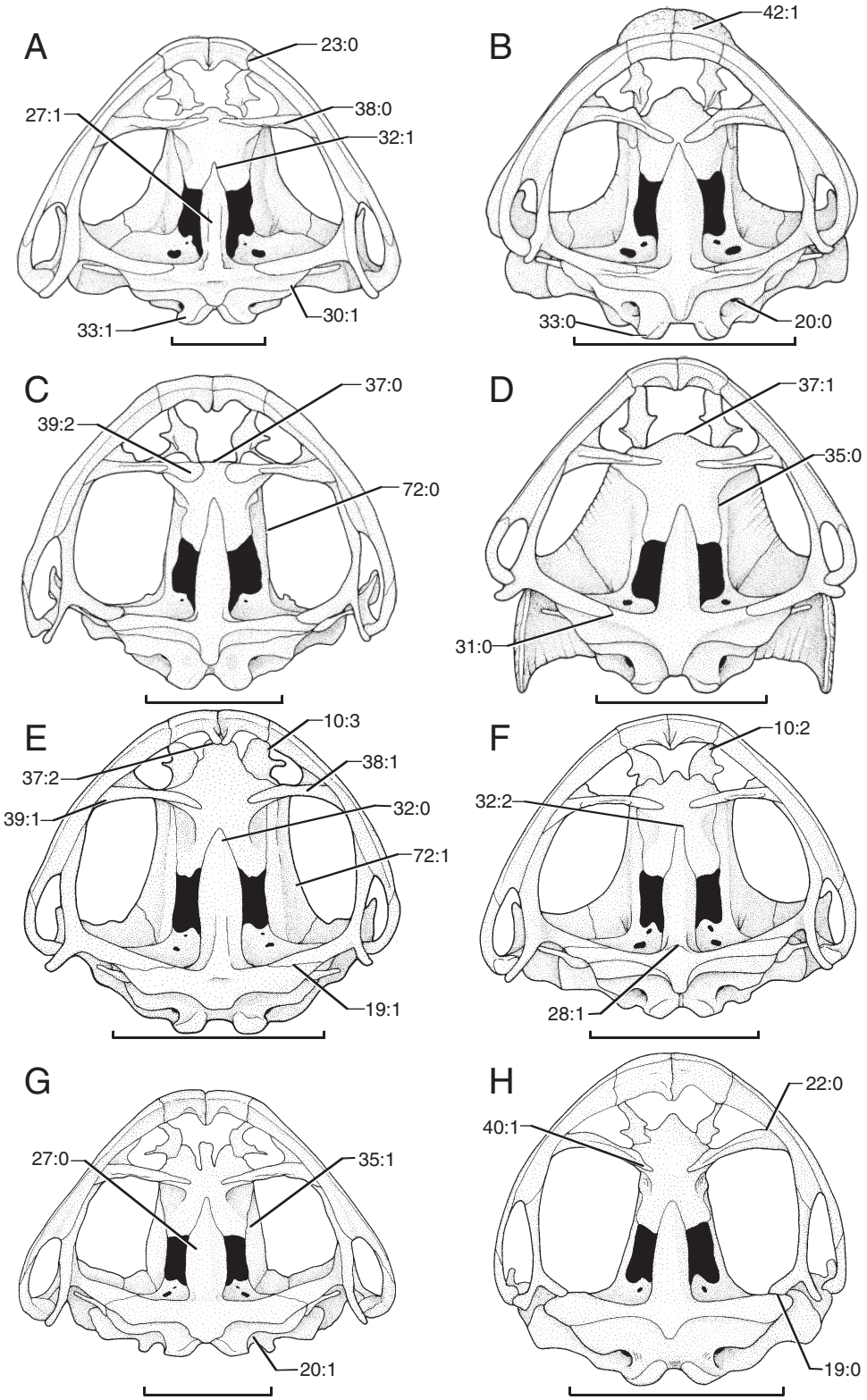

Figure 7. Ventral aspect of the skulls of representative South American *Bufo*. A, *B. crucifer* (KU 93112). B, *B. granulosus* (*B. granulosus* group; KU 170090). C, *B. amabilis* (*B. spinulosus* group; KU 124587). D, *B. margaritifer* (*B. margaritifer* group; KU 152057). E, *B. veraguensis* (*B. veraguensis* group; KU 164084). F, *B. valliceps* (*B. valliceps* group; KU 59873). G, *B. caeruleostictus* (*B. guttatus* group; KU 152057). H, *B. cophotis* (*B. variegatus* group; KU 218525). Scale bars = 1 cm.

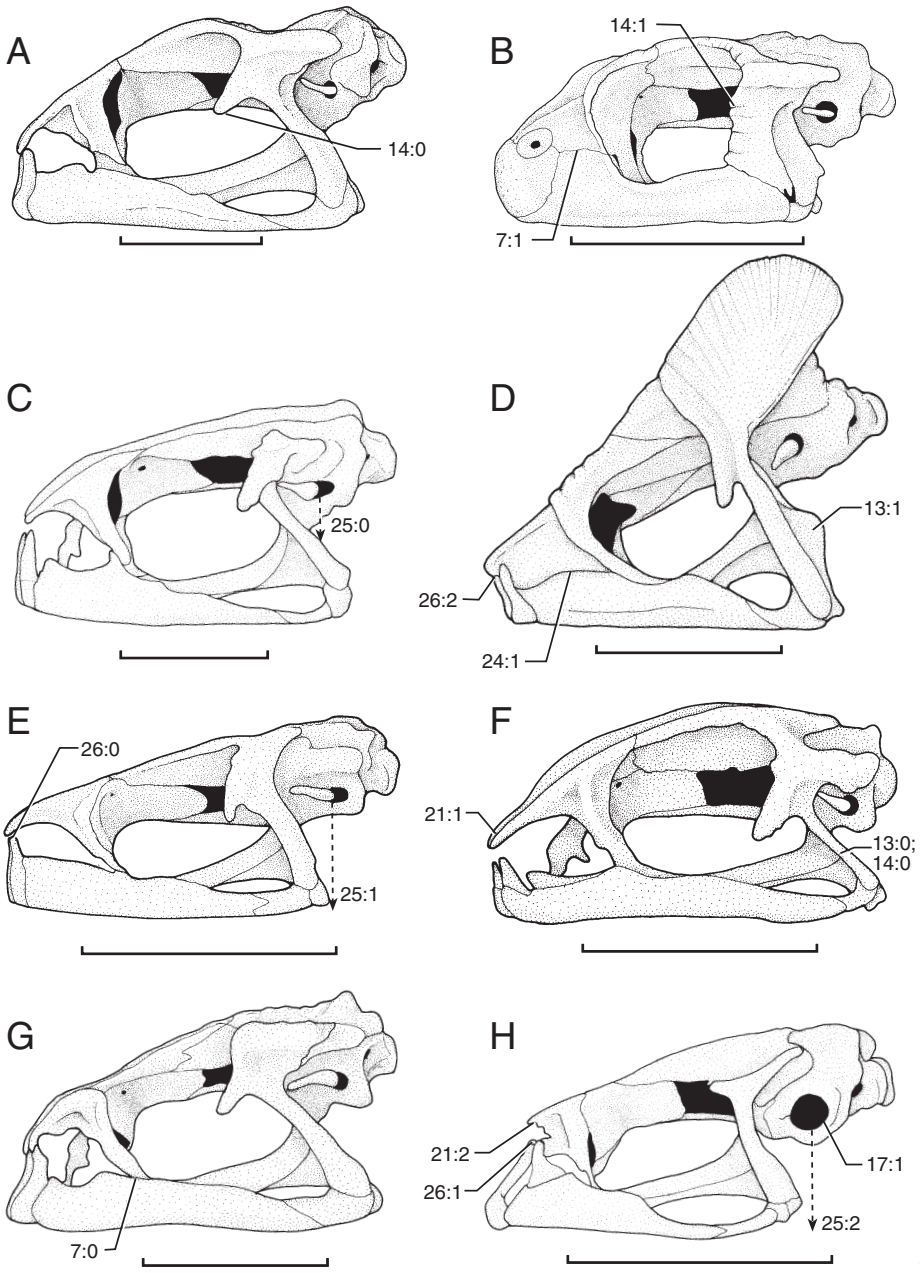

Figure 8. Lateral aspect of the skulls of representative South American *Bufo*. A, *B. crucifer* (KU 93112). B, *B. granulosus* (*B. granulosus* group; KU 170090). C, *B. amabilis* (*B. spinulosus* group; KU 124587). D, *B. margaritifer* (*B. margaritifer* group; KU 152057). E, *B. veraguensis* (*B. veraguensis* group; KU 164084). F, *B. valliceps* (*B. valliceps* group; KU 59873). G, *B. caeruleostictus* (*B. guttatus* group; KU 152057). H, *B. cophotis* (*B. variegatus* group; KU 218525). Scale bars = 1 cm.

included within the Central American lineage. This clade of medium-sized toads has moderate ossification of the skull and rather 'generalized' cranial morphology for *Bufo*. The cranial crests are well developed, with the parietal crests being particularly large compared with those of other New World *Bufo*. The nasals are not expanded dorsolaterally; the nasals and pars facialis of the maxilla do not articulate laterally; the zygomatic ramus of the squamosal is free and does not articulate with the maxilla and ventral ramus of the squamosal (as it does in the *B. granulosus* and *B. peltocephalus* groups). The crania of examined species of this lineage share the following characters: relatively broad skulls that are wider than long, with the greatest width at the level of the quadratojugals (Fig. 6F); nasals not expanded dorsolaterally;

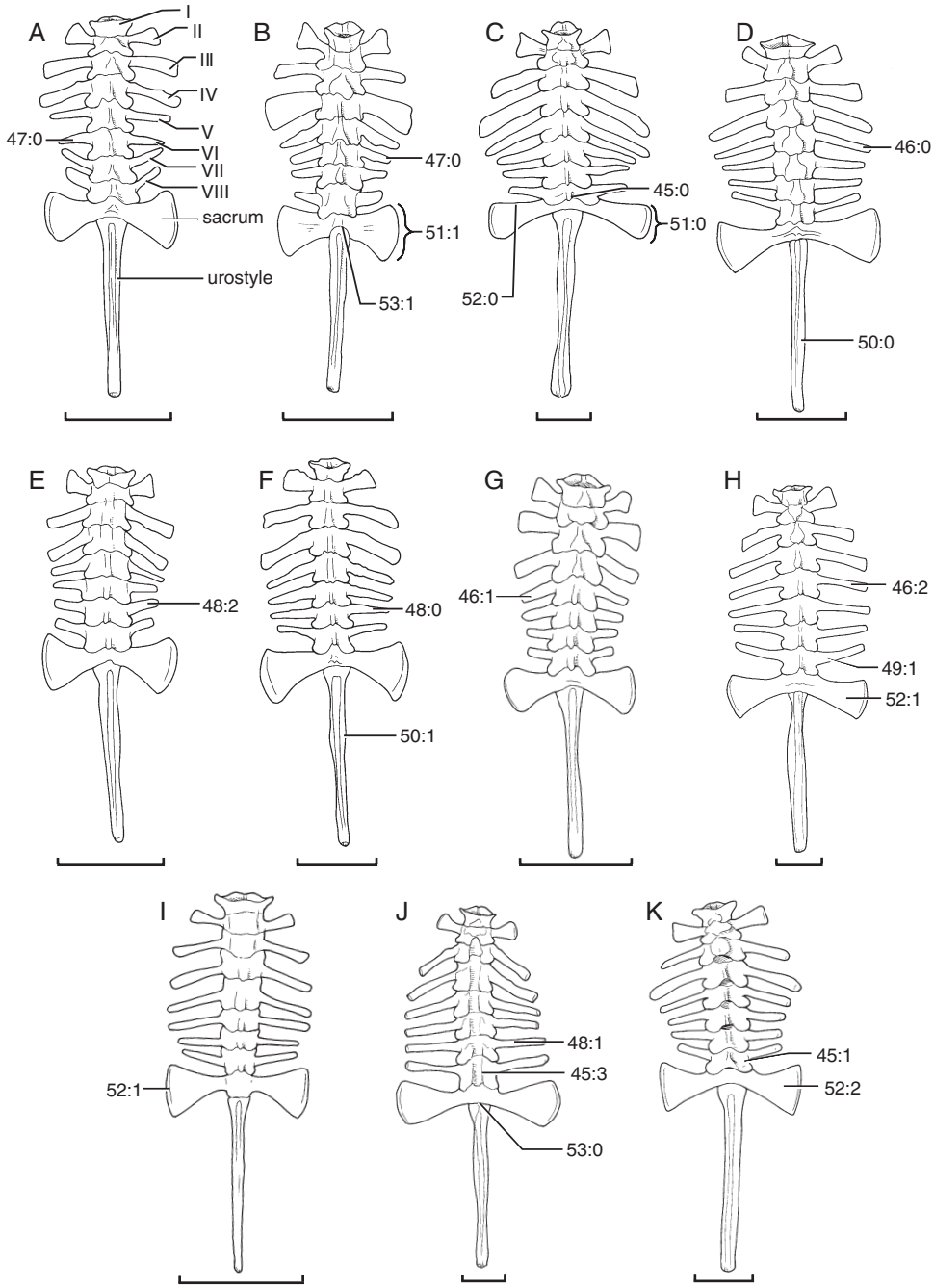

Figure 9. Dorsal aspect of vertebral columns of representative *Bufo*. The numbers refer to characters and their respective states discussed in the text. A, *B. spinulosus* (KU 160270). B, *B. granulosus* (KU 170090). C, *B. marinus* (ROM 20650). D, *B. margaritifer* (KU 104756). E, *B. veraguensis* (KU 164084). F, *B. valliceps* (KU 68155). G, *B. cophotis* (KU 218525). H, *B. guttatus* (KU 167631). I, *B. nasicus* (ROM 20650, drawn from a radiomicrograph). J, *B. asper* (KU 155584). K, *B. woodhousii* (KU 18185). Scale bars = 1 cm.

sphenethmoid not covered completely by medial articulation of nasals and frontoparietals; jaw articulation posterior to the level of the fenestra ovalis (Fig. 8D); a complete temporal arcade; and relatively acuminate nasals. The sacral diapophyses are moderately dilated (Fig. 9F). The monophyly of the Central American clade is supported by one unique and unreversed synapomorphy: character 28, the medial surface of the parasphenoid bears a pair of ridges that converge medially (Fig. 8F).

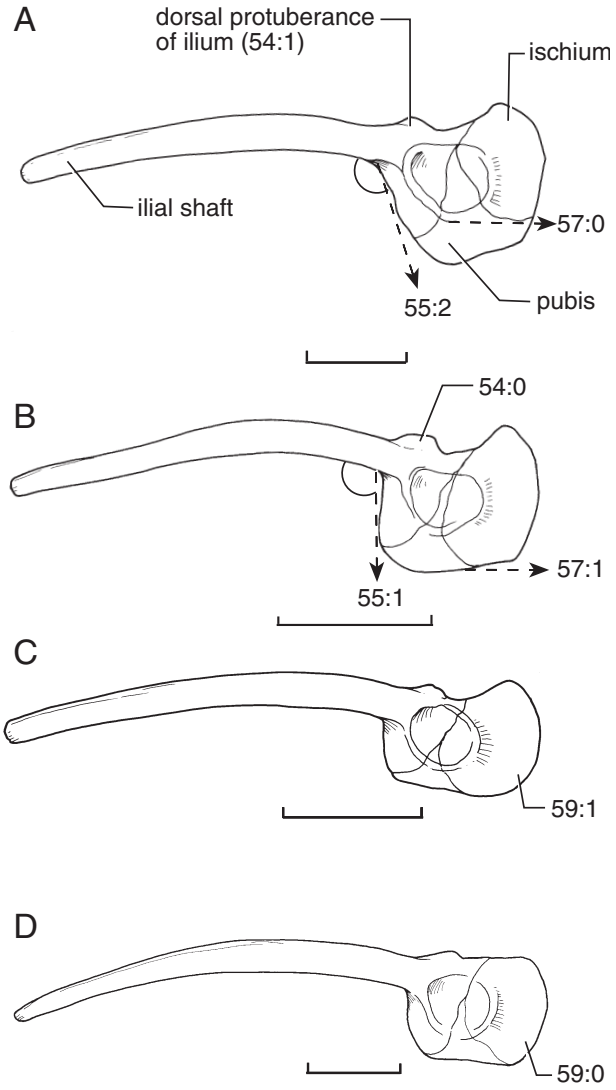

Figure 10. Lateral views of the ilia of representative South American *Bufo*, with relevant character states discussed in the text. A, *B. cophotis* (KU 218525). B, *B. valliceps* (KU 68155). C, *B. granulosus* (KU 170090). D, *B. margaritifer* (KU 104756). Scale bars = 5 mm.

Eurasian lineages (clades 9, 10, and 12 + Bufo melanostictus)

Eurasian taxa are represented in this analysis by only seven species. The analysis of combined data places the Eurasian species in two separate lineages that are basal to the New World clade (bpp = 0.97 and 0.64; Fig. 4), one lineage that is basal to the African clade (clade 12) and one species, *B. melanostictus*, that is sister to *Schismaderma* from Africa. Further understanding of Eurasian *Bufo* relationships awaits more extensive taxon sampling.

African lineage (clade 11)

The monophyly of the African clade (with the exception of *Schismaderma*) is well supported (bpp = 1.0) and is nested between two Eurasian lineages (Fig. 4). Relationships within the African clade are largely consistent with the results of a recent study based on the analysis of nuclear and mtDNA data (Cunningham & Cherry, 2004). However, in the present study, *B. garmani* is the sister to *B. xeros* (bpp = 1.0), whereas in the former study it was supported as the sister to *B. poweri*.

Bufo guttatus group (clade 13)

This group contains *B. blombergi*, the largest known species of *Bufo* (often with snout–vent length > 200 mm). However, other species assigned to this group (e.g. *B. haematiticus*) are more 'average' in size. Osteologically, members of the *B. guttatus* group are distinguished from all other *Bufo* by having well-developed omosterna. Moreover, their skulls are relatively broad and wider than long, with the greatest width at the level of the quadratojugals (Fig. 6G). The sphenethmoids of examined species are visible dorsally and the jaw articulation lies posterior to the level of the fenestra ovalis; the temporal arcade is complete. The sacral diapophyses of the examined species in this group are not broadly dilated (Fig. 9H) as they are in the *B. granulosus* and *B. veraguensis* groups. Members of the *B. guttatus* group share two unique and unreversed synapomorphies: character 35, the sphenethmoid in ventral view is distinctively broad (Fig. 7G); character 36, the posterior process of the prootic is prominent and notched (Fig. 6G).

In molecular and combined analyses, the *B. guttatus* group is basal to most other *Bufo* included in this study (with the exception of *B. cophotis*, *B. variegatus*, and the *B. peltocephalus* group); this relationship is not surprising, as members of this group have long been suspected of belonging to an ancient clade that is morphologically and biochemically distinct from all other South American *Bufo* (Blair, 1972a), and one member of the group (*B. haematiticus*) was recently supported as a basal clade within *Bufo* in an analysis of mtDNA data (Pauly *et al.*, 2004). Blair (1972a: 89) stated that the traits of this group differ decidedly from other Neotropical lines and tentatively suggested an independent origin from an unknown Tertiary ancestor. One unexpected result of all analyses is the support of *B. nasicus*, formerly assigned to the *B. margaritifer* group (Hoogmoed, 1990), as sister to the *B. guttatus* group. Synapomorphies shared by other *B. guttatus* group species and *B. nasicus* include the presence of a well-developed omosternum and an elongated transverse process of vertebra VI (Fig. 9H, I).

West Indian Bufo (clade 14)

Morphologically, this group is supported as the sister group to *B. granulosus* by the following synapomorphies: character 14, zygomatic ramus of the squamosal articulating with the dorsal surface of the maxilla; and character 41, a preorbital crest confluent with a suborbital crest, with anterolateral foramen present. Prior morphological and molecular phylogenetic analyses (Pramuk *et al.*, 2001, based on 1970 bp of 12S, 16S, and cytochrome *b* mtDNA; and Pramuk, 2002, based on combined morphological and molecular evidence) recovered *B. granulosus* + *B. marinus* as the sister taxon to the West Indian toads (Fig. 2B). West Indian toads are unique among bufonids for sharing a well-developed maxillary extension that forms a distinctively elongated snout common to most species of the group (with the exception of *B. fluviaticus*, in which the extension is present, but poorly developed; Pramuk, 2000). To test further the sister-group relationship of the West Indian toads, 1970 bp of previously published 12S and 16S mtDNA data (Pramuk *et al.*, 2001) for seven additional species of the *B. peltocephalus* group were combined and analysed (with MP and Bayesian methods) with the mtDNA data resulting from the present study. The analyses discussed previously, as well as the reanalysis of the previously published mtDNA data, indicate that the West Indian toads form a well-supported (bpp = 1.0) clade that is basal within most other *Bufo* included in this analysis (except *B. cophotis* and *B. variegatus*; Fig. 2A). Convergent morphological characters shared between the West Indian toads and *B. granulosus* have repeatedly led investigators to speculate on their shared ancestry (e.g. Pregill, 1981; Pramuk, 2002). The data presented in this study indicate that these two lineages do not share a recent common ancestor and that the *B. peltocephalus* group represents a relatively ancient and distinctive clade within *Bufo*.

Bufo variegatus group (clade 15)

I recommend resurrecting the *B. variegatus* group to contain *B. cophotis*, *B. corynetes*, and *B. variegatus*. (See comments under *B. spinulosus* group.)

DISCUSSION

The analysis of the morphological data failed to find unique and unreversed synapomorphies supporting the monophyly of *Bufo*. Moreover, none of the analyses supports the *Bufo* clade as strictly monophyletic, as it includes other non-*Bufo* bufonids, such as *Rhamphophryne* (in all analyses) and *Schismaderma* (in molecular and combined analyses). The genus *Rhamphophryne* Trueb, 1971 contains ten species that are distributed in eastern Brazil and the Andean slopes of the upper Amazon Basin of Ecuador and in moderate elevations of northern Colombia and eastern Panama (Frost, 2004). Graybeal & Cannatella (1995) noted that there are no unambiguous characters supporting the monophyly of this taxon. Therefore, it is not surprising that in the molecular and combined-evidence analyses, *Rhamphophryne* is nested well within the New World radiation. Moreover, in the molecular and combined analyses, *Schismaderma* (a bufonid genus native to Tanzania, the Republic of Congo, and South Africa) is sister to the Eurasian *B. melanostictus*, and is nested within *Bufo*. The results of other studies also indicate that *Schismaderma* is closely related to other *Bufo* (Maxson, 1981a, 1984; Graybeal, 1997; Pauly *et al.*, 2004). Continued recognition of *Rhamphophryne* and *Schismaderma* renders *Bufo* paraphyletic.

None of the data subsets supports the monophyly of South American *Bufo*. In most analyses resulting from separate and combined data sets, two clades of South American species (the *B. guttatus* and *B. variegatus* groups) and the West Indian *Bufo* (= *B. peltocephalus* group) fall outside of all other representatives of the genus; apparently these lineages are much older than other South American toads. These groups are quite distinctive morphologically from other *Bufo* included in this analysis. For example, members of the *B. guttatus* group share the presence of a well-developed omosternum and all species in the *B. variegatus* group lack columellae and share distinctively lightly ossified crania, with nasals that do not meet posteriorly with the anterior edges of the frontoparietals (Fig. 6H). In addition, the *B. peltocephalus* group is a lineage that is so distinctive from other *Bufo* that it was formerly assigned to its own genus (*Peltophryne* Fitzinger, 1843; see also Pregill, 1981). It could be argued that the 'odd', basal groups of South American toads (i.e. *B. peltocephalus*, *B. guttatus*, and *B. variegatus* groups) are so morphologically and genetically distinct from other *Bufo* and other New World species, that they should be reassigned to other genera. At this time, however, because of the lack of unique and unreversed morphological synapomorphies supporting the genus *Bufo* at any level, I refrain from reassigning the *B. guttatus* and *B. variegatus* groups to their own genera or from resurrecting the genus *Peltophryne* for the West Indian lineage.

MORPHOLOGICAL HOMOPLASY

The relationships supported by the analysis of morphological data (Fig. 1) vary considerably from those resulting from the molecular or combined analyses (e.g. Fig. 4). Although there is considerable conflict between the molecular and morphological data sets, these differences are poorly supported. Therefore, all data were combined and analysed jointly (following Wiens, 1998). There are several compelling reasons to

include even small components of morphological data in a phylogenetic analysis. For example, even relatively small subsets (< 5%) of morphological characters, in combination with large contigs of sequence data, can significantly influence a tree resulting from a combined analysis (Nylander *et al*., 2004). Also, the addition of morphological characters will be necessary to reconstruct relationships of fossil and recently extinct taxa, which compose > 99% of all species that have ever lived (Wiens, 2004). In addition, the inclusion of morphology allows for a discussion of morphological character evolution and descriptions of characters for the diagnosis of phylogenetically based taxonomic groups (*sensu* De Queiroz & Gauthier, 1990, 1992, 1994). The unique and unreversed morphological synapomorphies presented herein can be used to aid the diagnosis of the monophyletic groups of South American *Bufo*.

The strict definition of a 'broad' vs. 'narrow skull' *sensu* Blair (1972a) is related to the width of the frontoparietal, which is probably correlated with the overall amount of ossification in the skull. In *Evolution in the genus* Bufo, Blair (1972b) and Martin (1972a) discuss 'narrow-' and 'broad-skulled' groups at length, but nowhere do the authors explain how they quantified skull type. To account for this, and to simplify the coding scheme, I scored frontoparietals as 'broad' if they extended past the sphenethmoid laterally on the dorsal surface of the skull (see character 72). MACCLADE was then employed to trace the character states on the trees resulting from morphology and combined data (Figs 1, 4, respectively). Within the tree derived from morphological data (Fig. 1), the clustering of *Bufo* based on skull type indicates that the relationships supported by these data are largely affected by characters correlated with skull width. In contrast, the molecular and combined results do not support the monophyly of 'narrow-' or 'broad-skulled' lineages. It is apparent that characters correlated with skull width and the amount of overall ossification are highly convergent within the genus; as a result, relationships in the morphology-alone analysis should be interpreted with caution. Interestingly, Martin (1972a) was aware of the convergence in frontoparietal width among *Bufo* and noted that caution should be used in interpreting phylogenetic reconstructions of the genus based on osteological data.

In this study, phylogenetic groupings of *Bufo* resulting from molecular and combined analyses of DNA and morphology correspond more to historical geographical patterns than to skull type. Moreover, none of the analyses performed herein support 'broad-skulled' or 'narrow-skulled' clades (*sensu* Blair, 1972a). My molecular and combined-evidence analyses indicate that lightly ossified crania are highly convergent in *Bufo* and 'narrow-skulled' forms have conservatively evolved within at least six separate lineages (Fig. 4). It is evident that each skull type is intermingled with the other in each of the North, Central, and South American, and Eurasian lineages, and that skull width (or the amount of ossification affecting it) is prone to convergence. Morphological homoplasy within *Bufo* was also recovered by Pauly *et al*. (2004: fig. 5) and Graybeal (1997: fig. 10), who mapped skull type (coded from data presented in Blair, 1972b and Martin, 1972a) onto their resulting topologies.

Blair (1972b) speculated that an early dichotomy in skull type occurred in *Bufo* when 'narrow-' and 'broad-skulled' lineages became adapted to cold and warm habitats, respectively. Blair (1970, 1972b) suggested that cooler, upland environments selected against heavily ossified skeletons, given that a heavily ossified skeleton would not be as mobile in cooler environments. Some clades resulting from my combined analysis agree with Blair's (1972b) hypothesis: species with lightly ossified crania (e.g. members of the *B. spinulosus* and *B. veraguensis* groups) are generally restricted to montane and/or cooler habitats. However, there are broad exceptions to this pattern, as some species with lightly ossified skulls are endemic to warmer lowland environments (e.g. *B. atacamensis* of the *B. spinulosus* group, native to the Atacama desert of Chile, and species of the *B. margaritifer* group distributed throughout lowland forests of Amazonia). The causes of a correlation between a narrow skull type and cooler climates as noted by Blair (1972b) are not apparent, nor has a biological explanation for the convergence of 'broad' or 'narrow' skull types been investigated.

Prior authors have noted that the genus *Bufo* is morphologically conserved (e.g. Savage, 1973; Graybeal & Cannatella, 1995; Graybeal, 1997). Low levels of interspecies variation may explain why other investigators (Morrison, 1994; Graybeal, 1997; Mendelson, 1997a) employing morphological data to investigate bufonid phylogeny have obtained trees that were poorly resolved (e.g. Graybeal, 1997: fig. 11). Similarly, the lack of resolution in the strict consensus tree in the present study (Fig. 1) attests to the paucity of variation in characters of the osteology and integument of toads. However, the present study did not include myological, larval, or behavioural characters. In the future, it is possible that other kinds of morphological data (especially those coded from soft tissue and not correlated with the amount of skull ossification) could yield a wellspring of phylogenetically informative characters.

BIOGEOGRAPHY

In the Neotropical Realm, toads are a relatively minor component of the anuran fauna, representing approx-

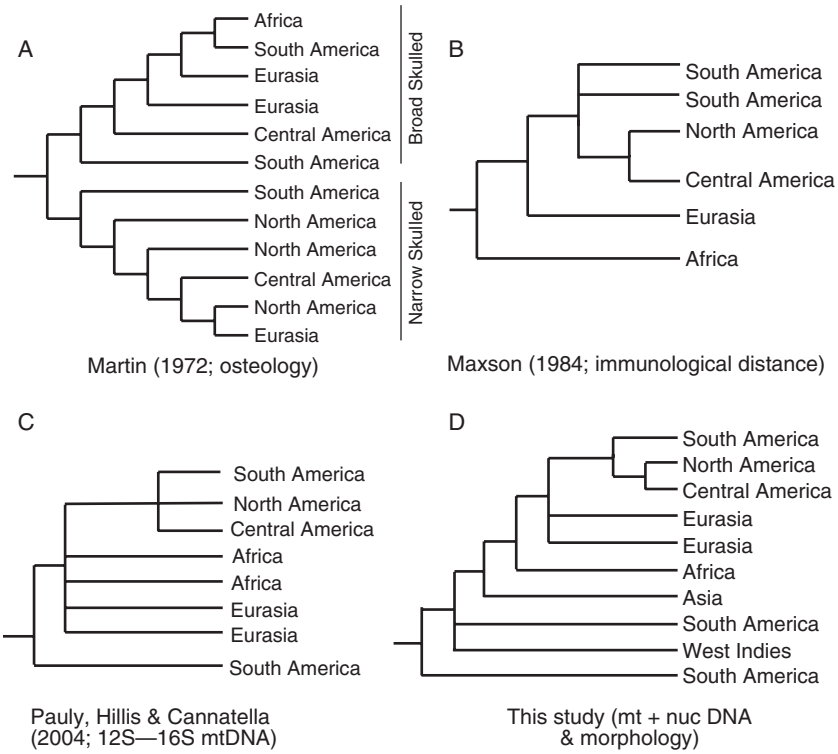

Figure 11. Area cladograms of previously proposed biogeographical hypotheses for the origin of *Bufo* compared (A–C) with the area cladogram resulting from the analysis of combined nuclear + mitochondrial DNA and morphology (D; this study). A, based on the osteological data and phenetic relationships of Martin (1972a). B, the cladogram of Maxson (1984) is based on immunological distance data. C, the hypothesis of Pauly *et al.* (2004) is inferred from 12S–16S mitochondrial DNA data.

imately 3.5% of species (calculated from data provided in Duellman & Sweet, 1999). However, the nearly cosmopolitan geographical distribution of *Bufo* is larger than that of any other amphibian genus. The widespread distribution and diversity of this group has prompted numerous systematic and biogeographical investigations of *Bufo*, some of which are reviewed herein and compared with the area cladogram resulting from this study (Fig. 11D).

The results of this study indicate that there is strong geographical structuring within trees resulting from both the combined and molecular data analyses, and most strongly supported clades are geographically homogeneous. Within the area cladogram (Fig. 11D), two South American and one West Indian lineage of toads are basally placed within *Bufo*, the African and Eurasian taxa are intermediate, and the remaining New World taxa are the most derived. Within the large New World clade, North and Central American taxa form a monophyletic group, which is sister to the derived South American lineage. A polyphyletic South American *Bufo* was also recovered in a recent study of Nearctic *Bufo* relationships, which included exemplars of South and Central American species (Fig. 11C; Pauly *et al.*, 2004).

Previously, other authors (e.g. Tihen, 1962a; Savage, 1966, 1973; Blair, 1972b; Martin, 1972a; Maxson, 1984; Graybeal, 1997) proposed hypotheses for the origin of South American *Bufo*. Pauly *et al.* (2004) provide a thorough review of the findings of these authors and discuss them in the context of their phylogeny of Nearctic toads. Herein I focus my discussion on how my results differ from those of Pauly *et al.* (2004) and from the few additional prior hypotheses based on objective methods (e.g. Martin, 1972a, based on a phenetic analysis of morphological data, Fig. 11A; Maxson, 1984, based on immunological distance data, Fig. 11B). Biogeographical scenarios presented in the literature as generalizations rather than with a branching diagram (e.g. Tihen, 1962a; Blair, 1972a; Savage, 1973; Tandy & Tandy, 1976) are not discussed. In addition, because the 16S data of Graybeal (1997) were recently found to be unreliable (Harris, 2001; Pauly *et al.*, 2004), the biogeographical hypothesis resulting from her data is not addressed here.

In *Evolution in the genus* Bufo, Martin (1972a: figs 4–16) was the only contributor to present a tentative phylogeny of *Bufo*, which was based on overall morphological similarity (Fig. 11A). Martin's phylogenetic tree proposes that South American taxa are polyphyl-

etic and contain descendants of both the 'broad-' and 'narrow-skulled' lineages. Intercontinental exchange of *Bufo* was offered to explain the occurrence on every continent of toads from both lineage types – convergence on 'narrow-' or 'broad-skulled' morphotypes was not widely entertained. In the same volume, Blair (1972a) proposed that the genus originated in South America, and subsequently dispersed to the Old World.

Maxson's (1984) immunological study failed to recover a paraphyletic South American clade consistent with Gondwanan origin (Fig. 11B), as recovered in the present study (Fig. 11D), as her single representative of the *B. guttatus* group (*B. blombergi*) fell out in a polytomy with other species of South American toads. However, using an 'albumin molecular clock' Maxson (1984) calculated the age of *Bufo* to be approximately 80 Myr (million years). Based on this estimate, Maxson (1984) hypothesized that African lineages separated from American and Asian lineages in the Late Cretaceous, corresponding with the breakup of western Gondwana (~100 Mya). Her results also suggest that North and Central American lineages are sister groups within the New World radiation, and that Eurasian species fall out as the sister to the New World clade. In contrast to the hypothesis of Martin (1972a), Maxson's tree does not group 'narrow-' and 'broad-skulled' individuals and is geographically cohesive (i.e. with species from most continents recovered as continent-specific clades, except South America, which was unresolved).

Recently, Pauly *et al.* (2004) presented their phylogeny of Nearctic toads and employed parametric bootstrapping to test previously proposed biogeographical hypotheses for the genus. Unfortunately, current MP and ML-based methods (e.g. Kishino–Hasegawa, parametric bootstrapping, Shimodaira–Hasegawa, and the Templeton test) used to test competing hypotheses do not allow for combined analyses with partitioned models (potentially leading to the use of inadequate models; Wiens *et al*., 2005b). Therefore, I opted not to employ MP and ML-based statistical methods to explicitly test competing biogeographical hypotheses. However, in lieu of statistical tests, we can evaluate the topology resulting from this study by comparing the bpp of corresponding nodes of my tree (Fig. 4) with those of Pauly *et al.* (2004: figs 2, 4). As with the present study, Pauly *et al.* (2004) identified South American, Central American, and Nearctic lineages within the New World clade. However, their ML analysis did not recover a sister-group relationship for the Nearctic clade, as their results weakly supported South America as sister to the Nearctic *Bufo* (bpp = 0.41) and reported slightly higher support of their data (bpp = 0.45) for a North America + Central America relationship. In contrast, my results recovered high support for the Central American clade as sister to Nearctic toads (bpp = 1.0). Pauly *et al.* (2004) also did not resolve the sister group to the derived New World clade, as their ML topology supported African and Eurasian lineages as successively basal clades (fig. 2), but with poor support (bpp = 0.81) for all of their deeper nodes. Here, I recovered two Eurasian lineages (bpp = 0.64 and 0.97) as successively basal sister groups to the New World radiation. After comparing my area cladogram with previously proposed phylogenetic hypotheses for *Bufo* (Fig. 11A–D), it is apparent that all three resulting from the analysis of genetic data (Fig. 11B–D) are broadly congruent. However, my area cladogram (Fig. 11D) is more similar to the results of Maxson (1984; Fig. 11B), recovering Central + North American lineages as well-supported sister areas and Eurasian *Bufo* as sister to the New World radiation, than it is with the findings of Martin (1972a; Fig. 11A) or Pauly *et al.* (2004; Fig. 11C). Nonetheless, my hypothesis does not agree completely with the topology of Maxson (1984), as she did not recover a polyphyletic South America.

The major biogeographical and phylogenetic conclusions resulting from this study are that: (1) The area cladogram supports Eurasian and African lineages as basal to a large New World radiation, with two South American lineages supported at the base of the tree. As has been proposed in prior studies (Maxson, 1984; Pauly *et al.*, 2004), this finding is consistent with an origin of *Bufo* that predates the breakup of Gondwana (~100 Mya; Goldblatt, 1993; Pitman *et al*., 1993). (2) Central and North American clades together form a well-supported monophyletic group with the 'derived' South American clade falling out as its sister group. (3) Eurasian *Bufo* comprise the sister lineage to the derived New World clade. Considering the area relationships supported by this study, it is possible that the ancestor of the 'recent' lineage of *Bufo* (comprising the African, Eurasian, and North, Central, and 'derived' South American lineages) arose in Africa following complete separation of the western Gondwana ~100 Mya (Goldblatt, 1993; Pitman *et al*., 1993).

This study provides our best insight yet into the major lineages within *Bufo*, and, as a result, provides a more thorough understanding of the biogeographical history of the genus. Unfortunately, the fossil record for true toads (reviewed in Pauly *et al.*, 2004) is particularly depauperate, with most described forms being of extant taxa primarily known from fragmented ilia and other pelvic girdle elements (Sanchíz, 1998). The oldest specimen attributable to *Bufo* dates from the Late Palaeocene of Itaborai, Brazil (~55 Mya; Báez & Nicoli, 2004). Therefore, there are currently no available fossil data to support the above-mentioned 'Gondwanan Origin' for *Bufo*, or to provide reliable calibration dates within the genus, making it difficult to

extend the results towards elucidating the historical biogeography of true toads. Greater taxon sampling (particularly of Eurasian and African species), as well as additional and accurately dated bufonid fossils, will aid our understanding of the biogeographical history of *Bufo*.

ACKNOWLEDGEMENTS

Financial support for this research was provided by The University of Kansas (KU) Natural History Museum Division of Herpetology and Panorama Society, and Joan and Bert Berkley of Mission Hills, Kansas; The KU Tinker Field Research Grants; and peripheral funding from the KU Department of Ecology & Evolutionary Biology. I am grateful to M. Mort (KU) for allowing me to use his sequencer during the earlier phases of my molecular data collection. Supplemental financial support was provided by NSF award DEB# 0132227 to J. Sites (BYU). I appreciate the comments and suggestions of the faculty and students in the Divisions of Herpetology and Ichthyology at KU, including L. Trueb, W. Duellman, E. Wiley, A. Bentley, E. Greenbaum, J. M. Guayasamin, N. Holcroft-Benson, C. Sheil, J. Simmons, and K. Tang. Many thanks to J. Caldwell, I. de la Riva, A. Gluesenkamp, A. Goebel, E. Lehr, J. Mendelson, P. Narvaes, G. Pauly, I. de la Riva, T. Reeder, A. Robertson, C. Vélez-R., and J. Wiens for help with field collections, molecular, taxonomic, and/or editorial expertise. Invaluable logistical support was provided by L. Krishtalka and L. Schlenkler. This research was made possible by loans of specimens from the following institutions, curators, and collections managers: AMNH (C. Myers, L. Ford), CAS (R. Drewes, Y. Vindum), MCZ (J. Cadle, J. Rosado), MNHNP (N. López-Kochalka), QCAZ (L. Coloma), ROM (R. Murphy, A. Wynn), TNHC (D. Cannatella), UMMZ (A. Kluge, G. Schneider), and USNM (R. Heyer, R. Wilson). The manuscript was greatly improved by comments from L. Trueb, W. Duellman, J. Sites, B. Noonan, G. Pauly, B. Shaffer, and J. Wiens.

REFERENCES

Alfaro ME, Zoller S, Lutzoni F. 2003. Bayes or bootstrap? A simulation study comparing the performance of Bayesian Markov chain Monte Carlo sampling and bootstrapping in assessing phylogenetic confidence. *Molecular Biology and Evolution* **20:** 255–266.

Alrubaian JP, Danielson D, Walker D, Dores RM. 2002. Cladistic analysis of anuran POMC sequences. *Peptides* **23:** 443–452.

Báez AM, Nicoli L. 2004. Bufonid toads from the Late Oligocene beds of Salla, Bolivia. *Journal of Vertebrate Paleontology* **24:** 73–79.

Blair WF. 1963. Evolutionary relationships of North American toads of the genus *Bufo*: a progress report. *Evolution* **17:** 1–16.

Blair WF. 1966. Genetic compatibility in the *Bufo valliceps* and closely related groups of toads. *Texas Journal of Science* **18:** 333–351.

Blair WF. 1970. Genetically fixed characters and evolutionary divergence. *American Zoologist* **19:** 41–46.

Blair WF. 1972a. Evidence from hybridization. In: Blair WF, ed. *Evolution in the genus Bufo*. Austin, Texas: University of Texas Press, 196–243.

Blair WF. 1972b. Summary. In: Blair WF, ed. *Evolution in the genus Bufo.* Austin, Texas: University of Texas Press, 329–343.

Bogart JP. 1972. Karyotypes. In: Blair WF, ed. *Evolution in the genus Bufo*. Austin, Texas: University of Texas Press, 171–195.

Boulenger GA. 1882. *Catalogue of the Batrachia Salientia s. Ecaudata in the collection of the British Museum*, ed. 2. London: British Museum (Natural History).

Bremer K. 1988. The limits of amino acid sequence data in angiosperm phylogenetic reconstruction. *Evolution* **42:** 795–803.

Bremer K. 1994. Branch support and tree stability. *Cladistics* **10:** 295–304.

Cannatella D. 1985. A phylogeny of primitive frogs (Archaeobatrachians). DPhil Thesis, University Kansas, Lawrence.

Cardellini P, Casas Andreu G, Goenarso D, Guidolin L, Martino R, Rasotto MB, Sala M, Scalabrin M. 1984. Globin evolution in some species of the genus *Bufo*. *Comparative Biochemistry and Physiology* **78:** 24–25.

Cei JM. 1972. *Bufo* of South America. In: Blair WF, ed. *Evolution in the genus Bufo*. Austin, Texas: University of Texas Press, 82–92.

Cordova JH. 1999. On karyomorphs, cladistics and taxonomic status of the *Bufo spinulosus* species group (Amphibia: Anura) in Peru. *Stuttgarter Beiträge zur Naturkunde Serie a (Biologie)* **28:** 1–28.

Cunningham M, Cherry MI. 2000. Mitochondrial DNA divergence in southern African bufonids: are species equivalent entities? *African Journal of Herpetology* **49:** 9–22.

Cunningham M, Cherry MI. 2004. Molecular systematics of African 20-chromosome toads (Anura: Bufonidae). *Molecular Phylogenetics and Evolution* **32:** 671–685.

Da Silva H, Mendelson JRM III. 1999. A new organ and sternal morphology in toads (Anura: Bufonidae): descriptions, taxonomic distribution, and evolution. *Herpetologica* **55:** 114–126.

Darst CR, Cannatella DC. 2004. Novel relationships among hyloid frogs inferred from 12S and 16S mitochondrial DNA sequences. *Molecular Phylogenetics and Evolution* **31:** 462–475.

De Queiroz K, Gauthier J. 1990. Phylogeny as a central principle in taxonomy: phylogenetic definitions of taxon names. *Systematic Zoology* **39:** 307–322.

De Queiroz K, Gauthier J. 1992. Phylogenetic taxonomy. *Annual Review of Ecology and Systematics* **23:** 449–480.

De Queiroz K, Gauthier J. 1994. Toward a phylogenetic system of nomenclature. *Trends in Ecology and Evolution* **9:** 27–31.

De Rijk PY, Van de Peer Y, Chapelle S, De Wachter R. 1994. Database on the structure of large ribosomal subunit DNA. *Nucleic Acids Research* **22:** 3495–3501.

Di Tada IE, Martino A, Sinsch U. 2001. Release vocalizations in neotropical toads (*Bufo*): ecological constrains and phylogenetic implications. *Journal of Systematic Evolutionary Research* **39:** 13–23.

Duellman WE, Schulte R. 1992. Description of a new species of *Bufo* from northern Peru with comments on phenetic groups of South American toads (Anura: Bufonidae). *Copeia* **1:** 162–172.

Duellman WE, Sweet S. 1999. Distribution patterns of amphibians in the Nearctic region of North America. In: Duellman WE, ed. *Patterns of distribution of amphibians: a global perspective*. Baltimore: Johns Hopkins University Press, 31–110.

Felsenstein J. 1981. Evolutionary trees from DNA sequences: a maximum likelihood approach. *Journal of Molecular Evolution* **17:** 368–376.

Felsenstein J. 1985. Confidence limits on phylogenies: an approach using the bootstrap. *Evolution* **39:** 783–791.

Fitzinger L. 1843. *Systema Reptilium Vindobonae.*

Ford L, Cannatella D. 1993. The major clades of frogs. *Herpetological Monographs* **7:** 94–117.

Frost DR. 2004. Amphibian species of the world: an online reference. V2.21 (15 July 2002). Electronic database available at: http://research.amnh.org/herpetology/amphibia/index.html.

Goebel AM. 1996. Systematics and conservation of bufonids in North America and in the *Bufo boreas* species group. DPhil Thesis, University of Colorado, Boulder.

Goebel AM, Donnelly JM, Atz ME. 1999. PCR primers and amplification methods for 12S ribosomal DNA, the control region, cytochrome oxidase I, and cytochrome *b* in bufonids and other frogs, and an overview of PCR primers which have amplified DNA in amphibians successfully. *Molecular Phylogenetics and Evolution* **11:** 163–199.

Goldblatt P. 1993. Biological relationships between Africa and South America: an overview. In: Goldblatt P, ed. *Biology relationships between Africa and South America*. New Haven, Connecticut: Yale University Press, 3–14.

Grandison AGC. 1981. Morphology and phylogenetic position of the West African *Didynamipus sjoestedti* Andersson, 1903 (Anura: Bufonidae). *Monitore Zoologico Italiano NS Supplemento* **15:** 187–215.

Graybeal A. 1993. The phylogenetic utility of cytochrome *b:* lessons from bufonid frogs. *Molecular Phylogenetics and Evolution* **2:** 256–269.

Graybeal A. 1997. Phylogenetic relationships of bufonid frogs and tests of alternate macroevolutionary hypotheses characterizing their radiation. *Zoology Journal of the Linnean Society* **119:** 297–338.

Graybeal A, Cannatella D. 1995. A new taxon of Bufonidae from Peru, with descriptions of two new species and review of the phylogenetic status of supraspecific bufonid taxa. *Herpetologica* **51:** 105–131.

Green DA, Parent C. 2003. Variable and asymmetric introgression in a hybrid zone in *Bufo americanus* and *Bufo fowleri*. *Copeia* **2003:** 34–43.

Harris DJ. 2001. Reevaluation of 16S ribosomal RNA variation in *Bufo* (Anura: Amphibia). *Molecular Phylogenetics and Evolution* **19:** 326–329.

Hass CA, Dunski JF, Maxson LR, Hoogmoed MS. 1995. Divergent lineages within the *Bufo margaritifera* complex (Amphibia: Anura: Bufonidae) revealed by albumin immunology. *Biotropica* **27:** 238–249.

Hauser D, Presch W. 1991. The effects of ordered characters on phylogenetic reconstruction. *Cladistics* **7:** 243–265.

Hillis DM. 1987. Molecular versus morphological approaches to systematics. *Annual Review of Ecology and Systematics* **18:** 23–42.

Hillis DM, Bull JJ. 1993. An empirical test of bootstrapping as a method for assessing confidence in phylogenetic analysis. *Systematic Biology* **42:** 182–192.

Hoegg S, Vences M, Brinkmann H, Meyer A. 2004. Phylogeny and comparative substitution rates of frogs inferred from sequences of three nuclear genes. *Molecular Biology and Evolution* **21:** 1188–1200.

Hoogmoed MS. 1990. Biosystematics of South American Bufonidae, with special reference to the *Bufo 'margaritifer'* group. In: Peters G, Hutterer R, eds. *Vertebrates in the tropics*. Bonn: Museum Alexander Koenig, 113–123.

Huelsenbeck JP, Ronquist F. 2001. MrBayes: Bayesian inference of phylogenetic trees. *Bioinformatics* **17:** 754–755.

Inger RF. 1972. *Bufo* of Eurasia. In: Blair WF, ed. *Evolution in the genus Bufo*. Austin, Texas: University of Texas Press, 102–118.

Kass RE, Rafferty AE. 1995. Bayes factors. *Journal of the American Statistics Association* **90:** 773–795.

Kluge A. 1989. A concern for evidence and a phylogenetic hypothesis of relationships among *Epicrates* (Boidae, Serpentes). *Systematic Zoology* **38:** 7–25.

Leão AT, Cochran DM. 1952. Revalidation and re-description of *Bufo ocellatus* Günther, 1858 (Anura: Bufonidae). *Memórias do Instituto de Butantan, São Paulo* **24:** 271–280.

Leviton AE, Gibbs RH, Jr, Heal E, Dawson EE. 1985. Standards in herpetology and ichthyology: Part I. Standard symbolic codes for institutional resource collections in herpetology and ichthyology. *Copeia* **1985:** 802–832.

Lewis PO. 2001. A likelihood approach to estimating phylogeny from discrete morphological character data. *Systematic Biology* **50:** 913–925.

Lynch JD. 1971. Evolutionary relationships, osteology, and zoogeography of leptodactyloid frogs. *University of Kansas Museum of Natural History Miscellaneous Publications* **53:** 1–238.

Mabee P. 1989. Assumptions underlying the use of ontogenetic sequences for determining character state order. *Transactions of the American Fisheries Society* **118:** 151–158.

Macey JR, Schulte IIJA, Larson A, Fang Z, Wang Y, Tuniyev BS, Papenfuss TJ. 1998. Phylogenetic relation-

ships of toads in the *Bufo bufo* species group from the eastern escarpment of the Tibetan Plateau: a case of vicariance and dispersal. *Molecular Phylogenetics and Evolution* **9:** 80–87.

Maddison WP, Maddison DR. 1992. *Macclade: analysis of phylogeny and character evolution*. Sunderland, Massachusetts: Sinauer Associates.

Martin RF. 1972a. Evidence from osteology. In: Blair WF, ed. *Evolution in the genus Bufo*. Austin, Texas: University of Texas Press, 37–70.

Martin RF. 1972b. Osteology of North American *Bufo*: the *americanus*, *cognatus*, and *boreas* species groups. *Herpetologica* **29:** 375–387.

Masta SE, Sullivan BK, Lamb T, Routman EJ. 2002. Molecular systematic, hybridization, and phylogeography of the *Bufo americanus* complex in eastern North America. *Molecular Phylogenetics and Evolution* **24:** 302–314.

Maxson LR. 1981a. Albumin evolution and its phylogenetic implications in African toads of the genus *Bufo*. *Herpetologica* **37:** 96–104.

Maxson LR. 1981b. Albumin evolution and its phylogenetic implications in toads of the genus *Bufo.* II. Relationships among Eurasian *Bufo*. *Copeia* **1981:** 579–583.

Maxson LR. 1984. Molecular probes of phylogeny and biogeography in toads of the widespread genus *Bufo*. *Molecular Biology and Evolution* **1:** 324–356.

Maxson LR, Song A-R, Lopata R. 1981. Phylogenetic relationships among North American toads, genus *Bufo*. *Biochemical Systematics and Evolution* **9:** 347–350.

McDiarmid RW. 1971. Comparative morphology and evolution of frogs of the Neotropical genera *Atelopus*, *Dendrophryniscus*, *Melanophryniscus*, *and Oreophrynella*. *Science Bulletin of the Los Angeles County Museum of Natural History* **12:** 1–66.

Mendelson JRM III. 1997a. The systematics of the *Bufo valliceps* group (Anura: Bufonidae) of middle America. DPhil Thesis, University of Kansas, Lawrence.

Mendelson JRM III. 1997b. A new species of *Bufo* (Anura: Bufonidae) from the Pacific Highlands of Guatemala and southern Mexico, with comments on the status of the *Bufo valliceps macrocristatus*. *Herpetologica* **53:** 14–30.

Mendelson JRM III. 1997c. A new species of toad (Anura: Bufonidae) from Oaxaca, Mexico with comments on the status of *Bufo cavifrons* and *Bufo cristatus*. *Herpetologica* **53:** 268–286.

Mendelson JRM III, da Silva HR, Maglia AM. 2000. Phylogenetic relationships among marsupial frog genera (Anura: Hylidae: Hemiphractinae) based on evidence from morphology and natural history. *Zoological Journal of the Linnean Society* **128:** 125–148.

Mickevich MF. 1982. Transformation series analysis. *Systematic Zoology* **31:** 461–478.

Mickevich MF, Weller SJ. 1990. Evolutionary character analysis: tracing character change on a cladogram. *Cladistics* **6:** 137–170.

Morrison M. 1994. A phylogenetic analysis of the *Bufo spinulosus* group (Anura: Bufonidae). DPhil Thesis, University of Kansas, Lawrence.

Mulcahy DG, Mendelson JRM III. 2000. Phylogeography and speciation of the morphologically variable, widespread species *Bufo valliceps*, based on molecular evidence from mtDNA. *Molecular Phylogenetics and Evolution* **17:** 173–189.

Narvaes P. 2003. Revisão taxonômida das espécies de *Bufo* do complexo *granulosus* (Amphibia, Anura, Bufonidae). DPhil Thesis, Instituto de Biociências da Universidade de São Paulo, Brasil.

Nylander JAA, Ronquist F, Huelsenbeck JP, Luis Nieves-Aldrey J. 2004. Bayesian phylogenetic analysis of combined data. *Systematic Biology* **53:** 47–67.

Palumbi SR. 1996. PCR and molecular systematics. In: Hillis D, Moritz C, Mable B, eds. *Molecular systematics*, 2nd edn. Sunderland, Massachusetts: Sinauer Associates, 205–247.

Pauly GB, Hillis DM, Cannatella DC. 2004. The history of a nearctic colonization: molecular phylogenetics and biogeography of the Neartic toads (*Bufo*). *Evolution* **58:** 2517–2535.

Pennington TR. 1996. Molecular and morphological data provide phylogenetic resolution at different hierarchical levels in *Andira*. *Systematic Biology* **45:** 496–515.

Pitman WC, Cande S, LaBrecque J, Pindell J. 1993. Fragmentation of Gondwana: the separation of Africa from South America. In: Goldblatt P, ed. *Biology relationships between Africa and South America*. New Haven, Connecticut: Yale University Press, 15–34.

Posada D, Crandall KA. 1998. Modeltest: testing the model of DNA substitution. *Bioinformatics* **14:** 817–818.

Powell R, Collins JT, Hooper DE. 1998. *A key to amphibians and reptiles of the continental United States and Canada*. Lawrence, Kansas: The University Press of Kansas.

Pramuk JB. 2000. Prenasal bones and snout morphology in West Indian bufonids and the *Bufo granulosus* species group. *Journal of Herpetology* **2:** 334–340.

Pramuk JB. 2002. Morphological characters and cladistic relationships of West Indian toads (Anura: Bufonidae). *Herpetological Monographs* **16:** 121–151.

Pramuk JB, Hass CA, Hedges SB. 2001. Molecular phylogeny and biogeography of West Indian toads (Anura: Bufonidae). *Molecular Phylogenetics and Evolution* **20:** 294–301.

Pregill G. 1981. Cranial morphology and the evolution of West Indian toads (Salientia: Bufonidae): resurrection of the genus *Peltophryne* Fitzinger. *Copeia* **2:** 273–285.

Rambaut A. 1996. Se-Al: sequence alignment editor. Available at http://evolve.zoo.ox.ac.uk/.

Rambaut A, Drummond A. 2003. Tracer v1.2. Available at http://evolve.zoo.ox.ac.uk/.

Ronquist F, Huelsenbeck JP. 2003. MRBAYES 3: Bayesian phylogenetic inference under mixed models. *Bioinformatics* **19:** 1572–1574.

Sanchíz B. 1998. Salientia, Part 4. In: Wellhofer P, ed. *Encyclopedia of paleoherpetology*. Munich: Verlag Dr Friedrich Pfeil.

Savage JM. 1966. The origins and history of the Central American Herptofauna. *Copeia* **1966:** 719–766.

Savage JM. 1973. The geographic distribution of frogs: patterns and predictions. In: Vial J, ed. *Evolutionary biology of the anurans: contemporary research on major problems*. Missouri: University of Missouri Press, 351–446.

Slowinski JB. 1993. 'Unordered' vs. 'ordered' characters. *Systematic Biology* **42:** 155–165.

Swofford DL. 2000. Phylogenetic analysis using parsimony (PAUP), vers. 4 0b10. Distributed by the Illinois Natural History Survey, Champaign, Illinois.

Tandy M, Tandy J. 1976. Evolution of acoustic behaviour in African *Bufo* (Anura: Bufonidae). *Zoologica Africana* **11:** 349–368.

Taylor WR, Van Dyke GC. 1985. Revised procedures for staining and clearing small fishes and other vertebrates for bone and cartilage study. *Cybium* **9:** 107–119.

Thompson JD, Gibson TJ, Plewniak F, Jeanmougin F, Higgins D. 1997. The Clustal–windows interface: flexible strategies for multiple sequence alignment aided by quality analysis tools. *Nucleic Acids Research* **25:** 4876–4882.

Tihen JA. 1960. Two new genera of African bufonids, with remarks on the phylogeny of related genera. *Copeia* **1960:** 225–223.

Tihen JA. 1962a. Osteological observations on New World *Bufo*. *American Midland Naturalist* **67:** 157–183.

Tihen JA. 1962b. A review of New World fossil bufonids. *American Midland Naturalist* **68:** 1–50.

Trueb L. 1971. Phylogenetic relationships of certain neotropical toads with the description of a new genus (Anura: Bufonidae). *Los Angeles County Museum Contributions in Science* **216:** 1–40.

Trueb L. 1993. Patterns of cranial diversity among the Lissamphibia. In: Hanken J, Hall BK, eds. *The skull*, Vol. 2*: Patterns of structural and systematic diversity.* Chicago: University of Chicago Press, 255–343.

Van de Peer Y, Van den Broeck I, De Rijk P, De Wachter R. 1994. Database on the structure of small subunit RNA. *Nucleic Acids Research* **22:** 3488–3494.

Venkatesh B, Erdmann MV, Brenner S. 2001. Molecular synapomorphies resolve evolutionary relationships of extant jawed vertebrates. *Proceedings of the National Academy of Sciences* **98:** 11382–11387.

Wanzhao L, Lathrop A, Jinzhong F, Datong Y, Murphy RW. 2000. Phylogeny of East Asian bufonids inferred from mitochondrial DNA sequences (Anura: Amphibia). *Molecular Phylogenetics and Evolution* **14:** 423–435.

Wiens JJ. 1998. Combining data sets with different phylogenetic histories. *Systematic Biology* **47:** 568–581.

Wiens JJ. 2001. Character analysis in morphological phylogenetics: problems and solutions. *Systematic Biology* **50:** 689–699.

Wiens JJ. 2004. The role of morphological data in phylogeny reconstruction. *Systematic Biology* **53:** 653–661.

Wiens JJ, Bonett RM, Chippindale PT. 2005a. Ontogeny discombobulates phylogeny: paedomorphosis and higher-level salamander phylogeny. *Systematic Biology* **54:** 91–110.

Wiens JJ, Reeder TW, Fetzner JW, Parkinson CL, Duellman WE. 2005b. Hylid frog phylogeny and sampling strategies for speciose clades. *Systematic Biology* **54:** 719–748.

APPENDIX 1

Specimens included in the morphological and combined analyses. Museum acronyms follow Leviton *et al*. (1985); [C&S], cleared and stained specimens.

SPECIMENS SCORED FOR MORPHOLOGICAL DATA

Alcohol-preserved specimes: **Outgroup taxa:** Leptodactylidae: *Leptodactylus ocellatus:* KU 289187–92 Paraguay: Parque Nacional San Rafael. Bufonidae: *Melanophryniscus stelzneri:* KU 93181–82 Argentina: Salta. *Osornophryne bufoniformis:* KU 117880, 189945 Ecuador: Carchi; KU 132126 Ecuador: Imbabura. *Pedostibes hosii:* KU 155590–93 Malaysia: Sarawak 4th Division Bintulu Dist. Tubau Camp on Sungei Pesu. *Rhamphophryne festae:* KU 209647 Ecuador: Morona-Santiago, W slope Cordillera de Cutucu, Camp 2, 1700 m; KU 217501 Ecuador: Pastaza, Locacion Petrolera Garza 1, NE Montalvo. *Schismaderma carens:* KU 195740, 195743 South Africa: Natal, 17 km N Mtubatuba, 60 m. *Truebella tothastes:* KU 196598 Peru: Ayacucho, Carapa, below Tambo on Tambo-Valle de Apurimac trail. *Truebella skoptes:* KU 196842 Peru: Junin, 5 km SW Comas, 2745 m. Bufonidae: *Bufo:* **North America:** *B. americanus:* KU 90141 USA: Iowa, Decatur, Graceland College; KU 109914 USA: Iowa, Mahaska, 0.8 km E Oskaloosa; KU 109916–17; Iowa, Mahaska, Pen Woods, Oskaloosa; KU 109918 USA: Iowa, Appanoose, 8.8 km E Moravia; KU 289469 USA: Whitehouse, Texas. *B. alvarius:* KU 43751–72 Mexico: Sinaloa. *B. boreas:* KU 51472 USA: Wyoming, Teton. *B. cognatus:* KU 98330 USA: South Dakota, Union County Park. *B. debilis:* KU 72961, 72966 USA: New Mexico, Doña Ana. *B. exsul:* KU 68824 USA: California, Inyo County, Deep Springs, 11 km S Deep Springs School. *B. punctatus:* KU 60519, 60525, 60533 Mexico: Tamaulipas, 5–8 km E Ciudad Victoria. *B. quercicus:* KU 90123 USA: Florida, Dade, 5 km W South Miami. *B. terrestris:* KU 187956 USA: Georgia, McIntosh, Sapelo Island; KU19161 USA: Georgia, Charlton, Folkston, Okefenokee Swamp. *B. woodhousii:* KU 220929 USA: Kansas, Ellis; KU 223460 USA: Kansas, Jefferson, 3 km W Nortonville. *B. fowleri:* USNM 314864 USA: Mississippi: Oktibbeha, Starkville. **West Indies:** *B. lemur:* KU 264172 Puerto Rico. **Central America:** *B. coccifer:* KU 184659, 184662 El Salvador: 16.5 km WNW Chalatenango. *B. coniferus:* KU 22098, 65437 Costa Rica: Cartago, Tapanti. *B. fastidiosus:* KU 107310 Panama: Bocas del Toro, N slope Cerro Pando; KU 107327 Panama: Bocas del Toro, N slope Cerro Pando 1300 m. *B. luetkenii:* KU 32810 Costa Rica: Puntarenas; KU 63734–38 Guanacaste, 4 km N Santa Rosa. *B. valliceps:* KU 86706 Mexico, Oaxaca, 11 km N Vista Hermosa, 900 m; KU 58336, 58359

Mexico: Oaxaca, 6 km N Palomares, 75 m. **Eurasia:** *B. andrewsi:* KU 208072 China: Sichuan, Ping-Wu-Co, Wang-Ba-Chu. *B. asper:* KU 40005 Thailand: Konsritamarat. *B. juxtasper:* KU 194730 Malaysia: Sabah, Ranau, Poring. *B. bufo:* KU 144228–29 Portugal: Baixo Alentejo, Sado Basin. *B. macrotis:* KU 194738 Thailand: Me Wang. *B. maculatus:* KU 63562, 63558 Liberia: Nimba, Sanniquellie. *B. melanostictus:* KU 150647–74 South Vietnam: Bien-hoa. *B. viridis:* KU 87796 Russia: Ukrainia, SSR, Kiev. **Africa:** *B. brauni:* KU 194719 Tanzania: Amani, E Usambara Mts. *B. pardalis:* KU 193374–75 South Africa: Cape. *B. regularis:* CAS 131373 Kenya: Rift Valley Province, Turkana District. *B. xeros:* KU 291138 Mali: Bamako. **South America:** *B. crucifer:* KU 93111, 93089, MNHNP 8738 Paraguay: Itapúa. *B. ocellatus:* KU 93115 Brazil: Para, Cachimbo. ***Bufo granulosus* group:** *B. azarai:* KU 290724–25 Paraguay. *B. dorbignyi:* KU 93096, Brazil: Rio Grande do Sul, Pelotas; KU 154590 Brazil: Rio Grande do Sul, Porto Alegre. *B. goeldii:* USNM 166294–95. *B. granulosus:* KU 73421, 73424 Paraguay: Boqueron, Loma Plata, Mennonite Colony. *B. major:* KU 136044–46 Bolivia: Cochabamba, 6.5 km N Chipiri, 260 m. *B. mirandaribeiroi:* USNM 28933 Brazil: Para to Manaos. *B. pygmaeus:* KU 93122–23 Brazil: Rio de Janeiro. ***Bufo guttatus* group:** *B. blombergi:* KU 169344 Colombia: Valle. *B. caeruleostictus:* KU 152059 Ecuador: Cotopaxi. *B. glaberrimus:* QCAZ 14708, QCAZ 13234 Ecuador. *B. guttatus:* KU 93108 Brazil: Para; KU 166712 Venezuela: Bolivar. *B. haematiticus:* KU 107364 Panama: Canal Zone. ***Bufo marinus* group:** *B. arenarum:* KU 93087 Brazil: Rio Grande, Torres. *B. ictericus:* KU 84873 Argentina: Misiones, Oberá. *B. marinus:* KU 98979 Ecuador: Sucumbios, KU 104742 Ecuador: Sucumbios. *B. poeppigii:* KU 183227–30 Bolivia, La Paz, Coroico. *B. rufus:* KU 196260 Brazil, Minas Gerais, Lagoa Santa. *B. schneideri:* KU 74326–7 Paraguay: Boqueron, Loma Plata, Mennonite Colony. ***Bufo spinulosus* group:** *B. amabilis:* CAS 9391417, KU 120361 120362–64, 120366–70 Ecuador: Loja. *B. arequipensis:* CAS 11140–41 Peru: Department Arequipa; UMMZ 64520, UMMZ 65898 Peru: Arequipa. *B. atacamensis:* KU 217349 Chile: Coquimbo. *B. chilensis:* KU 217359, 217362 Chile: Santiago, 2 km S Rungue. *B. cophotis:* KU 211685–729 Peru: 26 km NNW Cajamarca, S slope Abra Quilsh, 3500 m. *B. corynetes:* KU 173229 Peru: Cusco. *B. limensis:* KU 214802 Peru: Ancash; KU 215587 Peru: Ancash, 3 km ESE Casma, R'o Casma; UMMZ, 257557, 57553, USNM 120109 Peru: Ica. *B. rubropunctatus:* KU 179533, 179535 Argentina: Chubut, El Bolson (Río Negro). *B. amabilis:* KU 120361, 120362–64, 120366–70. *B. variegatus:* KU 161641 Chile: Llanquihue, 4 km W Lago Chapo. *B. vellardi:* KU 211764–67 Peru: Cajamarca. ***Bufo margaritifer* group:** *B. alatus:* KU 202271 Ecuador: Pichincha. *B. ceratophrys:* KU 154655 Ecuador: Pastaza, upper R'o Pastaza drainage. *B. dapsilis:* KU 139496 Colombia: Putumayo, San Antonio, Río Guamuez. *B.* cf. *margaritifer:* QCAZ 11597, 10601 Ecuador, KU 217492 Ecuador: Napo, Jatun Sacha; KU 217495, Ecuador: Pastaza. *B. nasicus:* ROM 20650 Guyana: Mazaruni-Potaro District, Potaro River, Tukeit, 100 m. *B. sternosignatus:* KU 185714 Venezuela: Aragua. ***Bufo veraguensis* group:** *B. arborescandens:* KU 209394 Peru: Amazonas, 5 km NW Mendoza. *B. chavin:* MTD 43789 Peru: Department Huánuco, Provincia Pachitea, Palma Pampa. *B. gallar*KU 198242 Argentina: Jujuy. *B. inca:* KU 136035, 136038 Peru: Cusco, Machu Picchu. *B. nesiotes:* KU 154921 Peru: Huanuco, W slope Serrania de Sira] UTA 53310 Bolivia: La Paz, Caranavi: Serran[apos]a de Bella Vista. *B. veraguensis:* KU 139115-31 Peru: Cusco] KU 163092 Peru: Ayacucho.

Osteological preparations

Leptodactylidae: *Leptodactylus ocellatus:* KU 289186 Paraguay: Parque Nacional San Rafael. Bufonidae: *Melanophryniscus stelzneri:* KU 93180 Argentina: San Luis [C&S]. *Osornophryne bufoniformis:* KU 144116 [C&S], KU 170103 Colombia: Cauca: Paramo Puracé; QCAZ 7684 [C&S]. *Pedostibes hosii:* KU 155595 Malaysia: Sarawak. *Schismaderma carens:* KU 195751 South Africa: Transvaal [C&S]; KU 195749 South Africa: Natal. *Truebella skoptes:* KU 196843 Peru: Junin [C&S]. *Truebella tothastes:* KU 196605 Peru: Ayacucho, Carapa [C&S]. Bufonidae: *Bufo:* **Africa:** *B. pardalis:* TNHC 33225 South Africa. *B. regularis:* CAS 122180; Africa: Kenya; CAS 131374 Africa: Kenya. *B. xeros:* CAS 122241, CAS 122245 Kenya: Eastern Province, Marsabit District. **North America:** *B. americanus:* KU 16457 KU 16444, 18194, 21146 USA: Kansas Douglas Co. Lawrence, Haskell Bottoms. *B. alvarius:* KU 14085, 25204 USA: Arizona. *B. boreas:* MVZ 142849 Canada: Vancouver Island. *B. cognatus:* KU 21149 USA: Kansas. *B. debilis:* KU 14099 USA: Texas; KU 73388 USA: New Mexico. *B. exsul:* MVZ 137717 USA: California. *B. fowleri:* AMNH 55672 USA: New York. *B. punctatus:* KU 73390 USA: New Mexico; KU 9107, 15314, 20984–85, 73391 USA: New Mexico. *B. quercicus:* KU 19474–77 USA: Mississippi. *B. terrestris:* AMNH 55551 USA: South Carolina. *B. woodhousii:* KU 7170 18185, 18209, 18249 USA: Kansas. **West Indies:** *B. lemur:* KU 288710 [C&S], USNM 226397, Puerto Rico: Santa Isabel. **Central America:** *B. coccifer:* KU 68147–48 Costa Rica: Puntarenas; KU 68151 Costa Rica: Cartago. *B. coniferus:* KU 68150 Costa Rica: Cartago. *B. holdridgei:* KU 103462 Costa Rica: Heredia. *B. luetkenii:* CAS 146942

KU 84927–28 Nicaragua: Managua; KU 84930, Nicaragua: Rivas *B. valliceps:* KU 59873 Guatemala: El Penten 10 km NNW Chinaga; KU 59874, KU 68155–56 Mexico: Chiapas; KU 52164 Nicaragua: Manaqua. Eurasia: *B. bufo:* CAS 98078, Spain: Madrid; KU 144227 Portugal: Baixo Alentejo. **Eurasia:** *B. asper:* FMNH 216228 Malaysia: Sarawak; KU 155584 Malaysia: Sarawak. *B. juxtasper:* FMNH 121320 North Borneo. *B. macrotis:* CAS 153004 Thailand: Nakhon Nayok Province. *B. melanostictus:* KU 129017 Singapore; KU 153941–42 Java: Central Java. *B. stomaticus:* KU 200370 India: Orissa, Sambalpur, Barpali. *B. viridis:* TNHC 51308 Europe. **Africa:** *B. maculatus:* AHR 121 Africa: Ghana, Tamara Island; CAS 103981; Ghana; ULM 192. **South America:** ***Bufo crucifer* group:** *B. crucifer:* KU 93112 Brazil: Espirito Santo. ***Bufo granulosus* group:** *B. goeldii*: USNM 290814 Brazil: Para; KU 292359, 292450 [C&S], 292453 [C&S], Brazil: Rondonia. *B. humboldti:* USNM 286985 Trinidad: St. George. *B. granulosus:* KU 110431 [C&S], 169346 [C&S], KU 10461, 110460 Colombia: Meta; KU 110462; KU 170090–92 Colombia: Magdalena. *B. mirandaribeiroi:* USNM 28934 Brazil: Para to Manaos. ***Bufo guttatus* group:** *B. blombergi:* KU 69843 Colombia: Santander; KU 59763, Ecuador, Collapi. *B. caeruleostictus:* KU 152057 Ecuador: Cotopaxi. *B. guttatus:* KU 167631 Venezuela: Bol'var. *B. haematiticus:* KU 41017 Costa Rica; KU 96160, Panama: Darien. ***Bufo margaritifer* group:** *B. margaritifer* 1: KU 93138 Brazil: Amapa; Brazil: Para; KU 205269 Peru: Madre de D'os. *B. margaritifer* 2: KU 104756 Ecuador: Napo; KU 127511. ***Bufo marinus* group:** *B. arenarum:* KU 71161 Uruguay: Artiga. *B. marinus:* KU 42566 Nicaragua: Managua; KU 69846 Mexico: Alta Verapaz; KU 84935–37 Nicaragua: Rivas; KU 152914 Ecuador: Napo. *B. poeppigii:* KU 18323435 Bolivia: La Paz. *B. scheideri:* KU 160307 Argentina: Santiago del Estero. ***Bufo spinulosus* group:** *B. amabilis:* KU 120365, 120371, 124587 Ecuador: Loja. *B. arequipensis:* KU 214793 Peru: Arequipa. *B. atacamensis:* KU 217351 Chile: Coquimbo. *B. chilensis:* KU 217363 Chile: Santiago. *B. cophotis:* KU 218517–18 Peru: Cajamarca [C&S]; 218525–26 Peru: Cajamarca. *B. corynetes:* KU 212555 Peru: Cusco. *B. limensis:* KU 209226 Peru: Lima. *B. rubropunctatus:* KU 159966 Chile: Llanquihue. *B. spinulosus:* KU 160270–72 Bolivia: Potos'; KU 163032; Peru: Puno; KU 163036 Peru: Puno; KU 163066 KU 163074 Peru: Ayacucho. *B. variegatus:* KU 161642 [C&S], KU 161651 Chile: Llanquigue. *B. vellardi:* KU 136053 Peru: Cajamarca. ***Bufo veraguensis* group:** *B. chavin:* MTD 43786–87 Peru: Department Huánuco, Provincia Pachitea, Palma Pampa; *B. veraguensis:* KU 164084 Peru: Cusco. *B.* sp. MTD 44751, Peru: Department Pasco.

APPENDIX 2

Taxa included in the molecular and combined analyses and their respective GenBank accession numbers. Order follows: family: taxon name: catalogue number; locality; GenBank accession number (gene order: 12S–16S, POMC, Rag-1). Museum abbreviations are listed in Leviton *et al*. (1985). Other abbreviations: DLR, Ignacio de la Riva private collection; AG, Andrew Gluesenkamp private collection; JRM, Joseph R. Mendelson private collection; AR, Alexander Robertson private collection.

Specimens used for DNA analyses

Outgroup Taxa: Hylidae: *Hyla cinerea:* KU 207358 (AY680271; AY819116; DQ158342). Leptodactylidae: *Ceratophrys cornuta:* KU 215537 (AY326014; AY819091; AY364218). *Eleutherodactylus w-nigrum:* KU 218136 (AY326004; DQ158260; DQ158344). *Leptodactylus ocellatus:* KU 289191; Paraguay: Parque Nacional San Rafael (DQ158417; DQ158259; DQ158343). Bufonidae: *Atelopus peruensis:* KU 211632; Peru: Cajamarca (DQ158419; DQ158261; DQ158345). *Dendroprhyniscus minutus:* QCAZ 883; Ecuador (DQ158420; DQ158262; DQ158346). *Melanophryniscus stelzneri:* KU 289071 Paraguay: Parque Nacional San Rafael (DQ158421; DQ158263; DQ158347). *Oreophrynella* sp. ROM 39649 Guyana, Mazaruni-Potaro District, Mount Ayanganna, NE plateau, 05°24′N, 059°57′W, 1500 m (DQ158422; DQ158264; DQ158348). *Rhamphophryne festae:* KU 217501 Ecuador: Pastaza (DQ158423; DQ158265; DQ158349). Africa: *Schismaderma carens:* MVZ 223386 Zimbabwe: Harare (DQ158424; DQ158266; DQ158350). Bufonidae: *Bufo:* **Africa:** *B. brauni:* FMNH 251853 Tanzania: Tanga Region, Muheza District (DQ158437; DQ158279; DQ158361). *B. cameruensis:* CAS 207288 Equatorial Guinea: Bioko Id (DQ158439; DQ158281; DQ158363). *B. garmani:* CAS 214829 Kenya: Kilifi Dist., Watamu (DQ158453; DQ158294; DQ158375). *B. gracilipes:* CAS 207620 Equatorial Guinea: Bioko Id (DQ158456; DQ158297; DQ158378). *B. gutturalis:* CAS 214842 Kenya: Kilifi Dist., Kararacha Pond II (DQ158460; DQ158301; DQ158382). *B. kisoloensis:* CAS 202005 Uganda: Rukungiri Dist., Bwindi Impenetrable National Park (DQ158464; DQ158305; n/a). *B. maculatus:* KU 290430 Ghana: Eastern Region, Muni Lagoon, Winneba (DQ158469; DQ158310; DQ158389). *B. poweri:* CAS 193885 Namibia: Okahandja (DQ158482; DQ158324; DQ158401). *B. regularis*: KU 290435; Ghana Eastern Region: Winneba (DQ158485; DQ158326; DQ158404). *B. steindachneri:* CAS 214839 Kenya: Kilifi Dist., Kararacha Pond (DQ158488; DQ158329; DQ158406).

B. xeros: AMNH 109826 (DQ158499; DQ158340; DQ158414). **Eurasia:** *B. andrewsi* 1: CAS 214911 China: Yunnan Province: Nu Jiang Prefecture (DQ158427; DQ158269; n/a). *B. andrewsi* 2: USNM 292081 China: Sichuan, Shimian, Shimian, *c.* 17 km SSE of, along Dahonggou Creek in forest reserve 2200 m (DQ158428; DQ158270; DQ158353). *B. asper:* FMNH 248148 Brunei, Belait Dist. Labi, Sg Mendaram (DQ158431; DQ158273; DQ158356). *B. bufo:* MVZ 230209 Turkey: Bursa Province (DQ158438; DQ158280; DQ158362). *B. galeatus:* FMNH 256443 Lao PDR: Khammouane Prov. Nakai Dist. Nakai Nam (DQ158452; DQ158293; DQ158374). *B. juxtasper:* FMNH 231245 Malaysia, Sabah, Lahad Datu Dist., Danum Valley Research Center (DQ158463; DQ158304; DQ158385). *B. macrotis:* FMNH 255318; Lao PDR: Champassak Prov. Mounlapamok Dist., Dong Khanthung National Biodiversity Conservation Area (DQ158468; DQ158309; DQ158388). *B. melanostictus:* FMNH 255309 Lao PDR: Champassak Prov Mounlapamok Dist, Dong Khanthung National Biodiversity Conservation Area (DQ158475; DQ158317; DQ158394). **North America:** *B. alvarius:* USNM 320001 USA: Arizona (DQ158425; DQ158267; DQ158351). *B. americanus:* KU 289469 USA: Texas (DQ158426; DQ158268; DQ158352). *B. boreas:* MVZ 223292 USA: California, Mendocino County (DQ158498; DQ158339; DQ158413). *B. cognatus* 1: LSUMZ H-457 USA: Arizona: Cochise Co., Chirichua Mts. 1.3 km E and 1.6 km N Portal along W side of Foot Hills Road (DQ158444; DQ158285; DQ158367). *B. debilis* 1: USNM 320116 USA: New Mexico (DQ158449; DQ158290; DQ158371). *B. exsul:* MVZ 137717 USA: California, Inyo Co., Deep Springs Valley, Buckhorn Spring (DQ158450; DQ158291; DQ158372). *B. fowleri:* USNM 314864 USA: Mississippi: Oktibbeha, Starkville (DQ158451; DQ158292; DQ158373). *B. microscaphus:* USNM 320147 USA: New Mexico (DQ158476; DQ158318; DQ158395). *B. quercicus* 1: LSUMZ 57048 USA (DQ158484; n/a; DQ158403). *B. quercicus* 2: LSUMZ H-2921 USA: Louisiana: St. Tammany Parish: Money Hill Plantation, Tailsheek Swamp NE of Abita Springs (DQ158483; DQ158325; DQ158402). *B. terrestris:* LSUMZ H2904 (DQ158489; DQ158330; n/a). *B. woodhousii:* KU 224658 USA: Kansas, Barber Sharon (DQ158498; DQ158339; DQ158413). **West Indies:** *B. lemur:* Anna Goebel; Puerto Rico (DQ158465; DQ158306; DQ158386). **Central America:** *B. coccifer:* KU 290030 El Salvador: Morazan, Perkin Lenca Hotel grounds, c. Perquin (DQ158443; DQ158284; DQ158366). *B. coniferus:* KU 217480 Ecuador: Pichincha, 1.0 km E Vicente Maldonado (DQ158445; DQ158286; DQ158366). *B. luetkenii:* KU 289850 El Salvador: Usulutan, Cerro del Tigre (DQ158467; DQ158308; DQ158387). *B. valliceps* 1: JRM 3870 Mexico: Veracruz: along road between Catemaco and Sontecomapan (DQ158492; DQ158333; DQ158408). *B. valliceps* 2: USNM 534129 Honduras: Colon (DQ158493; DQ158334; DQ158409). **South America:** ***Bufo crucifer* group:** *B. crucifer:* USNM 303015 Brazil: Sao Paulo (DQ158447; DQ158288; n/a). *B. ocellatus:* MZUSP 103261 Brazil: Peixe Tocantins (DQ158479; DQ158321; DQ158398). ***Bufo granulosus* group:** *B. granulosus* 1: USNM 302450 Brazil: Roraima (DQ158457; DQ158298; DQ158379). *B. granulosus* 2: AF0093 (DQ158458; DQ158299; DQ158380). *B. humboldti:* USNM 286986 Trinidad (DQ158434; DQ158276; DQ158358). ***Bufo guttatus* group:** *B. glaberrimus* 1: QCAZ 14708 Ecuador (DQ158454; DQ158295; DQ158376). *B. glaberrimus* 2: QCAZ 13234 Ecuador: Provincia Napo, Talag Alto (DQ158455; DQ158296; DQ158377). *B. guttatus:* LSUMZ 17418 Brazil: Rondonia: Parque Estadual Guajara-Mirim (DQ158459; DQ158300; DQ158381). *B. haematiticus* 1*:* QCAZ 13215 Ecuador: Esmeraldas, 5 km W of Durango (DQ158461; DQ158302; DQ158383). *B. haematiticus* 2*:* QCAZ 17083 Ecuador: Provincia Esmeraldas, Alto Tambo (DQ158435; DQ158277; DQ158359). ***Bufo marinus* group:** *B. arenarum:* AR305 Argentina (DQ158429; DQ158271; DQ158354). *B. ictericus*: AF 312 Brazil: Carapicuiba, Sao Paulo (DQ158462; DQ158303; DQ158384). *B. marinus* 1: KU 289750 El Salvador: Ahuachapan, Parque Nacional El Imposible, La Fincona (DQ158473; DQ158315; DQ158392). *B. marinus* 2: KU 217482 Ecuador: Loja, Vilcabamba (DQ158474, DQ158316; DQ158393). *B. poeppigii:* USNM 268824 Peru: Madre de Dios (DQ158481; DQ158323; DQ158400). *B. rufus:* AF 388; Brazil: Santa Barbara, Minas Gerais (DQ158486; DQ158486; n/a). *B. schneideri:* KU 289057 Paraguay: Parque Nacional San Luis de la Sierra (DQ158480; DQ158322; DQ158399). ***Bufo spinulosus* group:** *B. arequipensis:* KU 214792 Peru: Arequipa Arequipa Zamacola, 5 km NNW Arequipa, Distrito Cerro Colorado (DQ158430; DQ158272; DQ158355). *B. atacamensis:* KU 217352 Chile: Coquimbo, Cuesta Pajonales, 117 km N La Serena (DQ158433; DQ158275; DQ158357). *B. chilensis:* KU 217369 Chile: Santiago, 2 km S Rungue (DQ158442; DQ158283; DQ158365). *B. cophotis:* KU 211685 (DQ158446; DQ158287; DQ158369). *B. limensis:* KU 215587 (DQ158466; DQ158307; n/a). *B. spinulosus:* DLR 3837 Bolivia: La Paz, Creek between Charazani and Curva, prov. (DQ158487; DQ158328; DQ158405). *B. variegatus:* IZUA 3198 Chile: Puerto Edén, Isla Wellington, Provincia de Mafallanes, XII Región (DQ158494; DQ158335; DQ158410). *B. vellardi:* KU 211765 Peru: Cajamarca, 10 km SSE Cajabamba, 2900 m (DQ158495; DQ158336; DQ158411). ***Bufo margaritifer* group:** *B. castaneoticus:* LSUMZ 17429

Brazil: Para: 100 km S Santarem (DQ158440; DQ158282; DQ158364). *B. dapsilis:* QCAZ 3509 Ecuador: Pichincha, Bosque Protector La Perla, 5 km E La Concordia (DQ158448; DQ158289; DQ158370). *B.* cf. *margaritifer* 1: QCAZ 10601 Ecuador: Francisco de Orellana, Parque Nacional Yasuní (DQ158470; DQ158312; n/a); *B.* cf. *margaritifer* 2: QCAZ 13896 Ecuador: Cañar, Manta Real (DQ158471; DQ158313; DQ158390). *B.* cf. *margaritifer* 3: QCAZ 11597 Ecuador: Provincia Esmeraldas, Bosque Protector, 30 km from San Lorenz by way of Ibarra (DQ158472; DQ158314; DQ158391). *B.* cf. *margaritifer* 4*:* USNM 268828 Peru: Madre de Dios (DQ158490; DQ158331; DQ158407). *B.* cf. *margaritifer* 5: KU 215145 Peru: Madre de Dios (DQ158491; DQ158332; n/a). *B. nasicus:* ROM 20650 Guyana: Mazaruni-Potaro District, Potaro River, Tukeit, 05°13′N, 059°25′W, 100 m (DQ158477; DQ158319; DQ158396). ***Bufo veraguensis* group:** *B. chavin:* MTD 43789 Peru: Depto. Huánuco, Provincia Pachitea, Palma Pampa (DQ158441; n/a; n/a). *B. nesiotes:* UTA A53310; South America: Bolivia, La Paz (DQ158478; DQ158320; DQ158397). *B. veraguensis* 1: DLR 3820 Bolivia: La Paz (DQ158496; DQ158337; DQ158412). *B. veraguensis* 2: USNM 346048 Peru: Cusco (DQ158497; DQ158338; n/a).

APPENDIX 3

MORPHOLOGICAL CHARACTER DESCRIPTIONS

Transformation series are organized by anatomical region and numbered sequentially. Characters relating to a single structure or series of structures are grouped together. However, the order in which characters are presented within each anatomical region is arbitrary. Each account provides a description of the different character states and their codings; most characters are illustrated to clarify the description. Where appropriate, accounts also include references to prior investigators who included these characters in their analyses.

1. Ratio of head width to head length. To quantify overall head shape, the ratio of head width to head length was calculated from measurements. Head width was measured at the level of jaw symphysis; head length was measured from the tip of the snout to the posterior edge of the midline of the foramen magnum. Length less than width (0); length greater than width (1).

2. Sculpturing of dermal roofing bones. The dermal bones (i.e. frontoparietals, sphenethmoid, and nasals) display varying degrees of ornamentation that result from exostosis. Dermal bones of skull completely smooth (0); lightly exostosed (1); heavily ornamented with pits, striations, and rugosities (2).

3. Medial articulation of nasals. The nasal bones may articulate along their entire medial length, or as in some more lightly ossified species (e.g. *B. chilensis*), may be separated medially. Medial articulation present (0; e.g. *B. marinus*; Fig. 5A); nasals not articulating medially (1).

4. Nasals, shape of anterior margins. In dorsal view, the shape of the anterior margin of the paired nasal bones is variable. The shape of the anterior margins can be relatively blunt (0; e.g. *B. crucifer*; Fig. 6A) or acuminate (1; e.g. *B. margaritifer*; Fig. 6D).

5. Nasals, shape of posterior margins. In dorsal view, the shape of the posterior margin of the nasal bones is variable. The posterior margins may be arcuate (0), relatively blunt and perpendicular to the medial axis of the skull (1; e.g. *B. crucifer*; Fig. 6A), or extremely arcuate (2; e.g. *B. margaritifer*; Fig. 6D).

6. Contribution of nasals to orbital margin. In most *Bufo* examined, the nasals compose less than half of the orbital margin in dorsal view. The frontoparietal–nasal suture may be angled slightly anterolaterally (0), nearly transverse (1), angled slightly posterolaterally (2), or orientated extremely posterolaterally in relation to the medial axis of the skull, with half or more of the orbital margin being composed of nasal bone (3).

7. Lateral articulation of nasal bones. Typically, in anurans, the preorbital process of the maxilla articulates with the posterolateral margin of the maxillary process of the nasal (0; e.g. *B. caeruleostictus*; Fig. 8G). In all members of the *B. granulosus*, *B. margaritifer*, and *B. peltocephalus* groups, the nasals articulate with the dorsal margin of the pars facialis of the maxilla from the preorbital process to the posterior margin of the narial opening (1; e.g. *B. granulosus*; Fig. 8B).

8. Contact between nasal and frontoparietal. If the posteromedial edge of the nasal and the anteromedial edge of the frontoparietal are not in contact, the dorsal surface of the sphenethmoid is visible (0; e.g. *B. valliceps*; Fig. 6F); it is covered if the posteromedial edge of the nasal articulates with the frontoparietal (1; e.g. *B. granulosus*; Fig. 6B).

9. Occipital artery pathway. The occipital canal is formed by posterior elaboration of the frontoparietal and/or the involvement of the dermis of the head in coossification (Lynch, 1971; Mendelson, da Silva & Maglia, 2000). The canal encloses the occipital artery and lies over the prootic; the artery may be partially or entirely enclosed. Occipital canal uncovered (0; e.g. *B. cophotis*; Fig. 6H); partially covered (1; e.g. *B. veraguensis*; Fig. 6E); completely covered with bone (2; e.g. *B. valliceps*; Fig. 6F).

10. Articulation of anterior process of vomer and maxilla. The anterior process of vomer free (0; e.g. *B. quercicus*); articulating with maxilla only (1; e.g. *B. juxtasper*); articulating with maxilla and premax-

illa (2; e.g. *B. valliceps*; Fig. 7F); articulating with premaxilla only (3; Fig. 7E, *B. veraguensis*).

11. Medial contact of frontoparietals. In some taxa, the frontoparietals are in contact medially (0; e.g. *B. amabilis*; Fig. 6C), whereas in other species (e.g. *B. viridis*), they are separated medially (1).

12. Expansion of medial ramus of pterygoid. This character was described by Martin (1972a) as an occlusion of the suprapterygoid fenestra. Variation in this character is correlated with dorsal expansion of the medial ramus of the pterygoid. Medial ramus of pterygoid not enlarged, creating a large subprootic fenestra (0; e.g. *B. woodhousii*; Fig. 12A); enlargement covering half or less of the subprootic fenestra (1; e.g. *B. blombergi*; Fig. 12C); enlargement covering all of subprootic fenestra (2; e.g. *B. poeppigii*; Fig. 12D).

13. Expansion of posterior ramus of pterygoid. In examined members of the *B. margaritifer* group, the posterior ramus of the pterygoid is expanded to varying degrees (C. Vélez-R., pers. comm.). Posterior ramus not expanded (0; e.g. *B. valliceps*; Fig. 8F); posterior ramus expanded (1; e.g. *B. margaritifer*; Fig. 8D).

14. Articulation of zygomatic and ventral rami of squamosal. In most *Bufo*, the zygomatic ramus of the squamosal is free from the ventral ramus and the maxilla (0; *B. crucifer*; Fig. 8A). In examined species of the *B. granulosus* group, and in *B. lemur* of the *B. peltocephalus* group, the zygomatic ramus of the squamosal articulates with the maxilla, thereby completing the bony margin of the orbit; this is the 'closed orbit condition' of *B. granulosus*, *sensu* Cei (1972) (1; Fig. 8B).

15. Shape of otic (medial) ramus of squamosal. Otic ramus of squamosal present, not enlarged (0; e.g. *B. cophotis*; Fig. 6H); otic ramus of squamosal slightly enlarged, overlapping with the dorsal surface of the crista parotica (1; e.g. *B. amabilis*; Fig. 6C); otic ramus enlarged, in contact with posterolateral margin of frontoparietal, forming a continuous temporal arcade (2; e.g. *B. crucifer*; Fig. 6A).

16. Squamosal, angle of ventral ramus, posterior view. In posterior view, the ventral ramus of the squamosal may be angled ventrolaterally (0; e.g. *B. woodhousii*; Fig. 12A) or may be approximately perpendicular to the dorsal surface of the otic capsule (1; e.g. *B. granulosus*; Fig. 12B).

17. Columella (stapes). The columella is absent in several non-*Bufo* bufonids (e.g. *Melanophryniscus*, *Osornophryne*, *Schismaderma*, *Truebella*), as well as three examined species of the *B. spinulosus* group (*B. cophotis*, Fig. 8H; *B. corynetes*; *B. variegatus*). Columella present (0); absent (1).

18. Columella shape. The stapes of most anurans is a simple, rod-shaped bone. In some taxa (e.g. *Leptodactylus ocellatus*), the stapes is blade shaped and com-

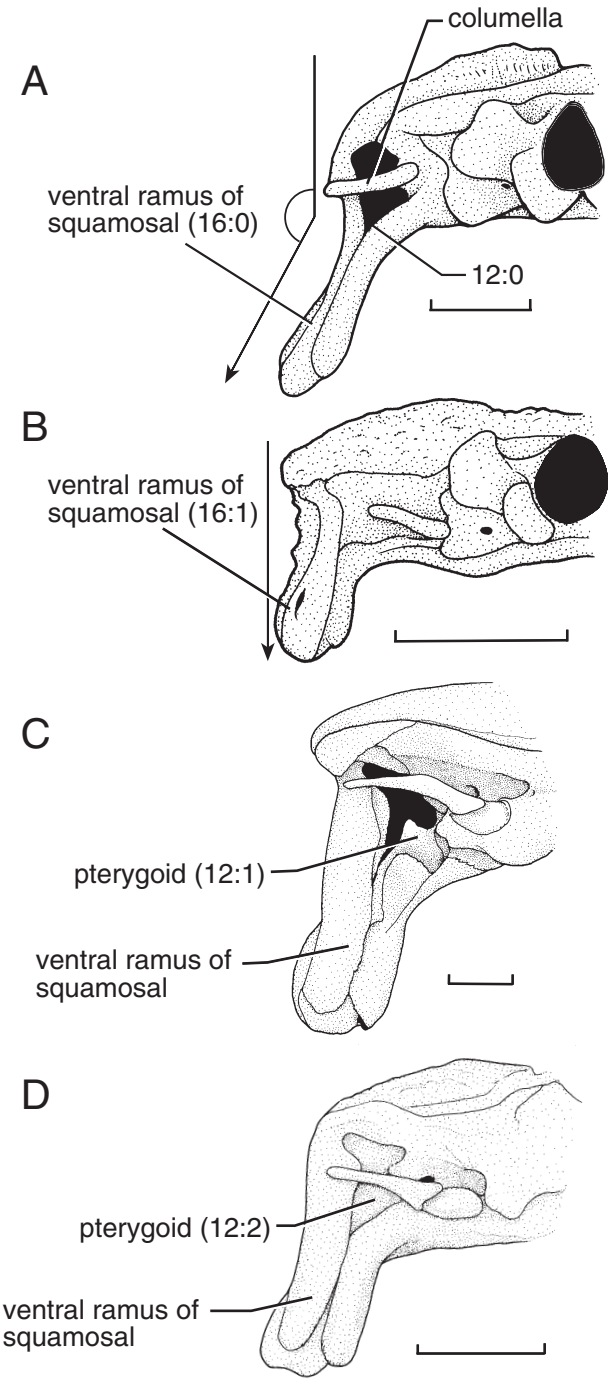

Figure 12. Occipital aspect of the skull. A, *Bufo woodhousii* (KU 18209). B, *B. granulosus* (KU 170090). C, *B. blombergi* (KU 69843). D, *B. poeppigii* (KU 183235). Characters 12 and 16 (expansion of the medial ramus of the pterygoid and angle of the ventral ramus of the squamosal, respectively) are illustrated. Scale bars = 5 mm.

pressed anteroposteriorly (0), whereas in other taxa (e.g. *B. marinus*), it is rod shaped (1).

19. Contact of medial ramus of pterygoid with ala of parasphenoid. The medial ramus of the pterygoid is not in contact or barely in contact with the anterolateral margin of the ala of the parasphenoid (0; e.g. *B. cophotis*; Fig. 7H), fused with the anterolateral margin of the parasphenoid (1; e.g. *B. veraguensis*; Fig. 7E), or fused and extending medially along approximately half the length of the parasphenoid ala (2; e.g. *B. marinus*; Fig. 5B).

20. Jugular foramina. In ventral view, the jugular foramina are round openings located on the ventral surface of the exoccipital (0; e.g. *B. granulosus*; Fig. 7B). However, in the *B. guttatus* group, they are orientated posterolaterally, and are not visible in ventral view (1; e.g. *B. caeruleostictus*; Fig. 7G).

21. Anterior margin of nasals. In lateral view, the anterior margins of the nasal bones are flush with the dorsal margins of the alary processes of the premaxillae (0; e.g. *B. marinus*; Fig. 5C), extend beyond the dorsal margins of the alary processes (1; e.g. *B. valliceps*; Fig. 8F), or lie posterior to the dorsal margins of the alary processes (2; e.g. *B. cophotis*; Fig. 8H).

22. Medial process. Pregill (1981) described a narrow, shelf-like process extending medially from the pars facialis of the maxilla that is present in the *B. peltocephalus* group; this was referred to as the preorbital process of the pars facialis by Morrison (1994). The process is visible in ventral view and articulates posteriorly with the neopalatine and laterally with the pars palatina of the maxilla. This process is reduced or absent in most outgroup taxa and some *Bufo* examined (0; e.g. *B. cophotis*; Fig. 7H) and is expanded and visible in ventral view in most *Bufo* examined (1; e.g. *B. marinus*; Fig. 5B).

23. Maxillary extension. In most *Bufo* (e.g. *B. crucifer*; Fig. 7A), the anterior edge of the maxilla abuts the premaxilla. However, in most members of the *B. peltocephalus* group (e.g. *B. lemur*) and one species of the *B. granulosus* group (*B. goeldii*), the paired maxillae overlap the lateral margin of the premaxillae (Pramuk, 2000: fig. 4). No overlap of premaxilla by maxilla (0); maxillae extending beyond lateral margin of premaxillae (1).

24. Expansion of pars facialis of maxilla. The pars facialis of the maxilla is a dorsally directed flange. The dorsal process can be relatively expanded at the point where it articulates anteromedially with the premaxilla (0; e.g. *B. marinus*; Fig. 5C) or be relatively equal in height from the anterior margin of the orbit to the point of articulation between the maxilla and the premaxilla (1; e.g. *B. margaritifer*; Fig. 8D).

25. Jaw articulation. In lateral view, jaw articulation may lie posterior to the fenestra ovalis (0; e.g. *B. marinus*; Fig. 5C), opposite the fenestra ovalis (1; e.g. *B. veraguensis*; Fig. 8E), or anterior to it (2; e.g. *B. cophotis*; Fig. 8H).

26. Alary process. The alary processes of the premaxillae project dorsally from the pars palatina of the premaxillae. Alary processes are perpendicular (0; *B. veraguensis*; Fig. 8E), angled posteriorly (1; e.g. *B. cophotis*; Fig. 8H), or angled anteriorly (2; e.g. *B. margaritifer*; Fig. 8D) to the anterior margin of the premaxillae.

27. Ridges on cultriform process of parasphenoid. In some taxa, the ventral surface of the cultriform process is smooth (0; e.g. *B. caeruleostictus*; Fig. 7G), whereas in others it bears a pair of ridges that are parallel to the medial axis of the skull (1; e.g. *B. crucifer*; Fig. 7A).

28. Ridges on medial surface of parasphenoid corpus. The medial surface of the parasphenoid corpus of some species is smooth (0; e.g. *B. marinus*; Fig. 5B), whereas in others it bears a pair of ridges that converge medially (1; e.g. *B. valliceps*; Fig. 7F).

29. Parasphenoid, shape of anterior edge of cultriform process. The anterior end of the cultriform process has one of two shapes; it may be acute and narrow (0), or broadly rounded anteriorly (1).

30. Direction of parasphenoid alae. The orientation of the long axes of the parasphenoid alae may be posterolateral (0), lateral (1; e.g. *B. crucifer*; Fig. 7A), or anterolateral (2; e.g. *B. marinus*; Fig. 5B).

31. Articulation of medial ramus of pterygoid and parasphenoid alae. In most *Bufo*, the suture between the medial ramus of the pterygoid and the parasphenoid is smooth (0; e.g. *B. margaritifer*; Fig. 7D), whereas in members of the *B. marinus* group it is jagged or scalloped (1; e.g. *B. marinus*; Fig. 5B).

32. Anterior extent of cultriform process. In some taxa, the anterior terminus of the cultriform process is at the level of, or barely beyond, the anterior edge of the optic foramen (0; e.g. *B. veraguensis*; Fig. 7E). In other taxa, the end of the cultriform process is midway between the optic and orbitonasal foramina (1; e.g. *B. crucifer*; Fig. 7A), whereas in others it extends beyond the orbitonasal foramina (2; e.g. *B. valliceps*; Fig. 7F).

33. Medial separation of occipital condyles. Tihen (1962a) proposed that features of the occipital condyles might indicate a close relationship between bufonids and genera of ceratophryine leptodactylids. Lynch (1971: 52) suggested that the degree of separation between occipital condyles (broad vs. narrow) might be size dependent. Because both conditions occur in small bufonids, the character is included in this analysis. Occipital condyles are widely separated (0; e.g. *B. granulosus*; Fig. 6B) or closely juxtaposed (1; e.g. *B. crucifer*; Fig. 6A).

34. Level of ossification of sphenethmoid. The sphenethmoid is lightly ossified, creating a large, tri-

angular exposure of the planum antorbitale cartilage (0; e.g. *B. marinus*; Fig. 13A), moderately ossified, creating a small triangular region of the cartilage exposed (1; e.g. *B. granulosus*, Fig. 13B), or highly ossified, extending to the dorsolateral edge of neopalatine, planum antorbitale not exposed (2; e.g. *B. veraguensis*; Fig. 13C).

35. Shape of sphenethmoid in ventral view. In most specimens examined, the ventral braincase is narrow (0; e.g. *B. margaritifer*; Fig. 7D), whereas in the members of the *B. guttatus* group, it is distinctively broad (1; e.g. *B. caeruleostictus*; Fig. 7G).

36. Posterior process of prootic. In many *Bufo* there is an elaboration of the dermal bone at the point of contact of the exoccipital and the posteromedial edge of the prootic. This process is distinctively large and notched in members of the *B. guttatus* group (0; e.g. *B. caeruleostictus*; Fig. 6G); in other taxa it is moderately prominent (1; e.g. *B. marinus*; Fig. 5A).

37. Anterior extension of sphenethmoid. In ventral view, the anterior margin of the sphenethmoid extends anteriorly only to the posterior margin of the vomers (0; e.g. *B. amabilis*; Fig. 7C), extends anteriorly approximately to the middle of the vomers (1; e.g. *B. margaritifer*; Fig. 7D), or extends to the posterior margin of the premaxillae (2; e.g. *B. veraguensis*; Fig. 7E).

38. Ventral ridge of neopalatine. In many species of *Bufo* the neopalatine bears a ventral, transverse ridge. Ventral ridge of neopalatine present (0; e.g. *B. crucifer*; Fig. 7A); or absent (1; e.g. *B. veraguensis*; Fig. 7E).

39. Neopalatine, relative width medial and lateral edge. The lateral end of the neopalatine may be broader than the medial end (0; e.g. *B. marinus*; Fig. 5B), the neopalatine may be the same width along its entire length (1; e.g. *B. veraguensis*; Fig. 7E) or the medial end may be broader than the lateral end (2; e.g. *B. amabilis*; Fig. 7C).

40. Neopalatine separation. The neopalatines may be nearly in contact at the midline of the sphenethmoid (0; e.g. *B. marinus*; Fig. 5B), or be separated widely, contacting the sphenethmoid only marginally (1; e.g. *B. cophotis*; Fig. 7H).

41. Anterolateral foramen. In species that bear a preorbital crest that is confluent with a suborbital crest (e.g. *B. lemur* and members of the *B. granulosus* group), a foramen perforates the ventrolateral surface of the nasal (1; e.g. *B. granulosus*; Fig. 13B), whereas in most *Bufo*, this foramen is absent (0; e.g. *B. veraguensis*; Fig. 13C).

42. Prenasal bones. These elements, described by Pramuk (2000), are paired, ovoid, dermal bones that lie posterior to the nares and are unique among bufonids to members of the *B. granulosus* group. Prenasal bones absent (0; e.g. *B. veraguensis*; Fig. 6E); present (1; e.g. *B. granulosus*; Fig. 6B).

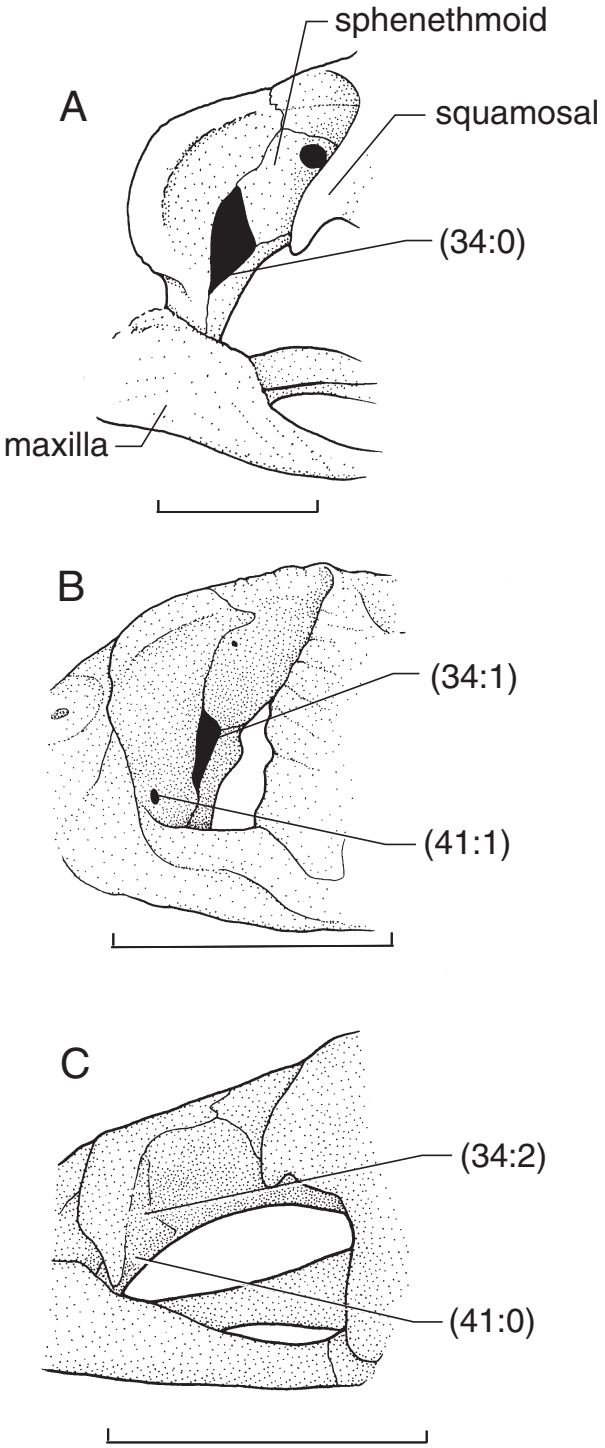

Figure 13. Posterolateral aspect of the orbits. A, *Bufo marinus* (KU 42566). B, *B. granulosus* (KU 170090). C, *B. veraguensis* (KU 164084). Character 34 (variable amount of ossification of the sphenethmoid) is illustrated. The black areas in (A) and (B) indicate the cartilage of planum antorbitale. Scale bars = 5 mm.

43. Articulation of maxilla and quadratojugal. In lateral view, the articulation of the posterior margin of the maxilla with the quadratojugal may have one of three orientations: posterior edge of the maxilla positioned ventrally to the quadratojugal (0); maxilla lateral to the quadratojugal (1); maxilla positioned dorsally to the quadratojugal (2); quadratojugal reduced and not in contact with the maxilla (e.g. *B. variegatus*; 3). In some taxa (e.g. *B. granulosus*), the condition of the quadratojugal is obscured by a heavy outgrowth of dermal bone; these were scored as unknown.

44. Number of presacral vertebrae. The anuran vertebral column is composed of the presacral, sacral, and postsacral regions; *Bufo* resemble most other neobatrachia in having eight presacral vertebrae and lacking ribs. In *Pedostibes hosii*, vertebra II is fused with III. However, this taxon was coded as having eight vertebrae present. Eight presacral vertebrae present (0); reduction in the number of presacral vertebrae (≤ seven) (1).

45. Posterior margin of neural arch. The posteromedial margin of the neural arches of the four posteriormost vertebrae may be spinous (0; e.g. *B. marinus*; Fig. 9C), relatively smooth (1; e.g. *B. woodhousii*; Fig. 9K), indented (2), or as in a few taxa there is a conspicuous channeled groove present that is visible in both whole and skeletal material (3; e.g. *B. asper*; Fig. 9J).

46. Relative lengths of transverse processes of vertebrae V and VI. The length of the transverse process of vertebra VI may be less than (0; e.g. *B. margaritifer*; Fig. 9D), approximately equal in length (1; e.g. *B. cophotis*; Fig. 9G), or greater than the length of vertebra V (2; e.g. *B. guttatus*; Fig. 9H).

47. Presacral vertebrae, orientation of transverse processes of vertebra VI. The transverse process of vertebra VI is orientated posterolaterally (0; e.g. *B. granulosus*; Fig. 9B) or perpendicularly in relation to the medial axis of the vertebral column (1; e.g. *B. debilis*).

48. Orientation of transverse processes of presacral vertebra VII. The transverse process of vertebra VII is orientated posterlaterally (0), perpendicularly (1; e.g. *B. asper*; Fig. 9J), or anterior in relation to the medial axis of the vertebral column (2; e.g. *B. veraguensis*; Fig. 9E).

49. Orientation of transverse processes of presacral vertebra VIII. The transverse process of vertebra VIII is orientated posterolaterally (0), or anteriorly in relation to the medial axis of the vertebral column (1; e.g. *B. guttatus*; Fig. 9H).

50. Lateral flange of the urostyle. In some species, the urostyle lacks lateral flanges (0; e.g. *B. margaritifer*; Fig. 9D). However, in other taxa, lateral flanges are present (1; e.g. *B. valliceps*; Fig. 9F) and in others (e.g. *Osornophryne bufoniformis*), the flanges are greatly expanded (2).

51. Shape of sacral diapophyses. The sacral diapophyses of some taxa (e.g. *Leptodactylus*) are relatively cylindrical, whereas those of the *B. peltocephalus* and *B. granulosus* groups are broadly dilated and flat. The width of the sacral diapophysis is smaller than its length (0; e.g. *B. marinus*; Fig. 9C), or equal to, or greater than, its length (1; e.g. *B. granulosus*; Fig. 9B).

52. Angle of anterior edge of sacral diapophyses. The anterior edge of the sacral diapophyses can be angled approximately posteriorly (0; e.g. *B. marinus*; Fig. 9C), perpendicularly (1; e.g. *B. nasicus*; Fig. 9I), or anteriorly (2; e.g. *B. woodhousii*; Fig. 9K) to the midline axis of the vertebral column.

53. Posterior margin of sacral diapophyses. The posteromedial margin of the sacrum is relatively smooth (0; e.g. *B. asper*; Fig. 9J), or bears a depression (1; e.g. *B. granulosus*; Fig. 9B) to accommodate the dorsal crest of the urostyle.

54. Dorsal protuberance of ilium. The dorsal crest of the ilium is large, and slightly directed anteriorly or more dorsally directed (perpendicular to the axis of the ilium in lateral view) (0; e.g. *B. valliceps*; Fig. 10B), or small, low and projected laterally (1; e.g. *B. cophotis*; Fig. 10A).

55. Symphysis of ilia of pelvis. In lateral view, the angle that the anteroventral margin of the symphysis of the ilia forms with the ilial shaft of the pelvic girdle can be acute (0; *Leptodactylus*), perpendicular to the plane of the ilia, forming a 90° angle (1; e.g. *B. valliceps*; Fig. 10B), or forms an obtuse angle (2; e.g. *B. cophotis*; Fig. 10A).

56. Dorsal crest of ilial shaft. In medial view, a dorsal crest on the ilial shaft can be absent (0; e.g. *B. margaritifer*), whereas in others it is present, but weak (1; e.g. *B. marinus*), or present and well developed (2; e.g. *B. asper* and *B. juxtasper*).

57. Relative contribution of ischium to pelvic girdle. In lateral view, the contribution of the ischium to the pelvic girdle is variable. The ischium can be relatively small, with its dorsal margin extending to the level of, or above, the ventral margin of the acetabulum (0; e.g. *B. cophotis*; Fig. 10A), or it can be larger, extending below the ventral margin of the acetabulum (1; e.g. *B. valliceps*; Fig. 10B).

58. Ilial crest in dorsal view. In some taxa there is a medially projecting ridge associated with the dorsal crest of the ilium that can be seen in dorsal view. The ridge may be present (0; e.g. *B. veraguensis*) or absent (1; e.g. *B. margaritifer*).

59. Acetabular expansion of ischium. In some taxa (i.e. members of the *B. granulosus* group), the ischium has a well-developed 'flag-shaped' posteroventral expansion of the ischium. Postventeral crest poorly

developed (0; e.g. *B. margaritifer*; Fig. 10D); well developed (1; e.g. *B. granulosus*; Fig. 10C).

60. Omosternum. The omosternum is a prezonal element of the pectoral girdle. The presence of this element is homoplastic among anurans and it is present in some *Bufo* examined (e.g. *B. guttatus* group and poorly developed in some members of the *B. valliceps* group). Omosternum present (0); absent (1).

61. Shape of ultimate phalanx of manus. The ultimate phalanx of the manual digits in *Bufo* may be pointed (0; e.g. *B. spinulosus*), or a modified T-shape (1; e.g. *B. lemur*; Pramuk, 2002: fig. 10).

62. Relative length of manual digits. Length of digit I >II (0); digit I = II (1); digit I < II (2).

63. Canthal crest. The terminology used for cranial crests follows Mendelson (1997a). The position of the crests is illustrated in Figure 14. The canthal crest is formed by a raised ridge of bone along the anterolateral margin of the nasal. Absent (0); present (1).

64. Parietal crest. The parietal crest is on the frontoparietal and squamosal. Absent (0); present (1).

65. Preorbital crest. The preorbital crest is located on the maxillary process of the nasal. Absent (0); present (1).

66. Pretympanic crest. The pretympanic crest is located on the frontoparietal and squamosal. Absent (0); present (1).

67. Suborbital crest. The suborbital crest is located on the pars facialis of the maxilla. Absent (0); present (1).

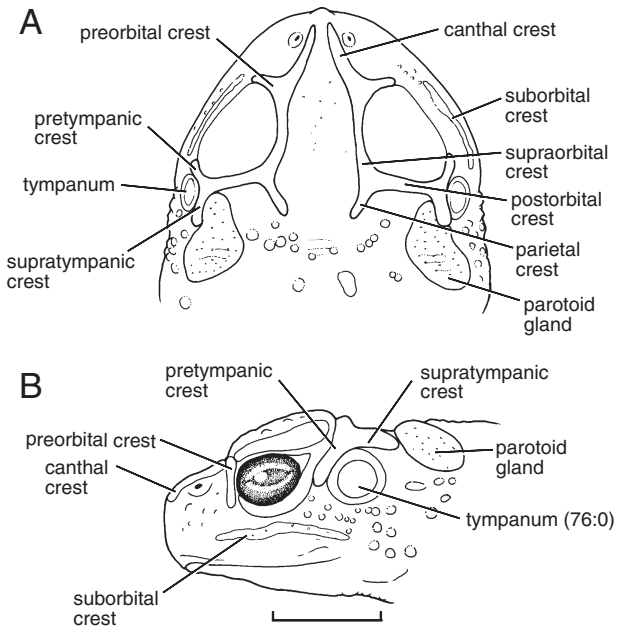

Figure 14. *Bufo luetkenii* (KU 289850), illustrating the nomenclature and position of dorsal (A) and lateral (B) cranial crests coded for the phylogenetic analysis. Scale bar = 1 cm.

68. Supraorbital crest. Absent (0); present, derived from the frontoparietal that is developed into a medially sloping, supraorbital flange (1); present, orientated vertically from the plane of the frontoparietal (2).

69. Supratympanic crest. The supratympanic crest is located on the otic ramus of the squamosal. Absent (0); present (1).

70. Pterygoid shape in dorsal view. In most species of *Bufo* the medial ramus of the pterygoid is relatively narrow (0), broad (1), or broad and flattened (2).

71. Angle formed by supraorbital and postorbital crests. Tihen (1962a) noted that in dorsal view the junction of the posterior margin of the supraorbital crest and the medial limit of the postorbital crest of some North American toads forms a distinct 90° angle. Junction of supraorbital and postorbital does not form a 90° angle (0); junction of crests forms a 90° angle (1).

72. Supraorbital flange on frontoparietals. In ventral view, the frontoparietal in some taxa extends laterally beyond the lateral margin of the sphenethmoid. The presence of this character approximately corresponds with a 'broad skull' morphology, *sensu* Blair (1972b) and Martin (1972a). Supraorbital flange absent (0; e.g. *B. amabilis*; Fig. 7C); present (1; e.g. *B. veraguensis*; Fig. 7E).

73. Shape of parotoid glands. The shapes and relative positions of the parotoid glands have been used as diagnostic characters for many groups within *Bufo*. Parotoid glands absent (0); present, longer than wide (1); present, ovoid or triangular (2); present, round (3).

74. Spade present on tarsus. Many species of *Bufo* bear a small spade-like structure on the skin overlying the astragulus of the hind limb; this spade presumably aids in digging. Linear ridge or 'spade' present on skin overlying astragulus absent (0); present (1); present, with thick keratinous edge (2).

75. Vocal slits. Vocal slits present, bilateral (0); present and unilateral (1); absent (2).

76. Presence/absence of tympanic annulus. The presence and absence of this character is difficult to judge accurately without dissecting the specimen to verify the absence of a tympanic annulus, which can be obscured by the overlying tympanum. To compensate for this, a tympanic annulus was coded as present if it was visible externally. Tympanic annulus visible externally (0; e.g. *B. luetkenii*; Fig. 14B); not visible externally (1).

77. Webbing on manus. Most bufonids lack webbing on the hand (0). However, a few taxa (e.g. *Osornophryne, Rhamphophryne*) possess it (1).

78. Webbing on pes. Most bufonids have webbing present on the feet (0), whereas a few species (e.g. *Truebella*) lack foot webbing (1).

79. Inguinal fat bodies. Da Silva & Mendelson (1999: fig. 2) described the presence of inguinal fat organs,

unique to bufonids; for phylogenetic analyses, the presence of this structure was coded from their publication. The function of these organs is unknown. Inguinal fat bodies absent (0); present (1).

80. Two-toned coloration. Some members of the *B. guttatus* and *B. margaritifer* groups have distinctive cryptic two-toned ('dead-leaf') coloration of tan on the dorsum and dark brown laterally and on the fore and hind limbs. Two-toned coloration present (0); absent (1).

81. Row of lateral tubercles on skin. Several species of bufonids have a distinct series of enlarged, lateral tubercles. The tubercles form a distinctive row that initiates near the posterolateral margin of the parotoid gland and continues in a descending row until they reach the mid-region of the flank where they become indistinct. Lateral tubercles absent (0); present (1).

82. Tibia gland. Enlarged glands on the hind limbs are rare among *Bufo*. However, they are present in a few species examined. Gland on skin overlying tibia absent (0); present (1).

83. Fibula gland. Gland on skin overlying fibula absent (0); present (1).